Anticipating and Adapting to Increases in Water Distribution Infrastructure Failure Caused by Interdependencies and Heat Exposure from Climate Change

by

Emily Bondank

A Dissertation Presented in Partial Fulfillment
of the Requirements for the Degree
Doctor of Philosophy

Approved June 2019 by the
Graduate Supervisory Committee

Mikhail Chester, Chair
Nathan Johnson
Benjamin Ruddell
Thomas Seager

ARIZONA STATE UNIVERSITY

August 2019

ABSTRACT

This dissertation advances the capability of water infrastructure utilities to anticipate and adapt to vulnerabilities in their systems from temperature increase and interdependencies with other infrastructure systems. Impact assessment models of increased heat and interdependencies were developed which incorporate probability, spatial, temporal, and operational information. Key findings from the models are that with increased heat the increased likelihood of water quality non-compliances is particularly concerning, the anticipated increases in different hardware components generate different levels of concern starting with iron pipes, then pumps, and then PVC pipes, the effects of temperature increase on hardware components and on service losses are non-linear due to spatial criticality of components, and that modeling spatial and operational complexity helps to identify potential pathways of failure propagation between infrastructure systems. Exploring different parameters of the models allowed for comparison of institutional strategies. Key findings are that either preventative maintenance or repair strategies can completely offset additional outages from increased temperatures though-- improved repair times reduce overall duration of outages more than preventative maintenance, and that coordinated strategies across utilities could be effective for mitigating vulnerability.

ACKNOWLEDGEMENTS

I would like to extend my sincerest thanks to the National Science Foundation, my dissertation committee, and my advisor Dr. Mikhail Chester, whose vision, support, and guidance made this journey possible and incredibly rewarding. I also am deeply grateful for my colleagues, friends, and family who provide joy and inspire me to think holistically and live fully.

TABLE OF CONTENTS

Page

APPENDIX Page

APPENDIX Page

LIST OF TABLES

LIST OF FIGURES

Figure Page

Figure Page

Figure Page

CHAPTER 1

INTRODUCTION

1.1 Motivation

Extreme weather events anticipated from climate change present major challenges for our society in the Anthropocene.[1] One challenge is in managing the vulnerability of civil infrastructure systems which were originally designed to operate under historical weather conditions.[2] Designs for historical weather conditions create the potential for climate-related extreme events to increase damages and loss of life. For example, in the 2010 earthquake in Haiti, poor building codes were identified to be a main factor for the resulting displacement of 1.2 million people and more than 200,000 deaths.[3] The World Risk Report states generally that "[Haiti's] vulnerability to disasters and its ability to cope with them are down to far more than simple geography. The disaster potential we see in Haiti… is not only driven by the strength of the hazard, but also by the real lack of coping capacity and very high fragility and susceptibility within society – we're talking very basic infrastructure – sanitation, healthcare centers and evacuation shelters".[4]

Engineers must adapt infrastructure systems to ensure reliability into the future. The American Society of Civil Engineers recognizes that "engineers should develop a new paradigm for engineering practice in a world in which climate is changing".[2] Part of this new paradigm will be to identify and explore vulnerabilities and prevent them from causing infrastructure failure or the cascading of failure to service losses. Without adaptation, increasing failures and service outages can occur without the means to properly respond.[5]

1.2 Climate Change Hazards for Water Infrastructure

Water distribution systems are one of the most critical infrastructure systems for the economic health of cities and they are vulnerable to climate hazards.[6] The delivery of safe and sufficient water to residents and commercial establishments is vital to almost all residential, commercial, industrial, and public operations. Therefore, disruption of this service from disasters is a threat to public and economic health. The overall reliability is dependent upon both the availability of the resource, the reliability of the infrastructure, and the quality of the water [7] and each are threatened by climate change events. Extreme temperatures, drought, frequency of freeze and thaw cycles, extreme precipitation, sea level rise, and increased frequency and extent of wildfires pose as hazards for water infrastructure.[6]

The availability of bulk water resources is sensitive to drought and sea level rise. Increased levels of drought causes decreased annual snowfall and precipitation, and sea level rise causes saltwater intrusion into groundwater aquifers.[8] With simultaneous increases in population and reduction of water supply, both surface water and groundwater could be insufficient to meet demands in some desert regions.[8]Additionally, increased bulk water temperatures can cause increased growth of pathogens in stagnant reservoirs that are difficult to treat at treatment plants.[9]

Common elements across all water systems are pumps and pipes which facilitate transport, treatment plants, and the operators who manage the infrastructure. Heat exposure can cause pumps to overheat and increase corrosion of thermoplastic, metal, and concrete materials in canal linings and pipes.[10–18] The freezing of water in pipes leads to blockages and outages, and an increased frequency of freeze and thaw cycles causes

increased cracking of pipes.[19–21] In places where temperatures will increase in the winter, climate change could beneficially decrease freeze-thaw cycles.[22] Additionally, increased amounts of standing water and infiltration from extreme precipitation events can cause stress loads to underground pipes from soil expansion, causing an increase in cracking.[23] Sea level rise threatens to affect both pumps and pipes along with treatment facilities. Salt water intrusion into soil causes increased corrosion and degradation of pipes and increased fracturing of pipes from land subsidence. Salt water intrusion could also cause flooding of pumping stations, sewers, treatment plants, and wastewater sewage backup.[24] From a human physiological perspective, extreme heat is known to increase water demand, and cause heat-stroke in water system operators.[25,26]

Each water infrastructure system has additional unique physical, chemical, and biological sensitivities to climate change events. Increases in frequency and expanse of wildfires can cause erosion, contaminating runoff and resulting in flooding.[27] Increases in the frequency or intensity of precipitation events are a major risk for these systems causing the following potential problems.[28] The infrastructure used to transport water to treatment plants is at risk to extreme precipitation events and heat exposure. The flooding of canals from precipitation and sewer infrastructure failure causes high turbidity and low pH levels which could exceed treatment capacity due to the lower-turbidity and higher-pH design of the treatment processes. This could lead to temporary outages of treated water to consumers.[29–31] Additionally, concrete canals with jointed panels can breach, leading to a shutdown of the larger system.[31] The chemical and biological treatment processes within water and wastewater treatment plants are sensitive to water temperature as well as from levels of turbidity from high precipitation events. Water temperature

correlates to the speed of chemical reactions and microbial growth. Higher water temperatures are generally beneficial for quickening the speed of reactions and growth of microbes that consume organic material and convert harmful chemicals into harmless ones.[22] If water temperatures become colder the treatment efficiency could be reduced. In contrast, increased chemical reaction rates in the distribution system are potentially problematic, causing an increased decay of the disinfectant residual, formation of disinfection byproducts, nitrification rates, and the growth of harmful bacteria like Mycobacterium Avium Complex and Legionella.[32,33,42,34–41]

1.3 Anticipating Impacts and Adapting Water Distribution Infrastructure

Though water utilities are largely aware of extreme weather hazards, they are challenged by how to adapt their specific systems. In a survey of water utilities, 17 out of 18 responded that they already experience the extremes attributed to climate change.[6] Most of the 17 utilities experiencing extremes are taking some form of action based on the extreme events that have already happened [6]. Once utilities identify the causal factors of failure within their systems during an extreme weather event, they are able to mitigate those factors. While they are acting on recent extremes they have faced, they neglect preparations for different future events resulting in planning that lacks foresight. Heyn & Winsor state that "A majority of the water and wastewater providers interviewed are already experiencing extremes, so convincing employees to prepare for a wider range or change in those extremes is difficult for a few of the utilities. Furthermore, there may be small, growing changes that accrue before substantial impacts take place, and these are hard to garner attention around".[6] Additionally, " several utilities have experienced dual

extreme events with different outcomes – for example drought and flooding. These events can result in different impacts to assets and infrastructure and certainly make it more challenging for utilities to plan for the future".[6]

Utilities that have not yet experienced extremes have the challenge of identifying any vulnerabilities in their system. While they can gain awareness of possible effects of extreme weather events that occurred at other utilities, they cannot directly infer that their systems are vulnerable in the same way, due to their different infrastructural contexts. The outcome of the 2010 earthquake in Chile provides some context. The earthquake was larger than the one that occurred in Haiti in the same year, however it produced much less damage and loss of life because Chile had stricter building codes.[3] Another example -- this time related to water infrastructure -- is that while the City of Phoenix and NYCDEP water utilities both face the hazard of extreme precipitation, the City of Phoenix anticipates possible water treatment plant shut downs from challenges in treating the high turbidity in the water, but NYCDEP does not. NYCDEP draws diversions from a different source, redirects high turbidity water, and has an interconnection with other bulk water providers.[6] Therefore, NYCDEP's network configuration and water flows make the anticipated impacts from extreme events different than those of the City of Phoenix. Moreover, the infrastructural context makes anticipating impacts for each utility challenging without direct historical experience.

New federal legislation requires considering context when developing adaptation strategies. The American Water Infrastructure Act passed in October 2018 requires US utilities to conduct resilience assessments for natural hazards.[43] As utilities conduct their assessments, they need contextual knowledge for the "Consequence Analysis" and the

"Risk and Resilience Management" steps as suggested by the Risk Analysis and Management for Critical Asset Protection (RAMCAP) Standard for Risk and Resilience Management of Water and Wastewater Systems, which serves as guidance for compliance with the new law.[5] The RAMCAP standard calls for an estimation of the duration and severity of service outage that could result from a hazard. They also ask that utilities "do not assume that all uncontrollable variables and unpredictable events occur simultaneously". [5] Therefore, a contextual knowledge of time and space is recommended for anticipating outages.

Reliability and climate impact assessments can help utilities anticipate impacts, but there is room for improvement in the potential of the assessments to capture the individual utility contexts. In the water infrastructure field, reliability assessments use quantitative methods for assessing a water system's ability to deliver service given scenarios of component failures. These models do not inherently have vulnerability assessments to different hazards, however. Climate impact assessments use selected methods from reliability assessments to anticipate the increased risks, costs, and/or service losses that could occur from a climate change hazard. A review of the types of information that were included in a sample of 46 existing reliability and climate change impact assessment studies for water treatment and distribution systems is shown in Figure 1. [6,44,53–62,45,63–72,46,73–77,47–52]

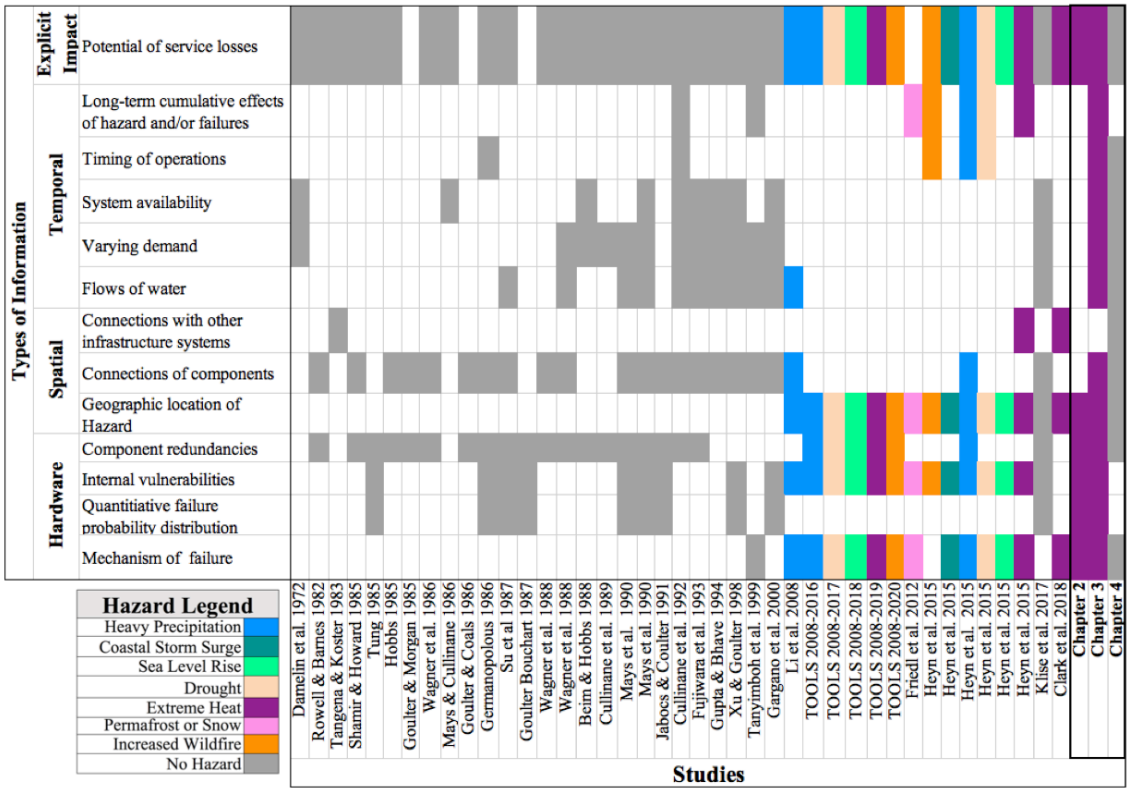

Figure 1 Types of Contextual Information Included in Water Reliability and Climate Impact Assessments

The types of information were divided into four categories: hardware, spatial, temporal, and information regarding explicit impact. Solid colors in Figure 1 represent the types of information that were included and each color represents a different climate hazards considered. White spaces in the figure indicate types of information that were not included in the studies. Studies are arranged chronologically from left to right. The overall takeaway is that while most studies aim to characterize potential service losses, they use a fraction of the identified types contextual information. The progression of studies through time, is promising, however. As time progressed, reliability studies included more contextual information (largely spatial and temporal network information) and by 2008, climate hazards were introduced. Not all quantitative information available in water reliability models has been utilized in climate change assessments. They largely

use qualitative assessments of probability and do not use spatial or temporal information. The WNTR model from EPA (2017) is a promising reliability assessment tool that considers much of the quantitative hardware, spatial, and temporal information as well as the ability to input climate hazard information to evaluate service losses.[50] Furthermore, only a few studies consider connections with other infrastructure networks, long-term cumulative effects, and repair dynamics.

1.4 Anticipating and Adapting Water Infrastructure to Impacts from Increased Heat Exposure

In warm regions like the US Southwest, the threat of heat to water reliability is of particular concern. It is especially important that water systems remain reliable as temperatures rise because in addition to greater consumption by individuals,[25] the viability of many services may also require increased consumption. The electricity generation and agricultural industries in particular may need increasing amounts of water in a hotter future.[78–80] For individuals, heat exposure can also cause a variety of health issues [81] that would be significantly exacerbated without access to clean water. Heat can also cause problems for traditionally cold places, but there may also be benefits from reducing periods of freezing.[19–21]

Anticipating effects from temperature rise and extreme heat events could be improved by considering additional types of information than was included in past reliability studies. Temporal dynamics are potentially important to consider because degradation from heat can accumulate overtime.[10–12,17,32,82–84] The two types of climate impact assessments that have addressed heat as a hazard to hardware and operations (shown in

Figure 1) are climate impact assessment tools[48,49,85] and a narrative crafted about the possibilities of effects.[47] Climate impact assessment tools contain geographically specific temperature projections and allow for input of information about component vulnerability to heat. They also allow for ranking of the criticality of components but do not help determine the vulnerability of failure and their potential to cause outages through mapping the network of components. The narrative written about water infrastructure vulnerability to heat also includes geographically explicit projection information and description of how the components could be vulnerable to failure from heat and connections to other infrastructure systems, but no analysis was performed to explore possible futures given hardware, spatial, or temporal context of particular water systems.

Assessments of heat impacts to other infrastructure systems include similar types of information to what is included in assessments of heat impacts to water systems (hazard information, criticality of components, qualitative component vulnerabilities). Assessments for power and transportation systems include additional types of information, however. Assessments of heat impacts to power infrastructure include additional information characterizing vulnerability of components quantitatively.[86–88] Assessments of roadway infrastructure include the additional information of expert rankings of vulnerability and criticality of components.[89–91] Moreover, while we know that infrastructure hardware are vulnerable, our ability to explore contextual scenarios causing service outages is limited.

1.5 Understanding and Managing Interdependencies

Another source of vulnerability of water systems to climate hazards is through their interdependencies with other infrastructure systems. Though managed separately, infrastructure systems share common space with each other and require one another to operate.[92] Thus, the vulnerability of one infrastructure system can propagate to other infrastructure systems. A key historical example of this propagation is the Baltimore's Howard Street tunnel event where the fire from a derailed freight train caused traffic congestion, fiber optic cable damage and telecommunication outage, along with a water main break. The water main break then caused flooding of transformers that resulted in power outages to 1,200 people in downtown Baltimore.[93] Thus, there has been a recognized necessity of also considering interdependencies in reliability and climate change impact assessments.[78,79,99–108,80,109–113,88,93–98]

Power systems are integral to water systems. The two are connected through water pumps, valves, and SCADA need for power,[7,114] possible load drops from pump failure, possible transformer flooding from pipe break,[115] and generator capacity drop from lack of treated water for cooling.[116] Power components are also vulnerable to heat in a variety of ways.[86] Therefore, exploring the impacts failures have on the coupled system could ultimately help understand the overall vulnerability of the coupled systems to heat.

Current models of interdependencies are insufficient to answer questions about propagation and vulnerabilities, however. Reliability and climate change impact assessments include quantitative information about interdependencies to better understand the strength of connections.[47,78,98–107,79,108–113,80,88,93–97] These studies focus on long-term use of resources and topographic connections, which do not provide

information to determine vulnerability from failure. Current failure propagation interdependency studies typically only use graph topologies without flow information.[96,103,110] Studies suggesting new model frameworks confirm that interdependency models should include more information. They recommend considering structure, flow characteristics [106], system operation [109,117], and temporal aspects [97]. This additional information would facilitate anticipating where, how, and under what operational circumstances the interdependencies could manifest given their spatial and operational context, and therefore how widespread resulting outages could be.

In addition to improving communication across utilities, literature suggests developing coordination between infrastructure managers, arguing that it could lead to more effective vulnerability mitigation. Derrible argues that "A more coordinated and better planned integration is highly desirable" because integrated systems can consider more of society's needs (health, equity, overall efficiency) (Derrible, 2017). Chester & Allenby (2018) citing Larence and Lorsch (1967) argue "Organic [organizational] structures allow for more internal specialization to respond to changing environments, thereby increasing responsiveness"[118] because "distributing the knowledge and decision-making at the bottom of the hierarchy becomes more effective when the environment [in which infrastructure operate] becomes unstable and high-level management cannot acquire all of the knowledge associated with the changing environment (Sherehiy et al., 2007)".[119,120] This generates the question for utilities, *do coordinated institutional strategies between utilities have the potential to reduce vulnerability better than other institutional strategies?* Models which identify the pathways of failure propagation can

serve as a baseline to explore different institutional strategy inputs to see how well they can mitigate failures.

1.6 Dissertation Objectives

The objective of the dissertation is to develop impact assessment models that improve water utilities' capacity to prepare for increased heat exposure and interdependencies by:

(1) Anticipating the water distribution infrastructure component and system-level responses from exposure to heat and exploring adaptation strategies related to reducing component probability of failure.

(2) Anticipating the impact of stochastic hardware failure on the service losses in a water network over time and exploring adaptation strategies related to reducing water outages.

(3) Presenting a modeling framework capable of anticipating pathways of failure propagation across coupled infrastructure systems and providing a tool to explore the benefits of coordination between water and power utilities.

The studies in the bolded box in Figure 1 highlights how the work of this dissertation would contribute to improving the types of information used in climate change assessments related to increasing heat for water distribution systems.

1.7 Chapter Summaries

Chapter 2: Water Distribution System Failure Risks with Increasing Temperatures	
Research Questions	What is the projected increase in risk of component failures and service losses within water distribution systems with increases in maximum summertime temperatures? Where should municipal water utility management strategies be focused to mitigate increases in risk?
Approach	i) potential temperature-induced sensitivities were identified for physical components and aspects of water quality; ii) quantitative relationships between failure and temperature exposure were identified; iii) ranges and distributions of major operating conditions impacting degradation were identified; iv) average maximum daily summertime temperature projection data were processed for Phoenix, Arizona and Las Vegas, Nevada; vi) Monte Carlo simulations were used to perform calculations of failure metrics for each temperature scenario given operating conditions; vi) probability distribution functions were fitted to Monte Carlo outputs; vii) projections of failure using failure rates for physical components and probabilities of water quality non- compliance were calculated from probability distribution functions; and, ix) fault trees were created to estimate how individual component failures and

	quality non-compliances could propagate to service outages given different operational scenarios.
Deliverable	Peer-reviewed journal article published in Engineering Science & Technology 2018.
Intellectual Merit	The probability of component failure is quantitatively estimated under future temperature scenarios and is compared across components. Probabilities are used to estimate the possible increase in service outages.

Chapter 3: Anticipating Water Distribution Losses from Climate Change	
Research Questions	What are the cumulative impacts of heat on water components? What are the impacts of increased component failures on service losses? What are some effective strategies for reducing the additional outages from climate change?
Approach	The Perses model is designed to simulate the reliability of water distributions systems into the future under long-term exposure to different possible temperature projections. Multiple temperature scenarios are considered including a baseline (where historical temperatures persist, i.e., no climate change) and futures with changing temperatures based on the Global Circulation Model (GCM) ensembles. A Python wrapper is used to stochastically fail components in each time step based on their temperature exposure and their individual

	robustness, and then implement the failed state of components in EPANET to track the consequential service outages, considering daily demand patterns and hydraulic flows. The program tracks the time of failed components and repairs according to given repair times. The results show a comparison of the increases in pipe and pump failures and how water outages increase under different temperature change scenarios. Two case studies are used to evaluate the effects of temperature on component failures and network service outages under extreme heat scenarios similar to those in the U.S. Southwest. The model is then used to explore adaptation strategies relating to probability of failure and repair times.
Deliverable	Peer-reviewed journal article.
Intellectual Merit	The Perses model shows the capability of a dynamic extended period simulation to aid decision making about climate adaptation by estimating the impacts to consumers. The use of Perses for projecting failures from increasing temperatures in water distribution systems shows that utilities in the Southwestern region of the U.S. that experience high temperatures will likely experience increases in component and consequential service level outages to consumers. We hope that the insight generated will help mitigate services losses into the future.

Chapter 4: Understanding and Managing Interdependent Power and Water Systems	
Research Questions	How can utilities model propagation of failure from interdependencies and anticipate vulnerability? How can they use these models to explore effects of institutional strategies?
Approach	Since sufficient modeling frameworks are not yet available, we present a modeling framework which uses real-time simulation of coupled network models and a case study of a specific coupled network. This modeling framework could then be used to answer the questions posed in the introduction for other coupled networks to answer the questions: Where are the locations in the network that are vulnerable to propagation of failure from interdependencies? How much vulnerability do interdependencies cause? Do coordinated institutional strategies between utilities have the potential to reduce vulnerability better than other institutional strategies?
Deliverable	Peer-reviewed journal article.
Intellectual Merit	This case study shows how failures can propagate across infrastructure systems in real time, which improves the knowledge we have about how interdependencies can cause additional vulnerability for utilities. Instead of only considering the resource flows between networks or the number of connection points, adding information about whether interdependencies cause failures given the resource flows within the network configurations, the operational settings of

	the components, and the operational management strategies, allows for anticipation of outages due to interdependencies. Anticipating outages from example propagations of failure in turn allows for the evaluation of outcomes from different institutional strategies both within and across systems. The result of the evaluation of strategies of this case study shows that there is potential for infrastructure systems managers to minimize impacts of interdependencies across systems by coordinating with other utilizes. We hope utilities use this finding as further motivation to consider coordination strategies across utilities.

CHAPTER 2

WATER DISTRIBUTION SYSTEM FAILURE RISKS WTH INCREASING TEMPERATURES

2.1 Introduction

Civil infrastructure systems are vital for delivering resources, providing protection, and facilitating most urban activities. Typically, these systems are designed to last for long periods of time, often on the order of decades, and some systems persist for over a century.[2] Today, infrastructure operational limits are designed based on historical climate conditions,[2] and global climate models project that these conditions will likely be more frequently exceeded in the future.[2] Consequently, the predictions of infrastructure reliability from historical climate data may over-predict the lifespans and reliability under future conditions. One particular climate change-related hazard is global temperature rise, and in regions that already have hot climates, further increases in temperature may pose serious risks for people and the infrastructure upon which they rely.[121] In the US, of particular concern is the Southwest region, where limited water supplies coupled with further increases in temperature may pose major challenges. For example, the National Climate Association reports that the Southwestern US "regional annual average temperatures are projected to rise by 1.4-3.0^{o}C by mid-century and by 3.0-5.3^{o}C by end-of-century with continued growth in global emissions (A2 emissions scenario), and with the greatest increases being in the summer and fall".[122] If urban densification occurs, it has the potential to cause even greater temperature increases via urban heat island.[123] In hot climates, it is reported that infrastructure components occasionally fail from high summertime temperatures because of overheating and increasing rates of undesirable

chemical reactions.[6,124] These failures can lead to service outages when there is not enough redundancy or emergency response.[125] Thus, increased temperatures have the potential to increase the probability of outages if design, operation, and management practices remain the same. An infrastructure of particular concern is that of potable water distribution, where heat may result in failures that lead to disruptions of quantity and quality.[125]

Water distribution systems are particularly critical to the economic health of cities and regions, especially in hot conditions. The delivery of safe and sufficient water to residents and commercial establishments is vital to almost all residential, commercial, industrial, and public operations, and the overall reliability is dependent upon both the availability of the resource, the reliability of the infrastructure, and the quality of the water. It is especially important that water systems remain reliable as temperatures rise because in addition to greater consumption by individuals,[25] the viability of many services may also require increased consumption. The electricity generation and agricultural industries in particular may need increasing amounts of water in a hotter future.[78–80] For individuals, heat exposure can also cause a variety of health issues that would be significantly exacerbated without access to clean water.[81] Additionally, research has shown that from increased evaporation and decreased snowmelt, the amount of fresh water available to some regions will diminish with increasing global temperatures.[122] When the availability, infrastructural reliability, and quality are all stressed by rising temperatures, there could be a significantly greater threat of provisional inadequacies and consequential human health and economic losses.

The reliability of water systems is already challenging to maintain under current temperature conditions. Utilities do not always implement asset management programs to track the failure rates of their components and strategically plan for preventative maintenance to decrease service outages.[126] Instead, components are typically operated to failure and utilities rely on their ability to quickly respond and repair, as preventative maintenance budgets are usually constrained.[7,127] There remains a question as to whether this strategy will continue to work under future conditions. Some utilities have identified potential threats of increased temperatures, but very few have formally included climate change in their design process.[6] The American Society of Civil Engineers notes that even when scenarios of climate change are explored, there will be "a tradeoff between the cost of increasing the system reliability and the potential cost and consequences of potential failure".[2] Utilities therefore need information to help them prioritize decisions in planning, design, maintenance, and operations.

Given the potential for increasing temperatures, utilities will need to know how their systems may be affected and where efforts should be most focused to prevent and prepare for changes in their system. More specifically, they will need to know how to prepare to mitigate failures ahead of time and how to prepare for the effects of failures.[128] This study strives to answer two questions in the context of seasonally hot cities where temperature increases risk of failure: (1) What is the projected increase in risk of potable water service loss with increases in maximum summertime temperatures? and (2) Where should municipal water utility management strategies be focused to mitigate increases in risk? To address these questions, the functionality of water system components and water quality are analyzed under temperature conditions characteristic of Phoenix, Arizona and

Las Vegas, Nevada, considering climate change. An exploration of the temperature-related sensitivities and consequential risk is valuable for understanding issues that may affect other cities in the future.

2.2 Methodology

To aid water utilities in understanding where their systems will be more vulnerable and how they can strategically mitigate temperature-related service interruptions, the following approach was used: i) potential temperature-induced sensitivities were identified for physical components and aspects of water quality; ii) quantitative relationships between failure and temperature exposure were identified; iii) ranges and distributions of major operating conditions impacting degradation were identified; iv) average maximum daily summertime temperature projection data were processed for Phoenix, Arizona and Las Vegas, Nevada; vi) Monte Carlo simulations were used to perform calculations of failure metrics for each temperature scenario given operating conditions; vi) probability distribution functions were fitted to Monte Carlo outputs; vii) projections of failure using failure rates for physical components and probabilities of water quality non- compliance were calculated from probability distribution functions; and, ix) fault trees were created to estimate how individual component failures and quality non-compliances could propagate to service outages given different operational scenarios. The resulting component projections of failure, percent increases in failure, and expected number of service outages under scenarios of the possible temperature exposure in the next 30 years considering best and worst case operating conditions are used to make recommendations for focused management strategies. A process flow diagram of the methodology is shown in SI Figure S1.

2.2.1 Quantifying Temperature-Related Exposure and Degradation

The physical components and aspects of water quality that have been shown to be sensitive to temperature were first identified through literature review to assess how operational failures might increase. Temperature sensitivities affect component wear and the rate of chemical reactions, the latter leading to the potential for increased pipe degradation and corrosion or quality non-compliance. Temperature-sensitivities are found in the motors[10–12,82] and electronics[83,84] used in pumping units, thermoplastic[16] and metal pipes[17], and in the chemical processes in the water from decay of the disinfectant residual[32] and increase in disinfection byproduct production (DBP)[33,34] (SI Table S1). While high temperature is known to affect water demand[25], soil expansion[129], material stress in pipes from temperature change[130,131], the health of system operators[132], nitrification rates[39–41,133], and the growth of harmful bacteria like *Mycobacterium Avium Complex*[37,38] and *Legionella,*[35,36] these effects were excluded from analysis because of lack of basic data and quantitative relationships.

There is ample evidence that summer temperatures contribute to degradation of water system components and quality. From experience of operation, the Las Vegas Valley Water District has found that their cooling systems for pumping units may be inadequate for higher summer temperatures and that thermoplastic pipes fail more frequently in the desert heat.[6,134] Observational studies of rates of corrosion and DBP production over year-long periods show that rates are higher during summer when the water is warmer.[17,33,34,135] Additionally, an experimental study of chlorine residual decay in water samples also shows that reaction rates increase when samples are subjected to warmer water temperatures under periods of about a day.[32]

Studies of environmental and public health hazards have found that the impact of a hazard depends on "the concentration, amount or intensity of a particular agent that reaches a target system in terms of its duration, frequency, and intensity".[136] It is therefore assumed that physical components and aspects of water quality would have varying levels of degradation as a function of their durations and magnitudes of exposure. While the empirical studies of water quality aspects and corrosion rates show that a summertime period or shorter is enough to cause the reported change in reaction rates, the exact duration of exposure that it takes for temperatures above rated thresholds to cause degradation to the physical components (i.e. PVC pipes, motors, and electronics) at the reported rates is unknown. We speculate that because degradation is cumulative for physical components, cumulative exposure duration might be important. No empirical data or models were identified to establish a useable relationship between cumulative exposure and degradation rate for these components, so we propose a theoretical relationship that is derived in Appendix A.2. However, we are not able to employ this cumulative temperature model in the current paper owing to a lack of empirical data on the effects of cumulative exposure. Fortunately, there is some information available on the relationship between maximum temperature exposure and component degradation rate. One source states that reported motor degradation rates apply "even if the overheating was only temporary".[12] We therefore interpret published degradation rates for PVC pipes, motors, and electronics as being appropriate to characterize degradation from brief but repeated exposure of water systems to peak temperatures over the components' service lives. When water systems are deployed in the field, they are exposed to exactly this type of pattern of "temporary", but repeated, maximum

temperatures; this exposure happens almost every summer afternoon. The hottest afternoons in U.S. cities tend to occur in June, July, and August, which is when temperatures sometimes exceed safe operating temperature ratings of components.

Since both physical components and aspects of water quality are affected by high summertime temperatures, this study models failure due to predicted averages of maximum daily summertime temperatures between June and August, during the hottest three hours of each summer day. This model has a cumulative-peak-exposure interpretation because a component in our model is exposed to this peak temperature for roughly 270 hours at least once and at most every year (the average temperature of the hottest 3 hours each day[137] for 3 months, referred to as "3x3" in this paper). If it is the case, however, that degradation rates of physical components increase every time the component experiences much smaller durations of exposure (e.g. during a minute, hour, or week), then the model underestimates projections of failure. If it is the case that the degradation occurs only given years of continuous exposure that are longer in duration than the 3x3 window time frame, the model overestimates failures. With empirical daily or monthly failure data, future studies could determine the specific duration of exposure needed to cause these rates of degradation to physical components.

2.2.2 Urban Water System Case Study

Given their large populations, hot environments, and modern infrastructure, a potable water system with characteristic conditions of the cities of Phoenix, Arizona and Las Vegas, Nevada was modeled as a case study. These metro areas are two of the largest and fastest growing regions in the Southwestern US, and experience some of the highest

temperatures of metro area across the US.[138,139,47] They both have populations of around 5 million people and experience 35 – 40°C average daily summer temperatures.[138,139] The largest water utilities in each metro region service around 1.5 million customers each.[140,141] Since studies on temperature affects to operation are sparse, the failure metric equations and ranges of operational characteristics from literature were used from systems around the world that do not necessarily represent the Las Vegas and Phoenix case studies. Therefore, the temperature data and number of components are the aspects of the system that are characterized by the case studies. A comparison of the relevant water utility characteristics is shown in SI Table S2.

Climate projections show significant increases in temperature in Phoenix and Las Vegas into the future. Phoenix and Las Vegas projections of the averages of maximum daily summer temperatures (3x3) are shown in SI Figure S3. Temperature projections were processed from CMIP5 12x12 km gridded data from Global Climate Model (GCM) projections of representative concentration pathway (RCP) scenarios 2.6, 6, 4.5, and 8.5.[121] The 3x3 maximum air temperature in Phoenix is projected to increase to at least 40°C in 2020 and at most 44°C in 2050 (including the GCM's standard deviation of temperature). In Las Vegas it is projected to increase to at least 36°C in 2020 and at most 41°C in 2050. The temperature range used to force the failure model considers the total range of both cities with GCM uncertainty, i.e., 36 – 44°C at 1°C intervals.

2.2.3 Modeling Increases in Component and Water Quality Failure

Failure can be measured as events where reliability requirements are not met.[7] Motors and electronics within pumping units failing to operate, pipes breaking and not

delivering water at required pressures, chlorine residual concentrations below regulation, and DBP concentrations above regulation each constitute failures. Estimated-time-to-failure (ETTF), which represents the lifetime of components in units of years, and chemical concentration therefore represent "failure metrics" that indicate the potential for failure of components and the aspects of water quality, respectively. With temperature sensitivities identified, a review was conducted to identify the quantitative relationships between temperature and component failure and chemical reaction rates to characterize failure metrics. The ETTF parameter was calculated when the quantitative relationship between exposure temperature and lifespan of component was given and was used to estimate effects of overheating on motors and electronics, degradation of polyvinyl chloride (PVC) pipes, and corrosion of iron pipes. Chemical concentration represents the failure metric of chlorine residual decay and the production of DBPs.

An increase in ambient temperature threatens overheating of motors and electronics that are vital to the operation of the pumping units. Motors can overheat from the combined dissipated heat from motor windings and the ambient temperature surrounding the motor, causing destruction of the insulation which can lead to burnt stator windings.[10–12,82] It is reported as a rule of thumb in the industry that for every 10°C increase in the operating temperature over the capacity of the insulation--155°C for class F motors -- the lifespan decreases by one-half (Appendix A.4.1.1).[10–12,82] Conversely, the lifespan increases by one-half for every 10°C decrease in the operating temperature below the capacity of the insulation. [11] The electronic controls that are used for pump operation are also sensitive to the combination of dissipated heat and the outside temperature within their enclosures, and for every 10°C rise in enclosure temperature

above 40°C, the lifespan of the electronics decreases by one-half (Appendix A.4.1.1).[83,84] It was assumed that electronics have the same property as motors when temperatures are below their capacity. With these relationships, we estimate the ETTFs that result from exposure to average peak summertime temperature scenarios.

Water temperatures in the distribution system rise in response to increases in ambient temperatures. The relationship between water and air temperatures was modeled using the empirically derived linear regression equations from a study of temperatures at water treatment plant outlets in Japan.[142] Coefficients of the regression range from 0.52 – 0.89 °C in water / °C in air and the constants range from 1.88 – 7.89 °C in water. Despite some novel research on the topic, [142,143] predicting water temperature within distribution pipes is challenging due to a lack of empirical data. With high water temperatures, thermoplastic pipes can experience overbearing pressures, with the greatest effects on PVC.[16] The derating of the PVC pipe is linear with increasing water temperatures (Appendix A.4.1.3). Iron pipes are sensitive to indirect effects of water temperature through internal corrosion.[17] The relationship between corrosion rate and water temperature over a year-long period has been reported in the literature for the cast iron pipe material, so this is the type of iron pipe modeled. Temperature may have a similar effect on the corrosion rate of ductile iron and steel pipes, though no relationship was found in literature. Corrosion rates for cast iron pipes are reported to be empirically different for water distribution systems (WDS) and water treatment plants (WTP) (Appendix A.4.1.4). [17] Corrosion rates and pipe age were used to calculate pit depth and then to the calculate the ETTF from the remaining life of the pipe according to Randall-Smith et al.[144]

Water quality is also affected by an increase in water temperature. Summertime temperatures increase the reaction rates between the organics and disinfectants in water, thereby increasing the formation of the cancerous DBP, total trihalomethane (TTHM), according to an empirical study on seasonal drinking water quality in Istanbul City, Turkey, where water is supplied through surface water and is treated through "aeration, prechlorination, coagulation, flocculation-sedimentation, filtration, and postchlorination" (Appendix A.4.1.5).[33] The concentration of another DBP, total haloacetic acid (THAA), is directly dependent upon the concentration of TTHMs and seasonal temperatures as well, according to an empirical study of three drinking water systems in the United Kingdom which represent a range of source water conditions – "upland surface water, a lowland surface water, and groundwater" with standard treatment mechanisms: aeration, filtration, coagulation, sedimentation, and chlorination (Appendix A.4.1.6)[34].

The other type of temperature-related quality concern is that of chlorine residual decay as water travels to the consumer. The final chlorine concentration was calculated based on the initial concentration of chlorine from dosage at a water treatment plant, the minimum allowable concentration of chlorine, and the chlorine decay constant (Appendix A.4.1.7). The decay constant's relationship with temperature experienced over day-long periods was taken from an experimental study with samples from two water distribution systems in Birmingham, Alabama, by Hua et al.[32] Table 1 shows the equations used to calculate the failure metrics for each component and aspect of water quality, though a more detailed discussion can be found in the Appendix A.4. All equations characterize temperature in terms of degrees Celsius because experiments and rules of thumb from the

literature measured temperature in Celsius. Equations would need to be modified to allow for the use of another unit of temperature.

Table 1 Failure Metric Equations. More detailed equations are shown in Appendix A.4. T= temperature rise above component threshold [ºC] , T_w = water temperature [ºC], *ETTF* (T/T_w) = estimated-time-to-failure after air or water exposure [years], $C(T_w)$ = chemical concentration after water temperature exposure, $MTTF_{T1}$ = historical mean-time-to-failure [years], r_d = lifespan degradation fraction per 10ºC above capacity [no units], t = age of pipe [years], t_w = water age, P_i = internal pit depth [cm], ∂ = pipe wall thickness [cm], C_0 = initial chlorine concentration [mg/L], *TOC* = total organic carbon [mg/L], Cl_2 = chlorine dosage [mg/L], *SUVA* = specific UV absorbance [l/mg*m], *Br* = bromide [mg/L], *ResT* = water age [h], *Season* = season of year, numerically expressed as: 1 for spring, 1.46 for summer, 1.31 for autumn, and 1.01 for winter.

Component/Aspect of Water Quality	***Failure Metrics***		
	ETTF (T or T_w) =	**C(T_w) =**	**Source**
Motors and Electronics	$MTTF_{T1} * (1 - r_d)^{T/10}$		10–12,82–84
PVC Pipes	$MTTF_{T1} * (-0.0123T_w + 1.293)$		16
Iron Pipes	$\frac{t}{0.5t(0.0774 * T_w - 0.1073) + P_i}\delta$		17,144
Chlorine Residual Concentration		$C_0 e^{-\frac{0.0050e^{0.0841Tw}}{C_o}t_w}$	32
TTHM Concentration		$11.967(TOC)^{0.398} * T_w{}^{0.158} * Cl_2{}^{0.702}$	33
THAA Concentration		$0.99(TTHM)^{0.64} * (Cl_2)^{0.15} * SUVA^{0.09} * (Br^- + 0.005)^{-0.12} * (ResT+5)^{0.07} * Season$	34

While temperature contributes to failure, the effects of operating characteristics can also be significant. Table 7 shows the characteristics used to calculate the failure metrics. Examples include the range in water temperature vs. air temperature regression coefficients, $MTTF_{T1}$ and heat dissipation of motors and electronics, and the age of water in pipelines. Estimates of the possible ranges and likely distributions of these characteristics were identified through literature review and were modeled as uniform or lognormal distributions to account for their uncertainty. Uniform distributions were used when there was no information available about the relative likelihood of certain values over others within the reported range. Lognormal distributions were used when there was evidence for a skewed distribution present in real water distribution systems.

Monte Carlo simulations were then performed to calculate and characterize probability distributions of the failure metrics. When performing the calculation of failure metrics for each temperature, the distributions of operational characteristics were sampled 5,000 times. To estimate the variation in failure metrics under different regimes of operating characteristics, the ranges of operational characteristics were divided into lower and upper halves (representing best-a worst- case operating conditions) and Monte Carlo simulations were run over both halves separately. The terms best- and worst- cases within the reported literature are not determined to be optimal and sub-optimal respectively from independent sources. Distributions of "failure metrics" were created for each average maximum summertime temperature and operational scenario by performing Monte Carlo simulations for each 1^{o}C increase in the range 36-44^{o}C, resulting in similar histogram outputs that are just shifted to higher values of failure metrics with increasing temperature. The output failure metric values from the

simulations were fit into probability distribution functions using Anderson Darling Statistics, probability plots, visualization and judgement about distributions that best fit the process underlying the data. [145] Weibull distributions were fitted to the physical components in pumping units and pipes because the form most accurately represents degradation with age and it also produced reasonable fits, as shown in figures S4-S11 .[146] These distributions characterize the histograms of component failures from a population of components overtime, and time represents ages of the components – starting at zero.[146] Motors and PVC pipes were the only components that had outputs that were statistically equal to the Weibull at the 10% significance level. The output distributions for chlorine residual concentration were fitted as exponential distributions based on best fit and the need to be consistent across operating scenarios. The output distributions for DBP concentration were fitted as Gamma distributions based on best fit. Output data and their fit distributions and probability plots are shown in figures S4-S20. Parameters of the distributions and Anderson-Darling Statistics are shown in Tables 9 and 10.

The projection of each component failure and type of water non-compliance was calculated through either hazard functions or integration of the distributions characterized by the failure metrics. The ETTF distributions of physical components were used to calculate components' annual failure rates with the hazard function of the Weibull distribution (units: % failed/year), which characterizes their failure behavior starting in the next instant of their lives, given that they had already lived a certain number of years. [147] The time period of the rate was then converted to be during the next summertime period of its life instead of a full year --as characterized by a period of 270 hours out of the total 8760 hours in a year (Appendix A.4.3.1).[147] It is necessary to calculate failure

rate after the components have operated up until a non-zero age because there would be very little likelihood of their failure given any temperature exposure if they were brand new. The DBP formation distributions were used to calculate the probability that a concentration from the distribution would be above the EPA regulated threshold of 80 µg/L and 60 µg/L for THMs and THAAs respectively[148] for each sampling station in the network for any point in time that the water temperature scenario is experienced, as shown in Appendix A.4.3.2. Similarly, the chlorine residual distributions were used to calculate the probability that a concentration from a sampling station would be undetectable and therefore non-compliant with EPA regulation for any point in time that the water temperature scenario is experienced.[149] A figure of the overall failure metric distribution formation and probability calculation methodology is shown in Figure 2.

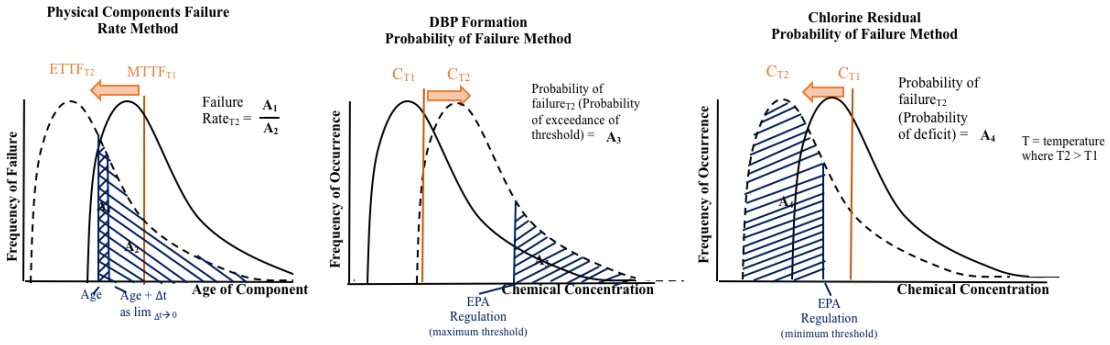

Figure 2 Methods of Projection of Component-level Failure Calculations. For physical components, the ETTF distribution is shifted to the left, which effectively shifts to the left through Monte Carlo analysis under increasing temperature scenarios. For disinfection byproducts, the failure metric, chemical concentration (C) is shifted to the right, and for chlorine residual is shifted to the left. Shaded regions represent integrated areas under the curves that are used to calculate failure rate and probability of failure.

2.2.4 Modeling Failure Cascades to Service Outages

Component probabilities of failure and failure rates were propagated to probabilities of systemic failure using a reliability engineering fault tree analysis to assess

the impact of component hierarchies, points of redundancy, and presence of back-up systems on the likelihood of systemic failure.[147] Water distribution systemic failure is defined as the pressure, flow, or quality falling below specified values at one or more nodes in the network. The three temperature induced pathways to service outages are pumping station outages, pipe breaks, and water quality non-compliance, and are shown as individual fault trees in Figure 3. Pipe breaks and pumping station outages can both directly cause failures in the water distribution system (WDS) and indirectly cause failures in the WDS due to failures of water treatment plants (WTP). The fault trees highlight which component failures lead to service outages. To calculate systemic probabilities of failure, physical components were assumed to have series behavior (meaning that if any one component fails, the sub-system fails), and failure rates were propagated from a component level to a system level according to the system reliability equations that state that individual component or sub-system failure rates are summed in a series system (Appendix A.5).[147] The use of the hazard function to calculate component failure rate allows for the characterization of failure behavior of all components during the same instant in time (when they are all at the certain ages in the scenario). To calculate the probability of water quality non-compliance, the probability of either a non-compliance from TTHM or chlorine residual decay occurring was found through the union of their probabilities (Appendix A.5).[147] Expected occurrences of service outages were calculated from these propagated failure rates and probabilities, along with the estimates of the number of components. Scenarios of numbers of available redundancies of components were explored in the calculation of pumping unit failure rate leading to pumping station failure rate, water treatment or water distribution failure rate, and

ultimately to distribution system failure rate (Tables 5 & 6). These values are relative to the average number of pipes, pumping stations, and quality sampling sites in Phoenix and Las Vegas (Table 6). An important type of redundancy is stored water in tanks throughout the network that can offset the pressure and flow lost during a pipe and pump station break and provide a location for re-dosing the distribution system with chlorine disinfectant. Without estimating water volumes at different times, water distribution tank storage was assumed to be 100% likely to be inadequate for stopping a pumping station outage or pipe break from causing some magnitude of water outage. A more specific representation of the availability of water storage would require knowing temporal and spatial information of the system structure and operations over time.

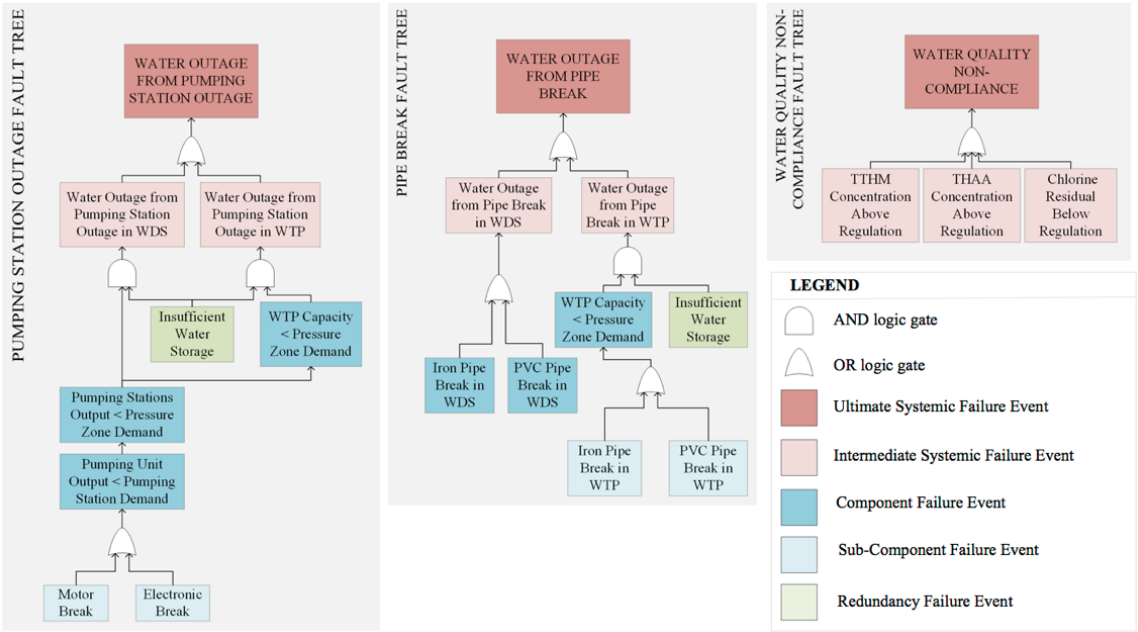

Figure 3 Fault Tree Diagrams showing three trees of systemic failure leading to a possible water service outage: 1) pump station outage, 2) pipe break, and 3) water quality non-compliance. The boxes represent failure events and their different colors represent hierarchies of failure (i.e. sub-component, component, intermediate systemic, ultimate systemic). It was assumed that if one out of two pumping units, pumping stations, and

water treatment plants failed, demand would not adequately be met and failure would propagate as detailed in SI Table S4.

It is possible that these individual pathways to outages could also happen simultaneously—leading to potentially longer and more severe supply and quality outages. For example, low pressures in the system from pipe breaks or pumping station outages not only independently cause quantity supply outages and seepage of contamination, but when coupled with pre-existing quality issues, pose a human health threat.[150] If both physical components and quality fail in the same time frame, the customers could experience longer periods of low pressures and durations of contamination because of the potential difficulty of rerouting and flushing water.[7,150] The probabilities of simultaneous occurrences of different types of water outages were thus also calculated, using standard probability law of simultaneous events for the expected values of service losses from physical component failure rates and water quality non-compliance probabilities (Appendix A.5). Simultaneous probability was estimated through viewing the conditional probability portion of the physical component failure rate as stand-alone under the certain time interval of 270 hours.

2.3 Results

2.3.1 Projected Increase in Component Risk

Over the full range of possible temperatures in all RCPs and including GCM uncertainty, the increase in component probability of failure from 2020 to 2050 ranges from 10-101% for the Phoenix and Las Vegas-characteristic utility. The average probabilities of failure and failure rates (between best- and worst- operating conditions) are the highest for chlorine residual and pumping stations, pumping units, motors and

electronics (within pumping units). This holds across all temperatures, as shown in Figure 4. Detailed results are shown in SI Table S10.

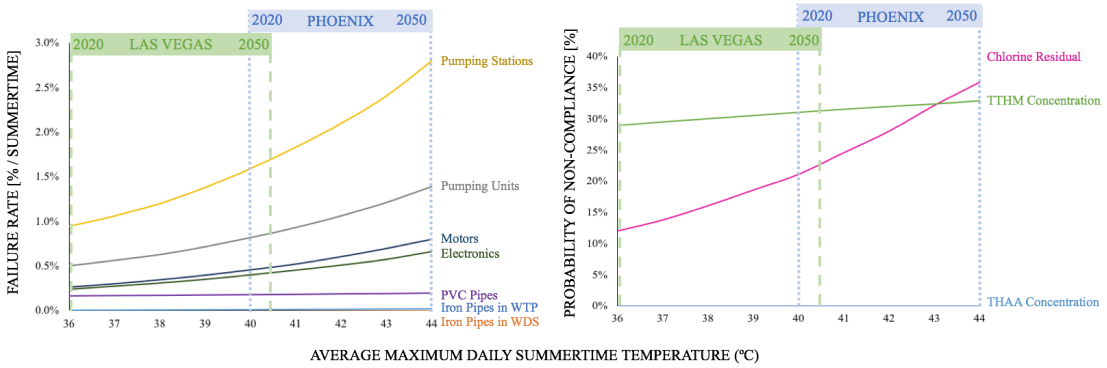

Figure 4 Average Component and Water Quality Projection of Failure: Component failure rates and probabilities of failure are shown as a function of temperature. Temperature ranges for Phoenix and Las Vegas are plotted on the abscissa. Chlorine residual, and pumping units are the components with the highest probability of failure. Pumping stations, inadequate chlorine residual, and motors are projected to have the greatest percent increases in failure.

The components that pose the greatest threat to reliability are those that have both the highest probability or rate of failure and the greatest percent increase in these values between the 2020 and 2050 scenarios. Thus, the most concerning aspect is water quality non-compliances due to the decay of chlorine residual and TTHM production. Chlorine residual decay will have the largest probability of failure and will also have a large percent increase with increasing temperatures. The relationship between inadequate chlorine residual and temperature is exponential, and therefore the percent increase in failure rates between 2020 and 2050 will be 53% ± 36% on average depending on operating conditions. There is no validation available for the historical frequency of non-compliances, though there is evidence that non-compliances have been non-zero. Annual

water quality reports show that out of the last 5 years in the City of Phoenix, there were 4 years where concentrations fell below the minimum residual concentration at least once sometime during the year.[151–155] TTHM production has the second highest probability of failure but has a lower percent increase of 17% ± 10% on average. It is unlikely however that the non-compliance thresholds of the other form of DBP, THAA, will be exceeded under this scenario of operational practices. This is because the calculated concentrations of THAA at different temperatures were only around 25% of the regulated levels. Though the chance of occurrence is high, it should be noted that there are no reports of DBP violations in the past in either city in recent years.[140,156]

The failure processes of second-most concern are those of electronics, motors, pumping units and pumping stations. Pumping station failure rates are projected to have a percent increase of 76% ± 15%, depending on operating conditions. The historical average failure rate of motors across a variety of industries in the US is on average 3-12% every year under current temperature conditions.[10] Extending the 270-hr failure rates to yearly values provides a value to check validity with historical data. The estimates of annual failure rates under all temperature scenarios from 36ºC (8.6% ± 5.6%) to 44ºC (26% ± 16%) fall within this historical range.

Pipe failures show a less significant increase in threat to utility reliability in the future compared to other component failures. Between the two types of degradation, corrosion causes a greater increase in probability of failure than does the degradation of thermoplastic pipes, though probability of failure of PVC pipes from degradation will be consistently greater than probability of failure of iron pipes from corrosion. The corrosion process associated with iron pipes causes the probability of failure to have a percent

increase of 52% ± 12% in the average WDS, and of 76% ± 8% in the average WTP. The PVC pipe failure rate has a percent increase of 10% ± 0.2% in the average WDS. The historical failure rates of polyethylene pipes, pipes with similar degradation rates to PVC pipes, in Las Vegas in 2005 was 2.2% (679 breaks out of 25,000 PE pipes) in the summer and 6.5% over the year (1623 breaks out of 25,000 PE pipes).[6,134,157] The PVC pipe failure rate estimate from the model given the average peak summer temperature of 2005 (44°C)[158] in Las Vegas is 0.2% ± 0.13% in the summer and 6.5% ± 4.3% over the year, so is consistent with historical data. Current annual iron pipe break rates are reported to be 6% on average in the United States.[141] For WTP iron pipes, the estimates of annual failure rates under all temperature scenarios from 36°C (0.32% ± 0.32%) to 44°C (0.84% ± 0.84%) fall below this historical range. Additionally, WDS iron pipe failure rates are negligible under all temperatures (0.005% ± 0.005% per year at 44 °C). Underestimates in modeled versus observed failure rates are in part due to the fact that there are multiple modes of pipe breaks in reality - longitudinal, circumferential, corrosion through hole, split bell/bell shear, and joint failure[129] - that are not accounted for in the model. In the results, the lifetime of the pipe is only modeled from an increase in corrosion and degradation. While the Weibull distribution can predict other forms of aging, it cannot account for the random breaks due to factors like inadequate bedding support and live loads caused by traffic that are independent of climate effects.[129] Moreover, results of pipe failure rates show that utilities should expect the high rate of PVC pipes to slightly increase, but should also anticipate an increase in WTP iron pipe breaks with increases in temperature.

2.3.2 Projected Increase in Service Outages

The probability of service outages increases as a result of propagated component failures. Individual water outages and water quality non-compliances are projected to have a percent increase within the 7-91% range and simultaneous water outages and water quality non-compliances are projected to have a percent increase within the 23-123% range, depending on the type of event and how the system is operated. Figure 5 shows the resulting expected occurrence of water outage and quality failure when all combinations of systemic probability are considered.

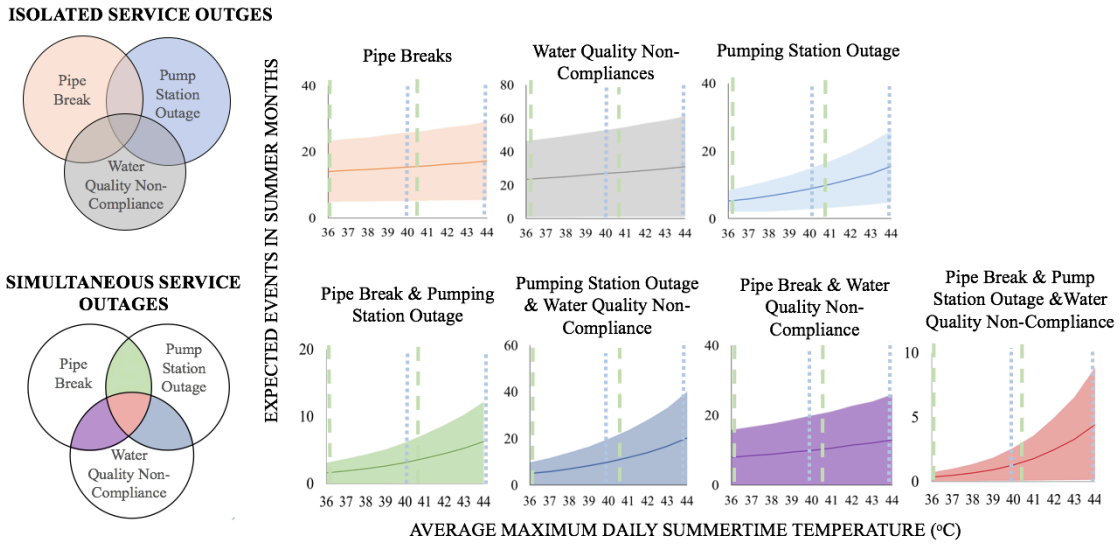

Figure 5 Isolated and Simultaneous Service Outages. Dashed lines represent Las Vegas temperature ranges from 2020 – 2050 while dotted lines represent temperature ranges in Phoenix. Venn diagrams in the first column show which type of systemic failure was analyzed. The ranges of failures due to changing operating conditions are shown in colored bands to characterize opportunities for risk mitigation. All best-case operating conditions together contribute to the lower range of expected number of failures and all worst-case conditions together contribute to the upper range of expected number of failures. The large range shown from the bands suggests that the expected number of failures is sensitive to changes in operating conditions.

Results show that the components that have the highest probability of failure and failure rates and that increase the most in failures - namely water quality non-compliances and pumping station outages - directly contribute to the greatest increase in service outages. The type of isolated water outage that is projected to increase the most is that from pump station failures. The expected number of water outages from pump station failures has a percent increase of 76% ± 15%. The second highest percent increase in water outages is from quality non-compliances of 17% ± 0.4%, and lastly, water outage percent increase from pipe breaks is estimated to be 10% ± 3%. Unfortunately, there was no identified available historical data for how many simultaneous outages currently occur currently for direct comparison.

Because the individual modes of water outage that increase the most are also more likely to happen simultaneously with other types of service outages, the simultaneous service outages that will have the greatest percent increase are those that include pump station outages and water quality non-compliances. This means that though utilities are used to responding to frequent pipe breaks, the increasing simultaneous occurrence of pipe breaks with pumping station outages and/or water quality non-compliances could cause outages that are increasingly difficult to recover from.

2.4 Priority Maintenance Strategies

Instances of water quality non-compliance and pumping station failures are also the failure modes that have the greatest potential for being prevented, and as such should be prioritized for failure prevention. The large sensitivity in failures for all events that are caused by water quality non-compliances and pumping station failures (as shown in the

colored bands in Figure 5) show that changing the operating conditions for these components would be the most effective way to reduce failures. The trends in failure shift from linear to exponential between operating conditions. Specifically, the results show that there is a maximum 79% absolute reduction in probability of inadequate chlorine residual failure when operators inject the higher range of dose of chlorine at the entrance point to the WDS, and make sure to maintain a low water age throughout the system. It should be noted, however, that injecting the maximum chlorine dosage and allowing for more organic carbon causes a 64% absolute increase in probability of non-compliances from TTHM production. Therefore, both residual chlorine and DBP concentrations should be monitored carefully under any chlorine dosing strategy. Pumping station failure rates are also sensitive to operating conditions as there is a maximum 15% absolute reduction in the pumping station failure rate when motors and electronics dissipate low amounts of heat, and there are cooling devices implemented that reduce operating temperatures. The expected value of pipe failures from corrosion and degradation is not very sensitive to changes in characteristics like pipe diameter and normal operating pressure (1% absolute reduction), and thus could not be easily decreased through changing these characteristics.

2.5 Model Uncertainty

Uncertainties associated with water temperature in underground pipes, the time it takes for degradation to occur, availability of water storage, component failures from waterhammer, and projections of future trends in model parameters should all be considered when assessing applicability of the risk projections to a specific water utility. These characteristics were necessarily inserted into the model as assumptions, but their

variability would have an effect on the output probabilities of failure. A 10% change to degradation rates results in a percent change of 0-22% of motor and electronic failures depending on the temperature and operating conditions scenario. Specific values are shown in Appendix A.3. The addition of this variance would make pumping stations more comparable to all other components in terms of percent increase in failure. Assuming that there is a 50% chance (instead of 100% chance) of an inadequate amount of water storage decreases the likelihood of outage from pipe break by 50% and an outage from pumping station failure by 50%. Additionally, if quantitative relationships to describe the effect of waterhammer from one component failure causing another became available, the frequency of pipe and pumping unit failure might increase. Lastly, it is hard to know what the resulting risk will be when normal structural and operational characteristics change over time from urban expansion, transformative designs, etc.

2.6 Discussion

The study is a critical first step towards helping utilities prepare for climate change and extreme events by identifying and characterizing the aspects of the system and chain of failure events most sensitive to heat. The results are modeled to show how discrete increases in temperature increase chances of failure. As framed, the results provide a *directionally reliable estimate* telling us that component and service failures will increase with increasing temperatures. While estimates of risk contain uncertainty, comparisons between the estimated increase in risk for each temperature-sensitive aspect of the system are nevertheless valuable for prioritizing where strategies should be focused.

The results also help identify several critical areas for future research and data collection. This model can be most directly applied to warm regions around the world

with modern centralized water distribution infrastructure, (e.g. the US Sun Belt, Middle East, North Africa, and South Asia), where a large and growing fraction of humanity lives and where a large fraction of global 21st century water infrastructure investment will occur.[159] Even in colder regions the model may be useful, with necessary further work because an increase in annual and summer temperature may benefit the system operation by helping to prevent pipes from freezing and accelerating the rates of beneficial chemical reactions needed for water treatment. [22] Additionally, a network model of components and iterative simulations through time would be beneficial to capture locations of component failures leading to different resulting magnitudes in outages, and the accumulation of degradation overtime by exploring the alternative assumption that shorter time periods (rather than the 3x3 duration) cause the reported degradation rates. More modeling work, combined with city-specific and component-specific engineering data quantifying heat-induced failure rates is necessary to more precisely quantify heat-induced service failure risk in particular WDSs. An analysis of relative costs of different suites of preparative actions and their consequences would also be valuable, but this requires data on preventative maintenance, repair, response, lost consumer use, and capital improvement costs for each type of failure. Furthermore, the methods of projecting risks of future external threats could be expanded to include other threats, including flooding and wildfires. It could also be used for the projection of risk in other infrastructure systems like transportation and electricity, which also have temperature and other climate change event sensitivities.[124,160]

Considering the possibility of other increasingly frequent extreme weather events, utilities should recognize that improved response times coupled with the capacity

for agile and flexible resources use (including money and equipment) will be critical. The water community should also work to phase out vulnerabilities by improving system design (e.g. increasing pumping unit insulation capacity, reducing water temperature in cooling towers, or adopting "smart" booster chlorination and network sensors[6,161]), and by improving training and institutional response capacity. Ultimately, in times when maintenance and response actions are severely constrained by budgets, it is of the utmost importance to identify and prioritize strategies by utilizing information on likely mechanisms of failure.

2.7 Acknowledgements

This material is based upon work supported by the National Science Foundation under Grant No. 1360509.

CHAPTER 3

ANTICIPATING WATER DISTRIBUTION LOSSES FROM CLIMATE CHANGE

3.1 Introduction

With increasing evidence of rapid changes in climate and resulting extreme events, infrastructure – the physical systems and managing institutions that deliver critical resources and protect us from hazards – must continue to perform reliably. Yet the design of infrastructure is often made assuming that past climatic and hydrological conditions will persist into the long term, [119] and the rules and codes by which they are designed do not change quickly.[2] The confluence of a rapidly changing climate and slow changing infrastructure, designed assuming stationarity of variability, results in a potential crisis.[119,162] Without strategic investment, increasing hardware failures and resulting service outages can occur without the means to properly respond. Serious questions remain as to whether our currently deployed infrastructure can remain functional as climate changes and during extreme events, the latter when people may need critical services the most.

In arid and semi-arid regions with hot temperatures, potable water delivery is an infrastructure system of particular concern. Water is a critical resource, not just for drinking, but often for industries that drive economies (such as manufacturing and agriculture), and even for power.[25,78–81] This is particularly true in the semiarid Southwest US where scarce water resources are transported long distances, populations have and are forecasted to grow significantly, agriculture remains a major activity, and thermoelectric power generation continues to supply a large fraction of energy.[163] If there is a continuation of the current path of global emissions, it is projected to lead to around 9-

10°F increase in average temp in the Southwest by the end of the century relative to the late part of the last century (RCP 8.5).[164] If total radiative forcing is instead stabilized shortly after 2100 without overshooting the long-run radiative forcing target level, there is projected to be an average 5-6°F increase (RCP 4.5).[164] There has been a great deal of work to understand how the accessibility of water resources might change as populations and climate change.[122] However, there remains a dearth of knowledge of how water infrastructure – in particular distribution – might perform under increasing local temperatures and what that means for water delivery reliability. It was found in a previous study that increasing temperatures affect the reliable operation of hardware within water infrastructure, and the failure of one or more pieces of hardware could lead to cascading effects.[46] Temperature affects component wear that results in the potential for overheating of motors [10,12,82,165] and electronics [83,84] used in pumping units. Temperature also affects chemical reaction rates that lead to the potential for increased pipe degradation and corrosion,[16,17] and water quality non-compliance. [32–34]

Modeling impacts to water delivery infrastructure systems from temperature change is a promising way to help identify and prioritize adaptation strategies. An important reliability metric is the loss of service to consumers. The guidelines for federally required water utility reliability and resilience assessments call for an estimation of both the duration and severity of service outage that could result from a hazard.[5] The severity of outages, or the number of consumers who experience outage, depend on mechanisms causing hardware component failures, the location of hardware failures within the spatial topology of the distribution network, and the timing of flows of water into and within the network.[7] The duration of outage depends on the repair times of the failed hardware.[125]

While models of either climate impacts to water infrastructure or water reliability have included a selection of these processes including climate stress to hardware or demand, [2,6,44,46,166–168] vulnerability of different types of components,[46,68,72,74,169–171] relative vulnerability of components of the same type, [63,69,172] historical hardware failure rates, [46,51,73,74,77,169,170,172–174,54,55,57,63,67,69,71,72] the use of flow-based networks,[62,63,174,69,72–74,76,77,170,172] changing demands, [76] and repair rates, [51,67,68,72,74,77,169,171,172,174] these elements are not typically incorporated into one model for anticipating service outages from the effects of heat, or any other hazard. The US EPA has developed a software tool that can be used to bring much of these pieces of information together, named WNTR, but the user must input component failure and repair probability information, and it has not yet been designed for simulating the cumulative impacts of long-term exposure.[50]

Understanding hardware exposure to changing temperatures and resulting dynamic hardware and service losses is central to understanding the challenge of reliable water delivery under climate change in semi-arid regions like the Southwest. Yet, there remains insufficient coordinated methods or models to fully explore these challenges considering ultimate outcomes and the following questions remain unaddressed: (1) What are the cumulative impacts of heat on water components? (2) What are the resulting impacts of increased component failures on service losses? and (3) What are some effective strategies for reducing these additional outages from climate change? To answer these questions, we develop a methodology and model to assess water infrastructure performance and reliability under changing temperatures. We call this model Perses (after the Greek god of destruction), with the hope that the insight generated will help mitigate services losses into the future.

3.2 Methodology

Perses is designed to simulate the reliability of water distributions systems into the future under long-term exposure to different possible temperature projections. Multiple temperature scenarios are considered including a baseline (where historical temperatures persist, i.e., no climate change) and futures with changing temperatures based on the Global Circulation Model (GCM) ensembles. A Python wrapper is used to stochastically fail components in each time step based on their temperature exposure and their individual robustness, and then implement the failed state of components in EPANET to track the consequential service outages, considering daily demand patterns and hydraulic flows. The program tracks the time of failed components and repairs according to given repair times. The results show a comparison of the increases in pipe and pump failures and how water outages increase under different temperature change scenarios. Two case studies are used to evaluate the effects of temperature on component failures and network service outages under extreme heat scenarios similar to those in the U.S. Southwest. The model is then used to explore adaptation strategies relating to probability of failure and repair times. An overview of the process is shown in Appendix B.1.

3.2.1 Developing temperature profile inputs

A set of six daily temperature profiles are used as alternative inputs to the model to anticipate possible futures given three types of uncertainty. There is uncertainty about the future emissions profile (i.e. different RCP types), the variables and interactions included in the climate models, and the initial conditions within the climate models.[175] Due to the uncertainty in the emissions profile, scenarios of possible daily maximum

temperature futures are characterized by a continuation of historical temperatures (baseline scenario) [121] and ensembles of daily RCP 4.5 and RCP 8.5 scenarios from the BCCAv2-CMIP5 projection. RCP 4.5 is used as a reasonable minimum bounding case, representing a modest instead of aggressive reduction in emissions by the end of the century. RCP 8.5 assumes a continuation of the increases in emissions. Due to the uncertainty in the variables, interactions, and initial conditions in the climate models of dynamics within each scenario, temperature profiles with minimums, averages, and maximum temperatures of all runs in all climate models within each RCP type were also used.

The increment of temperature inputs for all profiles is daily; therefore, the same temperature is used for each 2-hour timestep within a day in the simulation. Maximum daily temperatures are chosen to represent daily temperature for both baseline and future projections. Downscaling and projecting hourly temperature variation within a day could be used to get a more realistic characterization of the magnitude of exposure values and failures. Using maximum daily temperatures produces a consistent overestimation of exposure values and failures across scenarios. It is anticipated that the more realistic estimation would lead to the same relative changes between baseline and future scenarios.

3.2.2 Modeling Component Probability of Failure

The characterization of the probability of failure of pumps and pipes is used to determine whether components have failed in each time step of the simulation. Probability distribution functions (PDFs) of failure are generated using the procedure

developed in Bondank et al[46] by 1) providing variable inputs into temperature-degradation-failure equations[10,11,84,144,12,16,17,32–34,82,83] and 2) running Monte Carlo simulations holding each temperature constant.[46] Possible future temperature scenarios and ranges of operational parameters were used as inputs to these equations. For the analysis of the effects of climate change, mid-level ranges of reported operational parameters were used. The complete list of ranges of input parameters characterizing operating conditions can be found in Bondank et al 2018.[46] (Table 7). A separate PDF was generated for each daily temperature within the range of daily temperatures from the projections (0-57^{o}C). To evaluate the cumulative probability of failure at each time step, the PDFs are converted into cumulative distribution functions (CDFs) by integrating over each time step as shown in Figure 6. It can take many years of degradation accumulation for there to be one hundred percent chance of failure, especially in iron pipes under low temperature exposures.

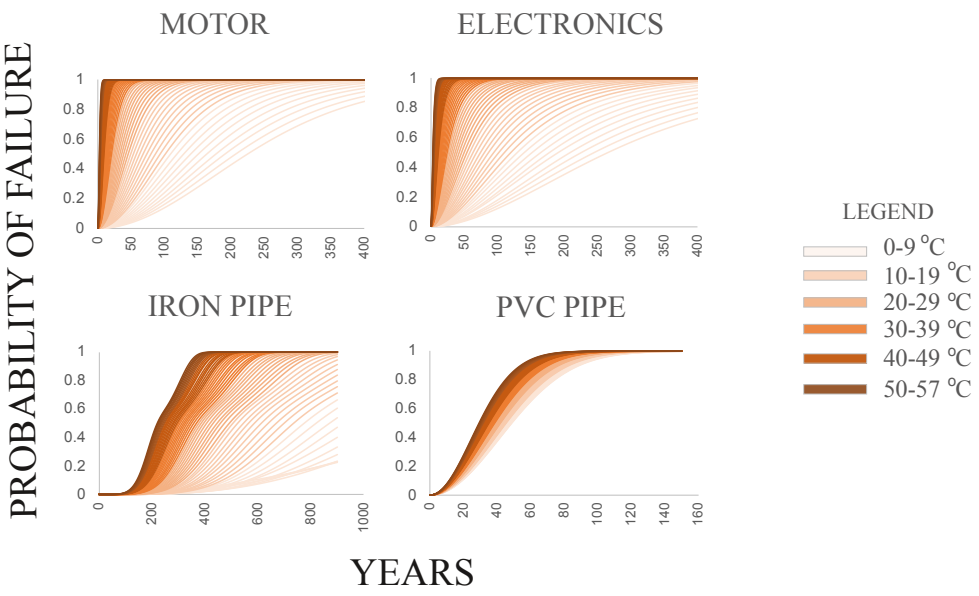

Figure 6 Temperature-Failure CDFs. CDFs are shaded in light orange to dark orange as the corresponding temperatures increase.

Each temperature-failure CDF represents the probability of failure of a component overtime given that it has been exposed to one specific temperature. In reality, however, components are exposed to multiple temperatures over their lifetimes. Therefore, to determine probability of failure of components, the temporal aspect of temperature exposure is considered. "Exposure" represents the temperature a component is exposed to, weighted by the amount of time the component is exposed. To calculate exposure values, duration and magnitude are multiplied to get units of degree-unit time ($℃ \cdot \Delta t$) as shown in Equation 1.

$$Exposure\ [℃ \cdot \Delta t] = magnitude[℃] \cdot duration[\Delta t] \quad (1)$$

This formulation of exposure assumes that magnitude and duration both have linear relationships with exposure. If there are any interactions between duration and magnitude, it may be the case that duration and magnitude have a non-linear relationship

with exposure, however. For example, the magnitude of exposure might increase as duration increases due to a feedback of additional amounts of heat generated from component degradation overtime. Without data available to analyze the exact nature of the relationship of exposure and its factors, it is uncertain as to which relationship is most accurate. Future studies could explore the results of employing an assumption of non-linear relationships between magnitude and duration of exposure.

A probability distribution of failure was generated for each component to reflect the effects of different exposure values over its lifespan. To generate the exposure-failure CDFs, probabilities from the temperature-failure CDFs with different durations and magnitudes of temperatures but with the same exposure values, were binned together and combined. Probability values from temperature-failure CDFs for the full range of historical and projected maximum daily temperatures in the City of Phoenix from 1950-2099 (0-57℃) were used to generate probabilities within the exposure bins. To obtain a probability value for exposure values that did not reflect other forms of aging characterized by the Weibull probability distribution, probability values within each exposure bin were combined through averaging. The other mechanisms of aging create a difference of probability of failure within the same exposure bins. For example, a PVC pipe with a 1,000 ℃ · yr exposure value under the combination of 20℃ for 50 years has a higher probability of failure (0.6) than the combination 50℃ for 20 years (0.2). The output temperature and exposed CDFs are shown in Figure 7. They represent probability of failure for each type of component given a certain levels of exposure.

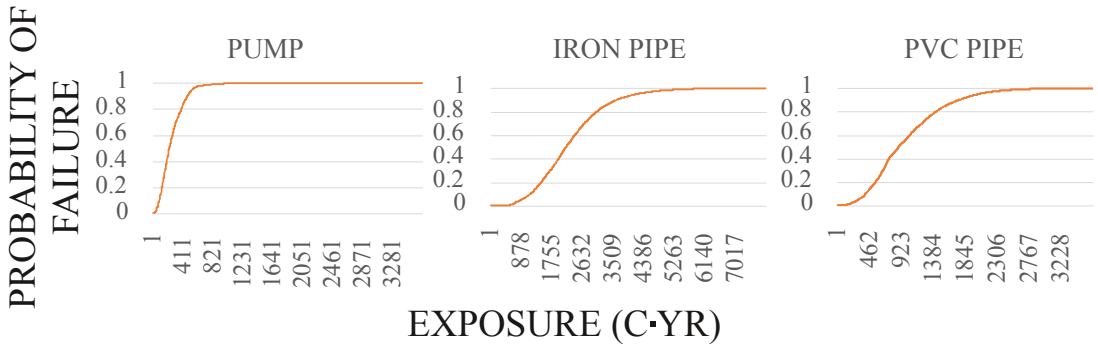

Figure 7 Exposure CDFs

3.2.3 Modeling Component States

In each time step, the simulation tracks the dynamic state of components relating to exposure, probability of failure, individual robustness, and operational state (failed or functional). The duration of each time step is set to the lowest increment of time taken to repair components, which is 2 hours for pumps. This time step ensures that pumps and pipes are replaced in the system when repairs are completed. The failure state of a component in any given time step is based on the probability of failure given its current exposure state at the component's age, its level of individual robustness, and whether or not the repair time has passed if it had already failed in the previous time step. Component ages are tracked overtime by the simulation as they fail and become repaired. Once failed, the component will be assigned a duration for that failure, which models the time to repair the outage. When they are repaired, their age returns to zero. This assumes that repairs restore the component functionality to new.

The components' cumulative exposure is tracked in each time step to evaluate its probability of failure using the exposure CDF curves. To do this, temperature profiles are used to determine the temperature experienced in each time step. The temperature values

of the time step are multiplied by the duration of the time step to get the current exposure value (Equation 1). The exposure values are iteratively summed together to get a current overall exposure value. This follows the mathematical representation of degradation of components as a function of the cumulative exposure, Equation 2, that was introduced in Bondank et al 2018[46]:

$$r_d = \int_{t_1}^{t_2} \alpha \cdot {T_e}^{\beta}\, dt \qquad (2)$$

Where r_d is rate of degradation from exposure [lifespan/^{o}C], T_e is temperature experienced by the hardware [^{o}C], and α and β are the linear and exponential parameters of degradation.

The determination of whether a component has failed or not in a certain time step is then performed by comparing the probability of failure of the component population (i.e. all pumps or all PVC pipes) at the current exposure state to the component's individual "robustness factor", which is a random value from a uniform distribution ranging from 0 to 1 representing the component's robustness or survivability compared to the rest of its population. Heterogeneities in components of the same type could arise from manufacturing defects or inconsistent treatment in operation across components. A uniform distribution is used because it is assumed that these heterogeneities cause random increases in the chance of individual component failure in each time step. The process of comparison of population probability of failure and individual robustness factors is shown in Figure 8. A component is determined to be in a failed state when its probability of failure is higher than its robustness factor. Robust components need more exposure to fail and less robust components need less exposure to fail.

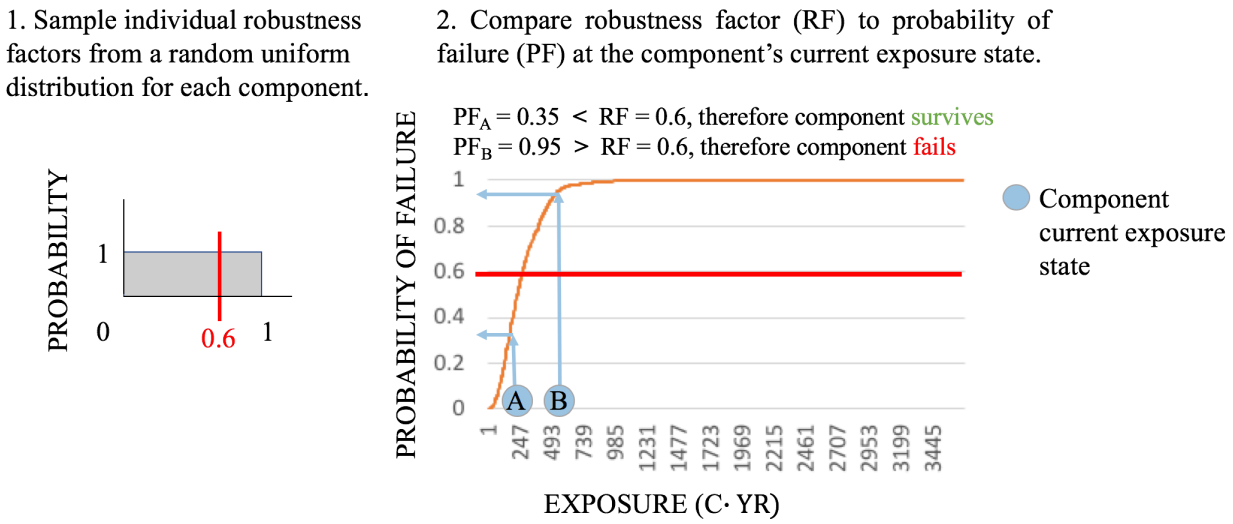

Figure 8 Rules of Component Failure. Exposure CDF and robustness factors are compared to determine whether or not a component has failed in a certain time step. Determination for two example time steps, A and B are shown.

3.2.4 Modeling Service Outages

The component failure analysis is input into the hydraulic solver, EPANET, to estimate service outages in each time step. Service outages are defined in this study as time steps in which a demand node pressure drops within 20-40 psi (service loss outage) or below 20 psi (vacuum pressure outage).[7] Multiple service outages can occur in one time step if multiple demand nodes are below pressure thresholds. EPANET is used as the hydraulic solver because it is authoritative and standard in that it 1) is the model of record for the U.S. EPA, and 2) because it is widely used by both academics and industry professionals. EPANET's algorithm is "demand-driven" and therefore outages are represented in terms of pressure losses. An EPANET network file is uploaded into Perses to generate component attributes automatically.

When components are failed, they are shut-off by changing their attributes within EPANET. Pipe statuses are set to "closed" to represent the response team isolating the

break using valves. Emitters are added to one node of the broken pipes to model water losses before operators are able to shut off valves to isolate the break. The magnitude of loss is modeled to be similar to what is experienced in fire-flow using a coefficient of 100.[7] Pumps are turned off by setting their status to "closed" as well. The change in status of components causes consequential pressure outages in nodes. The number of nodes that have outages is counted in each time step. Before counting service outages, however, 48 hours is run in the beginning of the simulation to obtain the correct output once the system equilibrates. EPANET allows for demands to vary by the hour according to daily demand patterns. Since the demand patterns are in 1-hour increments, the hydraulic time steps are also in 1-hour increments. The general simulation approach is shown in SI Figure 2.

3.3 Case Studies

Two case studies are used to evaluate the effects of temperature on component failures and network service losses under extreme heat scenarios like those in the U.S. Southwest. A full set of network data including spatial topography of components, pump and demand curves, nodal elevations, tank sizes, and pipe diameters for a Southwestern city would be ideal for this study, but were not available. A system based on the number of components in the City of Phoenix, Arizona network without any topological or water flow information is first used for a component failure analysis. We call this the Large-Scale System. The Large-scale System has populations of components representative of those in the City of Phoenix: 113 pumps and 61,500 pipes (7,000 total miles of pipe with 600 foot segments). [176,177] Half of the pipes are modeled as iron and the other half PVC.

To perform an analysis of service losses, a widely available network from North Marin County in California is used. The network, while small relative to the City of Phoenix, provides an opportunity to assess the effects of rising temperatures on a realistic system, where service losses can be estimated. We call this network the Realistic Network and the layout is shown in Figure 9. The Realistic Network has been widely used for research purposes and is provided in the EPANET user manual.[178–181] The network consists of 91 nodes, 115 pipes (of which we estimate 17 are PVC and 98 are iron from the roughness factors), 3 storage tanks, 2 reservoirs, and 2 pumps and serves a suburban population of around 53,000 people.[178] Nodal demands range from 0.87 to 1,856 gallons per minute. Details about the model including the pump head curves and controls are shown in Appendix B.3.1.

The case studies are also characterized by the component ages and component repair times. The ages of pipes and pumps in Phoenix are unknown, and as such it is assumed that the Large-Scale and Realistic systems were built in 1950, corresponding to the start of significant population growth and provision of new infrastructure in the City of Phoenix. [182] The Perses simulation thus begins with new components in 1950 for both the Realistic and Large-scale network. Repair times are set at 88 hours for pipes, 5 hours for motors, and 4 hours for electronics, consistent with the mean-time-to-repairs reported in literature for US water systems.[183] A sensitivity assessment is developed using varying repair times. The time associated with waiting for parts is not included in these mean repair times, but could be significant.

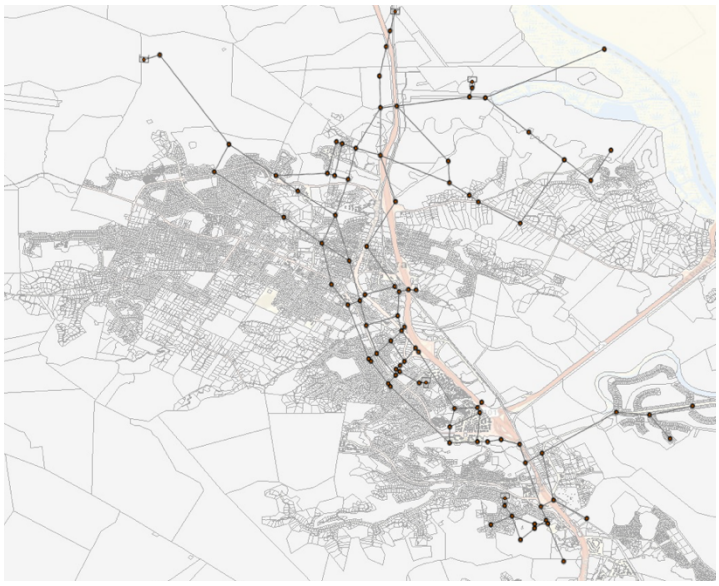

Figure 9 North Marin Water Distribution Network. Network is overlaid on a street and parcel map.

For both case studies, the current and projected future temperature profiles for the City of Phoenix, Arizona, are used. Projections have 1/8-degree spatial resolution and were averaged spatially within the region bounded by latitudes 33.3125 to 33.8125 and longitudes -122.1875 to -111.9375 (2414 km^2 that represent the City of Phoenix). There are 19 different climate models and 42 total runs in the RCP 4.5 emission scenario and 20 climate models with 41 total runs in the RCP 8.5 emissions scenario. Figure 10 shows plots of the different temperature profiles over time. The range of the historical data (grey error band) represents the daily temperature extremes within the year between the maximum daily temperatures of the hottest and coolest days within each year. Average RCP projections represent the average temperature estimates from all the runs of all the climate models for all the days in each year. The range of the future projections (orange and red error bands) also represent the maximum daily temperatures of the hottest and coolest days of each year, but in addition they are estimated from the runs of climate

models which have either the hottest or coolest estimates of all of the runs of climate models within each RCP scenario. At the daily scale at which the temperature data are dynamically used in the model, there are no extremes in regards to durations of time (i.e. years), the only uncertainty involved is in regards to the estimates of runs of climate models for each day. The averages of the scenarios show a clear increase in temperatures into the future with RCP 4.5 average rising from roughly 30 to 32.5°C and RCP 8.5 average to 35.5°C by end-of-century. The projections for the City of Phoenix are therefore cooler than the overall projections for the entire Southwest.

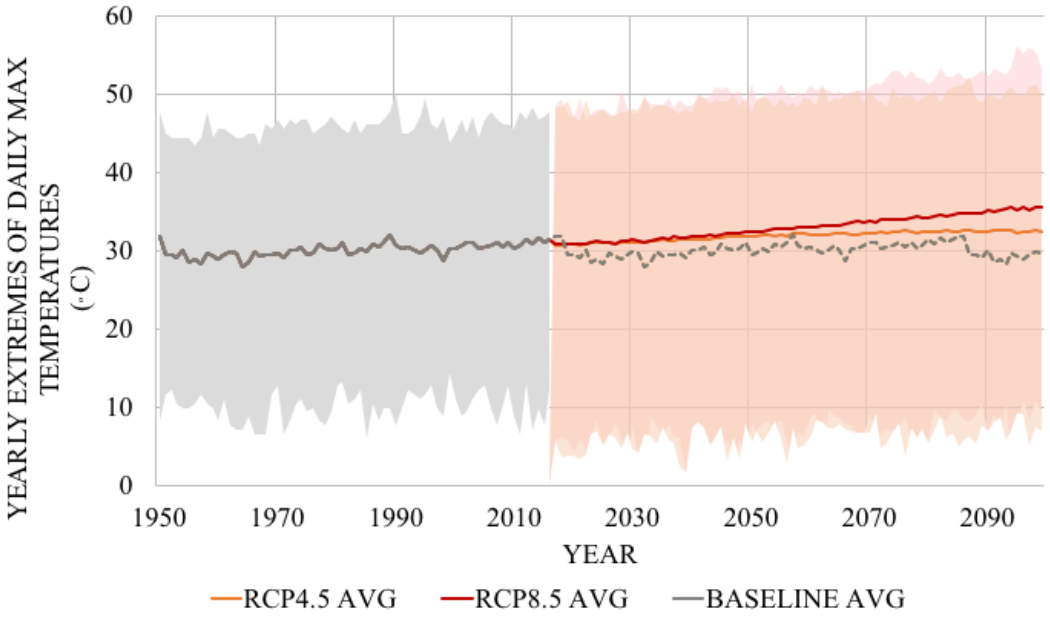

Figure 10 Historical and Future Projections of Maximum Daily Temperatures in the City of Phoenix. The range of projection scenarios is 0.72 – 56.2°C.

The averages of the climate models and runs of each emissions scenario (RCP 4.5 and 8.5) seem to be more representative of climate dynamics than the extreme minimum and maximum climate model runs are. The extremes show much more variance of

variables, interactions and initial conditions from baseline projections than the averages do. Therefore, we anticipate the results from average projections to be realized but also present the results from the extremes to show the bounding cases of possibility as modeled in the set of GCMs.

3.4 Results

3.4.1 Long-term Increases in Failures in the Large-scale System

In the Large-scale system, future PVC pipe, pump, and iron failures exceed estimates for the baseline case. Figure 11 shows the projections of cumulative component failure over time under the minimum, average, and maximum climate projection scenarios as compared to the baseline. By 2099, the anticipated increase in failures from the average temperature profiles of the RCP 4.5 and 8.5 scenarios are 5-8% more pump failures, 13-15% more iron pipe failures, and 5-7% more PVC pipe failures above the baseline scenario. The bounds of possibility from the extremes of weather pattern assumptions within RCP 4.5 -8.5 are at maximum a 16-18% increase in pump failures, 18-21% increase in PVC pipe failures, and 50% increase in iron pipe failures. The minimum bound of possibility of RCP 4.5-8.5 is a 7-9% decrease in pump failures, 8-10% decrease in PVC pipe failures, and a 20-23% decrease in iron pipe failures.

Components have different responses to cumulative heat exposure. Pumps and PVC pipes have a similar linear profile of yearly failure rates. Iron pipes experience exponential failure rates because it increases the *rate* of corrosion and therefore the rate of degradation of lifespan over time and not only the instantaneous *percent* of degradation of lifespan like is the case with pumps and PVC pipes. [17] Thus the impacts of temperature accumulate overtime for iron pipes. A result of this difference in behavior of

failure is that the first iron pipe to fail after the system is built is in 1977 whereas the first pumps and PVC pipes fail right away, in year 1951. Though the trends of yearly failure are different between pumps and PVC pipes, and iron pipes, all components reach 100% of baseline temperatures at the same time – in the average RCPs its 99.7% through the simulation and in maximum RCPs its 98.9% through the simulation. After these times, the exceedance of baseline failures of iron pipes increases above that of pumps and PVC pipes.

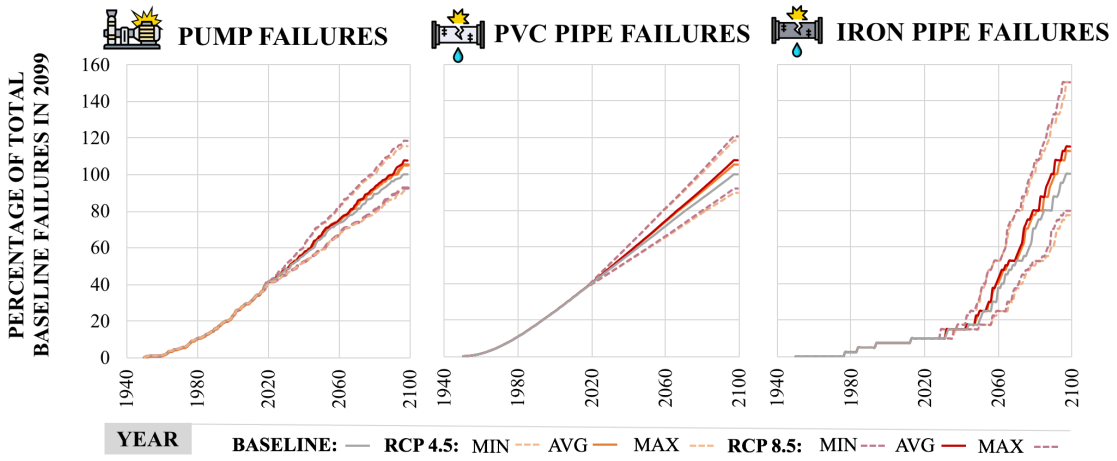

Figure 11 Cumulative Percentage of Baseline Component Failures in Large-scale System.

The exceedance of baseline failures in the average RCP scenarios reveals potential challenges for budgeting, management, and maintenance. If emissions and climate model scenarios at or above the average are realized and budgets do not adjust to include the increased need for preventative or corrective maintenance, either additional service losses will be realized or a last minute reshuffling of municipal funds may occur that could result in lingering overall deficit.[184] Because budgets are generated based on the past years' expenditures and new projects, there is no formal process to include projections of increased failure rates.[185] If utilities continue with this process of decision

making, they will have to see the pattern in the increased failures before they can budget in adaptation options. A survey of water utilities reveals that action is taken once extremes have been experienced.[6] The timing of the occurrence of increased failures could be important for whether utilities sense the increased rates of failure and are able to incorporate the increase into their future budgets. In the case of iron pipes, the large threshold of exposure needed to cause failure could cause situational surprise[186] by the end of the century when suddenly iron pipes fail before their expected lifespans. Because the cumulative failure curves for pump failures and PVC pipes are linear, if monitoring failure rates, utilities will know soon that pumps and PVC are failing more frequently and may be able to incorporate it into future budgets. Some utilities in the Southwest already report that they experience an increase in PVC and pump failure with extreme heat and therefore expect further increases from climate change.[6]

Historical data show that the model estimates of component failures under baseline temperature conditions are reasonable and thus serve as a source of validation for the model. The historical average failure rate of motors across a variety of industries in the US is on average 3-12% every year under current temperature conditions.[10] The average annual pump failure rate from the large-scale model under baseline conditions is 1.69% per year, which is near the historical range. The historical failure rates of polyethylene pipes, pipes with similar degradation rates to PVC pipes, in Las Vegas in 2005 was 6.5% over the year.[6,134,157] The average failure rate of PVC pipe from the large-scale model under baseline conditions is 1.72%. Furthermore, current annual iron pipe break rates are reported to be 6% on average in the United States.[141] The average failure rate of iron pipe from the large-scale model under baseline conditions is 0.001%. The discrepancy in

historical pipe break data and the modeled annual pipe failure rates shows that temperature related mechanisms of failure do not contribute as much to failures relative to other mechanisms of pipe failure—like freezing conditions, inadequate bedding support, or live loads caused by traffic, which are not modeled in this study. [129]

3.4.2 Long-term Increases in Failures in a Realistic Network

In the Realistic network, future PVC pipe and pump failures exceed estimates for the baseline case, and the criticality of infrastructure components becomes apparent. Figure 12 shows the projections of cumulative component failure overtime under the minimum, average, and maximum climate projection scenarios as compared to the baseline. By 2099, there is projected to be no increase in iron pipe and pump failures but 5% more PVC pipe failures than the baseline. The bounds of possibility from the extremes of weather pattern assumptions within RCP 4.5 -8.5 are at maximum a 25% increase in pump failures and a 15-16% increase in PVC pipe failures. The minimum bound of possibility of RCP 4.5-8.5 is a 25% decrease in pump failures, and a 10-13% decrease in PVC pipe failures.

In the Realistic Network, there is a smaller population of components than in the Large-scale System and therefore, there are fewer overall component failures. Because of this, the times between component failures are longer and it produces step-wise instead of smooth cumulative failure curves. In the case of iron pipes, the reason there were no failures at all was because the low percentages of failure of components relative to the total number of iron pipes in the Large-Scale System, 0.1-0.15%, translated to only 0.1 failure out of 98 iron pipes in the Realistic Network. Smaller utilities may not experience the increases in failure because they have fewer assets and therefore chances of failure.

Underlying trends of increases in component failure should therefore be interpreted from the Large-scale System. Additionally, though there are no projected increases in pump failures, the failures happen sooner under average and maximum projections than under baseline conditions. This could also be problematic because if failures happen sooner than expected under baseline conditions, they might not be covered in the budget in the years that the failures occur.

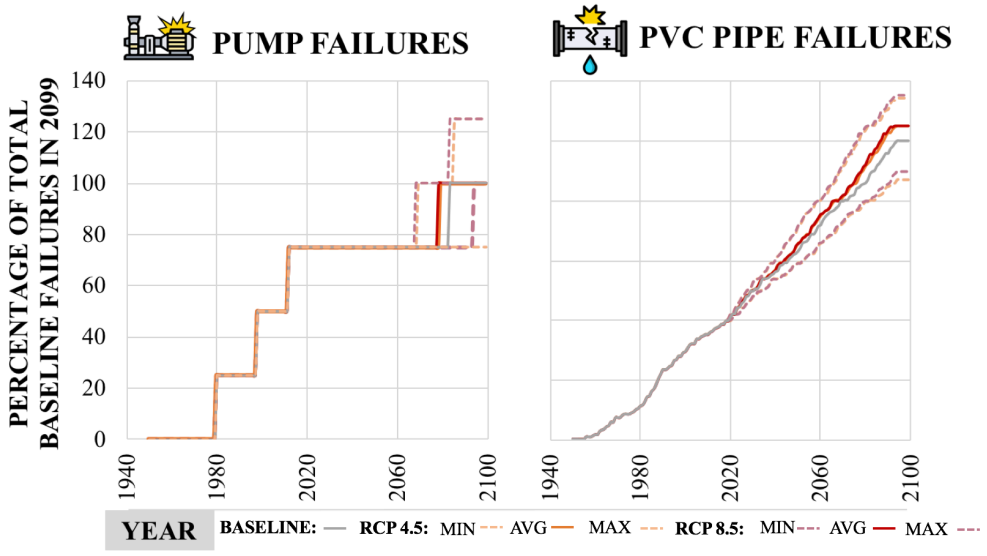

Figure 12 Cumulative Percentage of Baseline Component Failures in Realistic Network

Service outages (20-40 psi) that constitute inadequate pressure for domestic and commercial use are projected to increase by 3% above the baseline by 2099. Vacuum pressure service outages (below 20 psi) constituting inadequate pressure levels for fire-flow and vacuum pressure, are projected to also increase by 3% above baseline projections, as shown in Figure 13. The bounds of possibility from the extremes of weather pattern assumptions within RCP 4.5 - 8.5 are at maximum a 26-27% increase in service outages and a 27% increase in vacuum pressure service outages. The minimum bound of possibility of RCP 4.5-8.5 is a 4-5% decrease in service losses, and a 3-4%

decrease in vacuum pressure service losses. Similar to preventative maintenance and capital improvement budgets, if repair/response budgets do not have enough room to allow for the increase in service outages and find themselves unable to adequately respond, outages could have greater durations, thereby causing greater loss to human health and economic opportunity. Furthermore, if budgets neglect proper corrective maintenance, it could further increase components' chances of failure into the future.[146] This could cause the system to move into a state of deterioration that would be increasingly challenging to manage.[146] Unfortunately, there are no data available on historical instances of water outages to validate findings at the service loss level. However, since we have validated component failures, the outages should be reasonable since they are calculated using a standardly- used hydraulic solver.

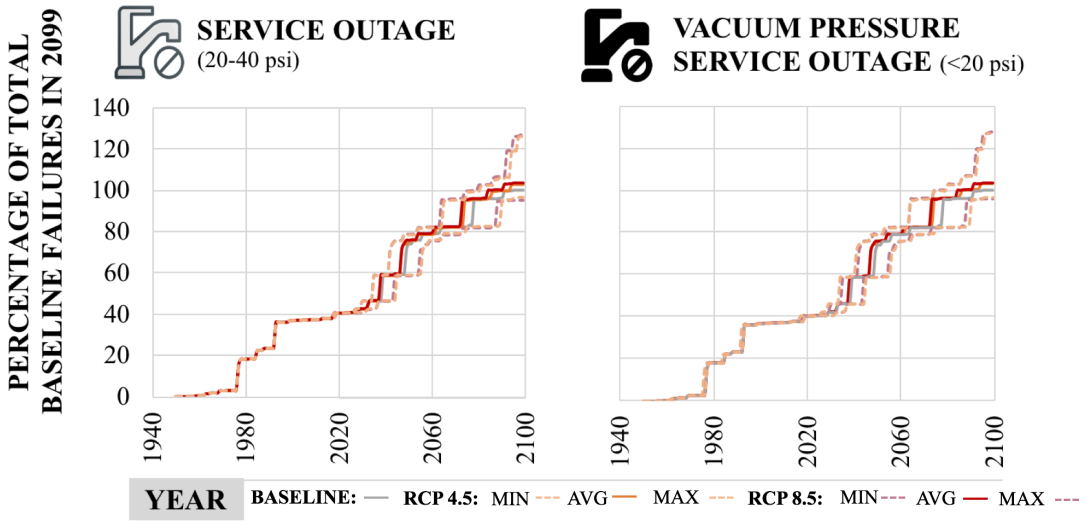

Figure 13 Cumulative Percentage of Baseline Service Losses from Component Failures in Realistic Network

Service outages are non-linear and emergent outcomes of the complex interactions between the component failures and the topology and flows within the network. This is evidenced by the fact that the number of service losses in the network

from component failures is not proportional to the number of component failures. For example, in year 33 of the simulation, 2 pipes failed and there were a resulting 6,511 service losses, but in the year 50, 4 pipes failed and there were only 264 resulting service losses. The nonlinearity is a driver behind the aspect of components called "criticality" that is referenced in network science studies.[187] Like other water reliability studies using simulation to find outages, we refer to critical components as ones that cause outages when failed.[63,69] From evaluating where those components are located within the network we find results consistent with studies that rely on topology of the network -- the critical components are ones which serve as the sole connection between demand nodes and the source of water, whether it be the reservoir or from the rest of the network.[58,59,61,183,188]

There are levels of criticality of components based on how many demand nodes the connecting component serves. Figure 14 shows the levels of criticality of components within the network from levels 1-5, with level one being the most critical. Criticality levels are characterized by the number of outages which occur when they fail. Components that are necessary for the initial conveyance of water out of the reservoir sources are most critical, especially those leading directly from reservoir 4 -- pipes 60, 329, pump 335. When they fail, the greatest number of outages occur (>12,000 outages) since much of the network are reliant upon the sources. Pipes and the pump leading from reservoir 5 (pump 10 and pipe 101) are less critical, however. A reason for this might be that reservoir 5 has a lower elevation and therefore provides less pressure for the network than does reservoir 4. The second most critical components are pipes that serve as the only connections between sections of the network (Pipe 238, 240, 241, and 243). They cause 2,000-12,000 outages when they fail. The third-most critical are the pipes that

connect small portions of the network to the rest of the network (Pipes 247, 237, 249, and 273). They cause 400-2,000 outages when they fail. Pipes that lead away from the network in a dendritic fashion to isolated nodes are fourth-most critical for individual nodes (Pipes 137, 149, 151, 180, 181, 185, 193, 233, 251, 257, 263, 277, and 291). They cause 1-400 outages when they fail. Components in level 5 criticality cause no outages when they fail. Overall, pumps are less critical than pipes. A failure of pump 10 has little effect (0-6 outages) and pump 335 causes 30-379 outages.. Criticality is the reason that the percent increases in outages from the maximum projection are greater that the decreases from the minimum projection. There was more opportunity for the critical component, pipe 329, to fail and cause many more outages.

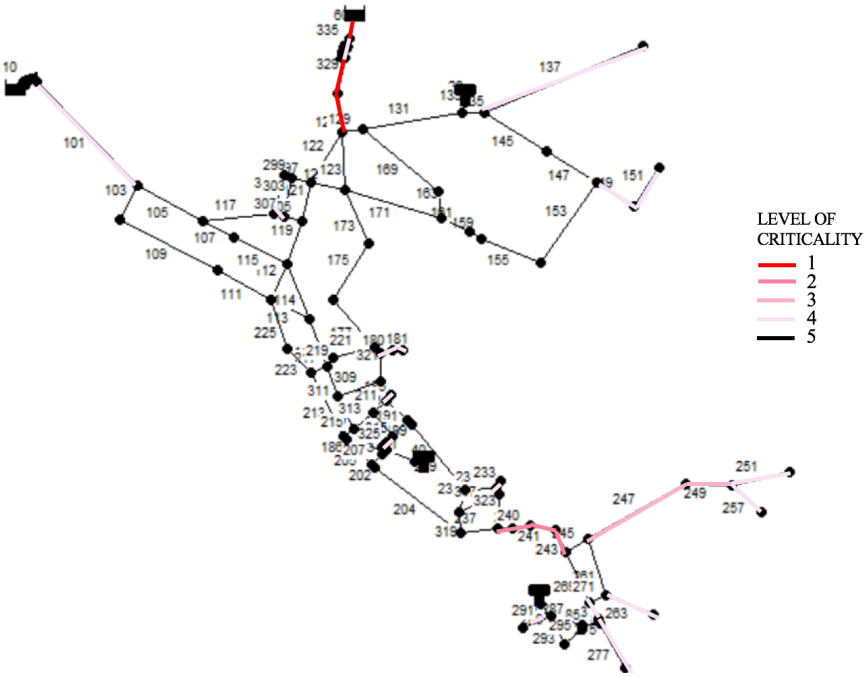

Figure 14 Criticality of Components in North Marin

Components that are individually non-critical can become critical when they fail within a day or so of another component. For example, the critical pipe, 329, when failed

alone creates 6,427 service loss outages. When failed on the same day as a pipe that does not cause any failures by itself, pipe 261, there are 6,429 service loss outages. Another example is that when the minimally critical pipe, 137, fails by itself it produces 92 service loss outages, but when failed within 6 days of an individually non-critical pipe, 131, there are 96 service losses.

3.5 Evaluating mitigation potential of adaptation strategies

Contextual variables in the simulation that are temperature-independent represent opportunities for exploring how well adaptation strategies could mitigate failures from climate change. The two contextual variables which failures and outages are sensitive to are the operational parameters used to generate the temperature-failure CDFs, and the repair times of components. Ranges of operational parameters that produce relatively low probabilities of failure represent the implementation of improved preventative maintenance strategies. An example of a preventative maintenance strategy in this context is changing the range of internal heating in motors within pumping units. When the internal heating from friction of the bearings is kept at 100-105^{o}C via good bearing lubrication practice, the motor has a lower probability of failure than if the internal heating is kept at 105-110^{o}C via poor lubricating practice.[11]

To evaluate how well preventative maintenance and fast repair times could mitigate outages, we compare the percent of additional outages from climate change that were offset from implementing three independent possible adaptation strategies: (1) improved preventative maintenance at 50% above mid-levels, (2) improved repair times at 50% above mid-levels (i.e., 88 and 8 hours respectively), and (3) both improved preventative

maintenance and repair times 50% above mid-levels. We then explore why those offsets occurred and form recommendations from the findings. We explore how strategies would offset failures if either the average or maximum projections within each RCP were realized. The minimum projections are not included because they produce fewer failures than baseline scenarios and therefore would require no offsets from strategies. The strategies are compared based on the number of times they offset the additional failures from climate change, which we refer to as "factor of offsets". Figure 15 shows the different resulting offsets provided by each strategy under the different temperature scenarios.

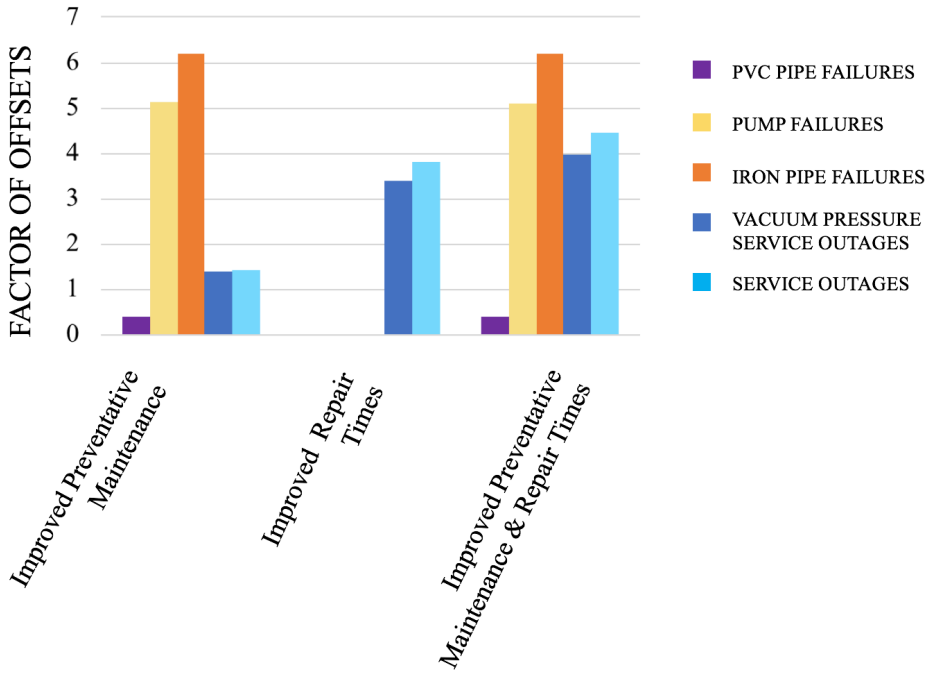

Figure 15 Offsets of Additional Failures from RCP 4.5 Average Temperature Projections

An exploration of the mitigation potential of adaptation strategies shows that (1) strategies are capable of offsetting 100% of the additional failures from climate change, (2) improvements in repair times offset the most outages, and (3) strategies have different

effects under different climate futures. Improved preventative maintenance offsets outages by decreasing component failures. For pumps, improved preventative maintenance will provide a 3-5 factor offset under average temperature conditions and a 1.5 factor offset under maximum temperature conditions. For iron pipes, improved preventative maintenance will provide a 5-6 factor offset under average temperature conditions and a 2 factor offset under maximum temperature projections. Offsets of PVC failures never reach a factor of 1 in any temperature scenario. Improved preventative maintenance will provide a 23% offset of additional PVC failures under average temperature conditions and 7% at maximum temperature conditions. These component failure offsets translate to a 1.4 factor offset of service outages. Improved repair times offset service outages directly without offsetting component failures. Implementing improved repair times has a 3.4-3.8 factor offset of all service outages under average conditions. Improving repair times is therefore about three times as effective for reducing the duration of outages than is improving preventative maintenance. Improved preventative maintenance paired with improved repair times produce an even greater offset at a factor of 4-4.5 times. An additional insight is that the comparison of offsets across average and maximum projections reveals that both repair and preventative strategies are less effective in hotter futures, especially for improved repair time strategies. This is because there are more failures to offset at higher temperature projections, and the strategies only provide a constant decrease in failures. Therefore, utilities should expect different levels of offsets from strategies depending on which temperatures are realized out to the end of the century.

3.6 Discussion

The Perses model shows the capability of a dynamic extended period simulation to aid decision making about climate adaptation by estimating the impacts to consumers. The use of Perses for projecting failures from increasing temperatures in water distribution systems shows that utilities in the Southwestern region of the U.S. that experience high temperatures will likely experience increases in component and consequential service level outages to consumers. If allowance is not provided in budgets for the increased need for repair, replacement, and response required from increased failures, and for maintaining the quality of repairs, outages to consumers could be more frequent and could extend even to longer periods.

The knowledge Perses generates could be especially useful for resilient decision-making regarding assessing consequences and management strategies since the American Water Infrastructure Act passed in October 2018 requires US utilities to conduct resilience assessments to natural hazards.[43] As utilities in warm regions of the US conduct their assessments, they could use the Perses results especially for improving the "Consequence Analysis" and the "Risk and Resilience Management" steps in their assessments as suggested by the Risk Analysis and Management for Critical Asset Protection (RAMCAP) Standard for Risk and Resilience Management of Water and Wastewater Systems which serves as guidance for compliance with the new law.[5] The RAMCAP standard calls for an estimation of the duration and severity of service outage that could result from a hazard. This is then used to define resilience as a function of the duration and severity of consequence instead of just the estimation of ultimate consequence. They ask that utilities "do not assume that all uncontrollable variables and

unpredictable events occur simultaneously".[5] Therefore, a more detailed knowledge of time and space is needed to estimate this aspect. Additionally, the evaluation of the results under different maintenance scenarios using Perses also helps with "assessing the options by analyzing the facility or asset under the assumption that the option has been implemented—" by "re-estimat[ing] the risk and resilience levels and calculating the estimated benefits of the option." Utilities could improve the context considered by inputting utility specific information like the number and topology of components and demand profiles.

There are aspects of resilience dependent upon an understanding of social capacity, transformative designs, and system decompensation that are not yet considered. Perses does not yet quantify the impacts to the communities from experiencing service losses. The low pressures that constitute outages could be translated to loss of demand (in gallons per minute) and the consequence of different consumers losing this amount of water could be estimated according to their critical need. Including this in future versions of Perses could help utility managers better prioritize where they will invest in adaptation options for specific locations in their networks so that their most vulnerable populations remained served under increasing hardware stress.[52] Additionally, system decompensation, representing the diminished "capacity to deploy and mobilize responses as disturbances grow and cascade" from neglected budgets, [189] could be incorporated into Perses by having components repaired to lower levels in response to constrained budgets.

The applicability of Perses to water systems decision-making is specific to certain spatial and temporal contexts. Perses is applicable to a certain type of climate in warm regions that does not experience freezing temperatures (e.g. the US Sun Belt, Middle

East, North Africa, and South Asia). In cold regions, the effects of temperature include additional dynamics regarding changing freeze-and-thaw cycles which have a large impact on pipe breaks. [22] Additionally, Perses is most applicable to structure of water infrastructure that is currently prevalent in developed countries today. Future designs of water systems that for example incorporate decentralization, direct reuse treatment, and more robust materials, could transform the nature of the relationship of the hazard to the system, thereby changing the form Perses would take to aid decision-making. Perses could model the impact of temperature on some of the hardware components of more decentralized systems, e.g., pumps and pipes in rainwater treatment systems, but would need to consider more internal dynamics of how a hardware failure causes systemic failure of the rainwater treatment system. Additionally, if systems that connect wastewater treatment to water treatment and water distribution become more common, Perses could account for the increased number of connections in the network that could cause more widespread cascades of failure and therefore more service losses. Additionally, building robustness into the material design of the hardware could be included in the model, decreasing the initial impact of temperature exposure. Improving the robustness of materials used for motors, electronics, and pipes would reduce the rate of temperature-related degradation and the need for any action to counter act the temperature rise.

The analysis of adaptation strategies to temperature effects does not consider costs or all of the stressors need to make complete practical recommendations for utilities. Including cost in the comparisons of adaptation strategies may produce different recommendations of strategies. The functional unit in this analysis is one independent

adaptation strategy. If costs of improvements of strategies were quantified, the functional unit could be the benefit from strategies provided by an investment dollar amount. The repair times which cost as much as preventative maintenance may offset fewer failures than the preventative maintenance strategy because they are relatively expensive.[127] For example, for pipes, it may take a lot more money to reduce repair times to consistently 44 hours for all failed components than it would be to invest in reducing corrosion. Additionally, the analysis of these strategies does not include other mechanisms of degradation which contribute to our infrastructure aging crisis. [127] There is evidence that in the case where many of the pipes are at the end of their useful life at once, strategies like rehabilitation or scheduled replacement are much less costly than relying on repair.[127]

Ultimately, Perses shows the potential for simulation methods to aid water infrastructure decision-making by providing the basis to consider dynamic parameters and spatially-explicit aspects of the system. Climate impacts to other infrastructure systems that depend upon network connections and operations of the flow of materials could be modeled in a similar fashion considering the specific mathematical formulations of degradation from the hazard, component operations, and the connections between components. We ultimately hope that using spatial and temporally explicit information becomes a more common practice for anticipating and preparing for changing conditions which underlie successful provision of vital infrastructure services.

CHAPTER 4

UNDERSTANDING AND MANAGING INTERDEPENDENT POWER AND WATER SYSTEMS

4.1 Introduction

Interdependencies between infrastructure systems present management challenges for utilities in maintaining reliable service. Though infrastructure systems are managed separately, they share common space and can require inputs from one another to operate.[92] Thus, the vulnerability of failure of one infrastructure system can propagate to other connected infrastructure systems. One historical example of an occurrence of vulnerability propagation is Baltimore's Howard Street tunnel event where the fire from a derailed freight train caused traffic congestion, fiber optic cable damage and a telecommunication outage, along with a water main break. The water main break then caused flooding of transformers that resulted in power outages to 1,200 people in downtown Baltimore.[93] The vulnerability of infrastructure systems given their interdependencies is only predicted to become more of a challenge as the connectivity with information and communications infrastructure increases [109,117,119] and as climate change increases the reliance on services of other infrastructure systems. [47,99,116] The ability to manage interdependencies is becoming a more complex task.[190]

Though appropriate in the past, literature suggests that separate management of infrastructure systems may limit the capacity to prepare systems for disturbances. The "dichotomy of responsibility" was developed due to "the global push toward safety, accountability, and higher efficiency".[191] "The mechanistic approach has been shown to be…effective in environments that require routine operation and little change. In these

environments high-level management possesses the appropriate amount of knowledge to make decisions and organize work″.[119] This type of structure was desirable in the 20th century "since it was the first time they reached such as large scale and level of complexity".[191] However, "This separation of responsibility inhibit[s] communication and coordination between departments", and leads to "solutions that are oriented around a short-term, stable system perspective".[191] Under these conditions, "in some instances, incremental adaptation can actually lead to the degradation of a safety-control structure over time due to asynchronous evolution, where one careful change is made, but fails to relate with changes in connected parts.[190] In such cases, flawed expectations about the behavior of the change may lead to undesired consequences".[128,192]

There is evidence that infrastructure utilities are limited by lack of communication. The use of incomplete information about the state of other utilities' infrastructure and their plans for improvement produces sub-optimal vulnerability mitigation strategies. For example, after the 2003 Northeast blackout, the water utilities which had outages of their power supply expressed the desire to communicate with power utilities to "learn about isolating failures and creating redundancy".[114] Unfortunately, power utilities did not want to share information because of the competitive nature of the information. One water utility ultimately resorted to hiring an outside consultant in order to assess the reliability of their infrastructure because of the challenge of information sharing from the power utility.[114] Additionally, a lack of communication breeds false expectations between utilities. A study on decision-making within interdependent infrastructure systems shows that utilities try to anticipate what other utilities are doing to try to benefit from their decisions and reduce their own costs, especially regarding adaptation strategies that affect

all of the utilities in the geographic region.[193] However, because they do not communicate, (1) the utilities incorrectly anticipate benefits, and (2) the acting utilities do not factor the perceived benefits to the other utilities into their decision making.[193]

The incomplete information about other infrastructure systems leave the following questions unanswered for utilities: *Where are the locations in the network that are vulnerable to propagation of failure from interdependencies? How much vulnerability do interdependencies cause?* Considering the lack of direct information, modeling the causes of the propagation of failure between utilities can help answer these questions. Utilities can gain insights about possible failure events from past failures of different utilities, but this information is also insufficient because utilities cannot expect the same exact impacts to occur due to their different contexts. For example, the water utilities affected by the 2003 Northeast Blackout were all affected differently due to their differing network configurations.[194] Therefore, to anticipate pathways of failure propagation and vulnerability impacts for specific utilities, a predictive or exploratory model of interdependencies, contextual information about the utility, and the consequential outcomes would help utilities explore impacts for their specific systems. There are not enough case study data available to generate a statistical predictive model, so a model exploring the effects of the underlying dynamics would be useful. Current models of interdependencies are insufficient to answer questions about propagation and vulnerabilities, however. Reliability and climate change impact assessments include quantitative information about interdependencies to better understand the strength of connections.[47,78,98–107,79,108–113,80,88,93–97] These studies focus on long-term use of resources and topographic connections, which do not provide information to determine

vulnerability from failure. Current failure propagation interdependency studies typically only use graph topologies without flow information.[96,103,110] Studies suggesting new model frameworks confirm that interdependency models should include more information. They recommend considering structure, flow characteristics [106], system operation [109,117], and temporal aspects [97]. This additional information would facilitate anticipating where, how, and under what operational circumstances the interdependencies could manifest given their spatial and operational context, and therefore how widespread resulting outages could be.

In addition to improving communication across utilities, literature suggests developing coordination between infrastructure managers, arguing that it could lead to more effective vulnerability mitigation. Derrible argues that "A more coordinated and better planned integration is highly desirable" because integrated systems can consider more of society's needs (health, equity, overall efficiency) (Derrible, 2017). Chester & Allenby (2018) citing Larence and Lorsch (1967) argue "Organic [organizational] structures allow for more internal specialization to respond to changing environments, thereby increasing responsiveness"[118] because "distributing the knowledge and decision-making at the bottom of the hierarchy becomes more effective when the environment [in which infrastructure operate] becomes unstable and high-level management cannot acquire all of the knowledge associated with the changing environment (Sherehiy et al., 2007)".[119,120] This generates the question for utilities, *do coordinated institutional strategies between utilities have the potential to reduce vulnerability better than other institutional strategies?* Models which identify the pathways of failure propagation can

serve as a baseline to explore different institutional strategy inputs to see how well they can mitigate failures.

4.2 Case Study Approach

Since sufficient modeling frameworks are not yet available, we present a modeling framework which uses real-time simulation of coupled network models and a case study of a specific coupled network to answer the questions: *How can utilities model propagation of failure from interdependencies and anticipate vulnerability?* and *How can they use these models to explore effects of institutional strategies*? This modeling framework could then be used to answer the questions posed in the introduction for other specific coupled networks. The case study includes (1) a description of the pathways of failure propagation and outages, which characterize vulnerability, that result from an initial hardware failure and an example set of dependencies in the coupled networks, and (2) a comparison of the avoided outages from implementation of institutional strategies within and across the infrastructure systems. We use flow-based infrastructure networks that incorporate temporal and spatial information and are connected to each other through operational resource needs and geographic location. The individual connections are unidirectional *dependencies* which together form *interdependencies* between the networks since "the state of each infrastructure influences or is correlated to the state of the other".[92] We hope that this case study will provide motivation for utilities and researchers to further explore resulting failure propagations and outages and coordinated institutional strategies for different coupled networks with different configurations and dependencies.

We use a case study of the interdependencies between water and power distribution networks because they are critical lifeline infrastructure systems, there are a variety of types of interdependencies between them, their interdependencies are expected to grow stronger in the future, and their interdependencies are largely unexplored at the operational level. The disruption of water or power systems poses a significant threat to human health and economic activity. For example, in the 2003 Northeast blackout, 50 million people were without power for around 4 days[195] and parts of Detroit and Cleveland experienced temporary water outages that resulted in boil water advisories and in one case, the National Guard was called in to distribute water to the elderly and the frail.[196] The blackout was also estimated to have caused $6.4 billion dollars of economic loss due to productivity impacts, costs to governments and utilities, and lost or spoiled commodities.[197] In this example, the failure was due to the physical interdependency between water pumps and electricity. There are other physical and geographic interdependencies between the water and power systems according to Rinaldi et al.'s classifications.[198] The physical interdependencies between the systems are through water pumps, valves, and SCADA's need for power,[7,114] and in the drop in power generator capacity from lack of treated water for cooling.[116] Geographic interdependencies include possible transformer flooding from pipe break [115] and the transient overvoltage effect of a unexpected failure of a large water pump.[199] Future conditions such as climate change, population growth, and increasing complexity threaten to make these connections stronger, therefore increasing the vulnerability of propagation. For example both power and water hardware are expected to fail more frequently from increased heat exposure,

[46,47] and increased residential and generator demand from heat and increase in population served for the same amount of infrastructure is expected to further stress the systems.[114]

Existing efforts at identifying water-power interdependencies reveal what the physical interdependencies are that could potentially cause a cascade of failures under the right circumstances. They are beneficial for showing how much the production of one resource requires of the other resource and vice versa.[78,79,98–100,200–202] Studies with projections into the future include actionable suggestions about conservation measures to sustainably decrease demands [78] or predictions of how much new infrastructure might be built to accommodate coupled rising demands.[79] Optimization models even help utilities decide how much output to produce to sustain interdependent systems. [200,201] Water-power interdependency studies that address how failure events could cascade into the other infrastructure systems consider temporal flows of water and power within spatially contextual networks, but focus on contingency scenarios of component failure and only include physical interdependencies.[113,203]

4.3 Case Study Description

We build and simulate a realistic coupled water-power network using the hydraulic solver, EPANET, the power flow simulator, OpenDSS, and a coupled network solver we helped develop called the Resilient Infrastructure Simulation Environment (RISE). To identify the pathways of failure propagation, we establish dependency connections between components within the networks and a set of rules that cause propagation of failure through the dependency during the simulation (e.g. if real power at a load is zero, then connected water pumps fail). We then simulate the coupled network

over a short period of time until all resulting failures have occurred under the single-hardware scenario (a few minutes) and see which dependencies had failures propagate through them given the initial failure. To estimate how much of a threat interdependencies can pose to reliable service, we count the resulting outages at demand nodes. For water systems, an outage is considered to occur when the pressure at the node goes below 40 psi.[7] For power systems, an outage is considered to occur when real power drops to zero. We calculate the percentage of the demand nodes that have outages within the interdependent network and compare to the percentage of demand nodes that have outages within the uncoupled independent networks from the same initial hardware failure. To answer whether coordinated institutional strategies between utilities have the potential to reduce vulnerability better than other institutional strategies, we compare the number of avoided outages from the implementation of individual institutional strategies.

4.3.1 Network Configuration

Example power and water networks are modeled separately and then connected through their dependencies. The example electric power network is modeled using the IEEE 14-bus system for a single distributed generation network.[204] The 14-bus system operates at 12 and 120 line-to-line kV and consists of 2 generating units, 9 loads, 9 distribution line branches, 4 transformers, and 2 capacitors. The input data are shown in the respective data sheets.[204] OpenDSS models assume a constant power model wye-grounded connection, minimum per-unit (PU) voltage of 0.9, and maximum PU voltage of 1.1 for the generating units and loads according to NERC example voltage deviation standards.[205]

There is no existing water network that is complementary to the IEEE 14-bus system so we generated one using the power loads and network layout. A water distribution network was generated based on the text network provided in the EPANET manual that spatially (i.e., location) and functionally (i.e., rated capacity) complements the IEEE 14-bus electric power system.[206] The water network contains one source of water modeled as a reservoir in EPANET, 2 tanks throughout the network that store and cycle water, 2 pumps, and 14 junctions or nodes with water demands. Appendix B includes all input data for the water network.

The base average annual water demand of the junctions was modeled by calculating the population served by the power load and then calculating what the water demand would be for that same population. We calculated the number of power customers at each node by converting the peak single-phase power of load into three-phase power and dividing by the per customer electric load value of 5.8 kW per customer.[207] Electric power customer demand at each node was used to estimate the water demand at each node. It was assumed that each electric customer is a domestic unit, and that a domestic unit in Phoenix consists of 2.85 people.[208] The number of people at each junction was then multiplied by the per capita water demand value of 0.792 gallons per minute.[209]

4.3.2 Network Solvers

Water and power flows between the sources of the resources and the nodes that require resources (demand nodes) were calculated using topological and temporal information about rate of supply. The software program, EPANET was used to solve the hydraulics of the water distribution network [206]. EPANET calculates pressures at demand nodes given rates of inputs from reservoirs and tanks, considering elevation, and the

increases in pressure provided by pumping units. OpenDSS was used to solve the power flow of the power distribution system [210]. OpenDSS "captures both the time- and location-dependent value of distributed generation by modeling distributed generation in its actual location on the circuit and by having extraordinary loadshape modeling capability to support sequential time simulations" [210]. To connect the networks through their dependencies in real time, we use RISE [211]. RISE allows users to (1) generate water and power networks and place them on the same map, (2) place different types of dependency connections between individual components across the networks, (3) change operational settings of components to explore causing failure or bringing service back after failure, and (4) run a solver that considers dependency connections for a chosen time step. When a hardware component fails and is connected to a component in the other network, the logic from the interdependency connection will cause that component to also fail (geographic interdependency). When a demand node loses service and is connected to a component in another system, the logic from the interdependency connection will cause the component to lose capacity to operate relative to the amount of flow lost (physical interdependency). Therefore, although the possible dependency connections are input into the model from case studies, the real time occurrence of failure propagation and the resulting outages are emergent from the initiating failure, the network topology, and flows overtime.

4.3.3 Dependencies

The dependencies modeled in the case study are those connecting water pumps and power loads. One dependency is the physical connection from power loads to water

pumps due to the water pumps' need for power. The other dependency is the geographic connection from water pumps to power loads from the possible transient overvoltage effect of an unexpected failure of a large water pump. Together these dependencies form a case study of the interdependencies between the networks.

4.3.4 Coupled Network

An overview of the coupled network modeled in RISE is shown in Figure 16. The water network is displayed in blue, the power network is displayed in orange, and the interdependency connections are displayed in green. The networks were overlaid onto an example map showing that power lines and water pipes roughly follow the street network. The data of the networks has no direct tie to the geographic location of the map.

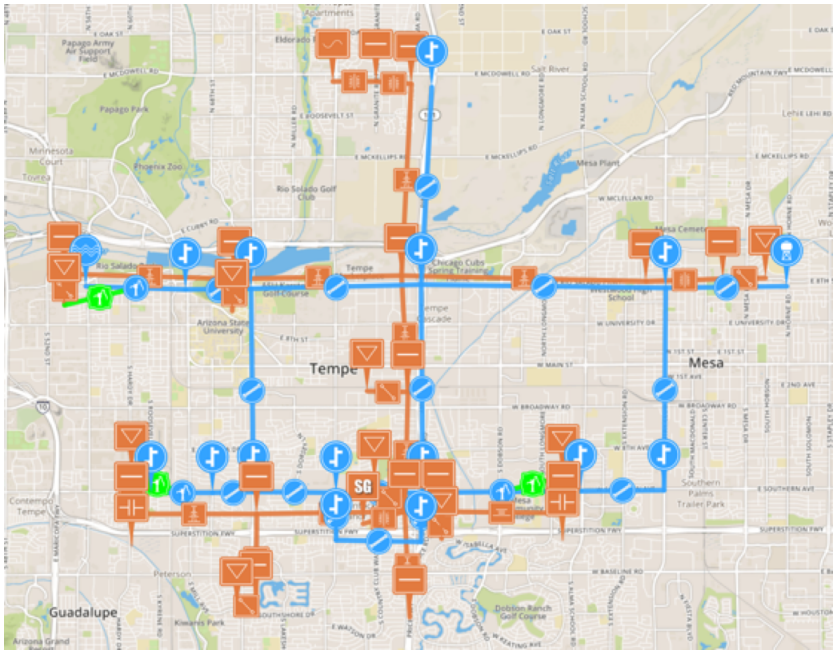

Figure 16 Water and Power Coupled Network Case Study in RISE

4.4 Emergent Failure Propagation Pathways and Resulting Vulnerability

The emergent propagation of failure through dependencies and the resulting vulnerability from interdependencies for the case study coupled network is illustrated with an initiating single-hardware failure. The consequential emergent failure events are described in detail below. The failure events in the case study are categorized using terminology from Rinaldi et al 2001[92] and the distinction between direct and indirect from Markolf et al 2019[212] to demonstrate examples of the theoretical types of failures. In Rinaldi et al 2001 "orders" represent the number of times failures have propagated across systems, "cascading" failures specifically refer to outages that occur in one system because of a propagated failure from the other system, and "escalating" failures are ones that happened without interdependencies but were exacerbated by interdependencies.[92] In Markolf et al 2019, direct physical failures are those which are characterized as "impact to physical infrastructure" while indirect physical failures are characterized as "disruption resulting from other interconnected or co-located infrastructure".[212] It should be noted that in different configurations of coupled networks with different types of dependencies at different locations and under different initial failure conditions, different failure events and vulnerabilities from interdependencies would emerge.

To initiate the events, a pump in the water system (Pump 2) is failed (set to closed in the EPANET model). Example stressors that cause pumps to fail are age, heat stress, or flooding.[6] The lack of pressure produced by the failed pump then causes a decrease in pressure within the network, and consequentially water junction 18 drops below the reliability threshold of 40 psi. Junction 18 has a high elevation relative to other junctions and needs Pump 2 to be operational in order to receive adequate pressure. A close up

view of the connection between Pump 2 and Load 675 and the graphical representation of the water junction 18 service outage is shown in Figure 17. The dotted lines represent the pressure thresholds of safe operation. The area below the 40-psi threshold in the graph is shown in red. Red arrows point to the time step of interest for each failure event.

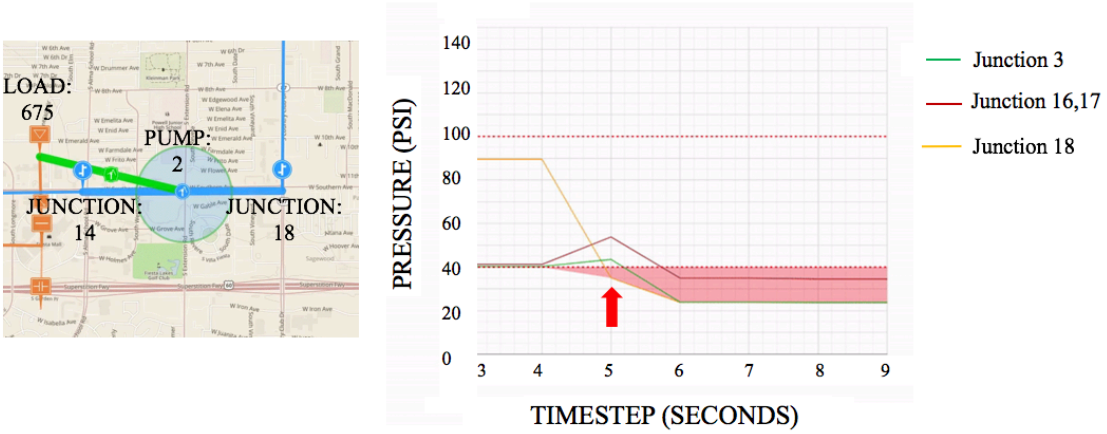

Figure 17 Direct Physical Failure and Service Outage Outcomes. The pressure at Junction 18 drops to below the 40-psi threshold. Junctions 16 and 17 have the same pressure.

Since Pump 2 and power Load 675 are connected and pump 2 has a large power load of 225 kW, the sudden failure of the pump causes a transient spike (downward) in the power network at Load 675 because power is no longer being used for the operation. This effect characterizes a first-order cascading effect from the interdependency with the water network. Figure 18 shows the location and effects of the drop in Load 675.

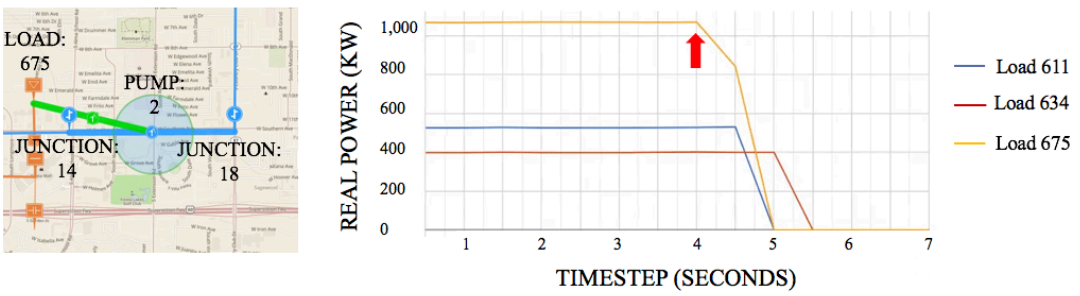

Figure 18 First Order Indirect Physical Failure. Pump 2 failure causes Load 675 to drop.

The transient spike at Load 675 causes an imbalance of voltage in the power grid assuming that the synchronous generator's output is not adjusted in time. The spike in voltage causes lines 1 and 2 to exceed their continuous ampacity of 250 amperes. The assumption is made that when lines exceed continuous ampacity the lines trip. Figure 19 shows the locations of the tripped lines within the network and shows the graph of the current magnitudes with a highlight of when the current exceeded the continuous ampacity.

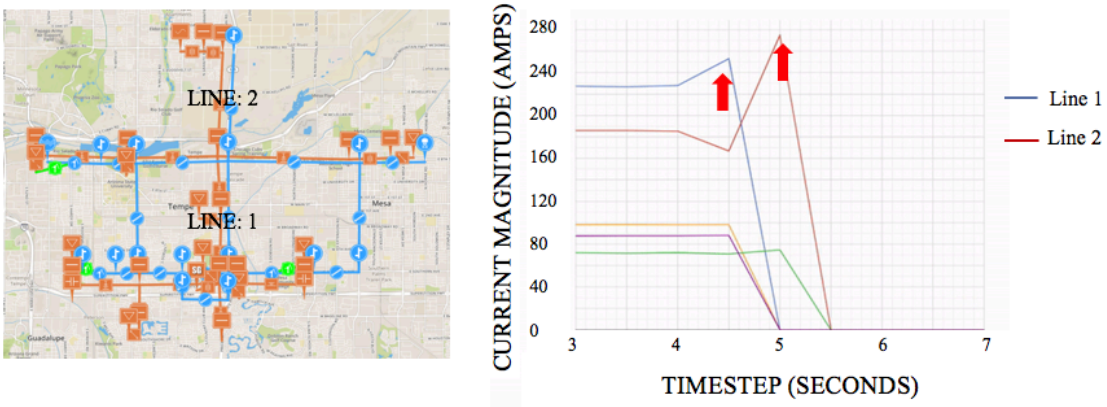

Figure 19: Secondary and Tertiary Indirect Physical Failures. Currents rise in power lines and cause trips in lines 1 and 2.

The tripping of the aforementioned power lines then causes a blackout where Open DSS calculates that all power loads drop to zero. Figure 20 shows a graph of the real power of three example loads from the network dropping to zero after the lines trip.

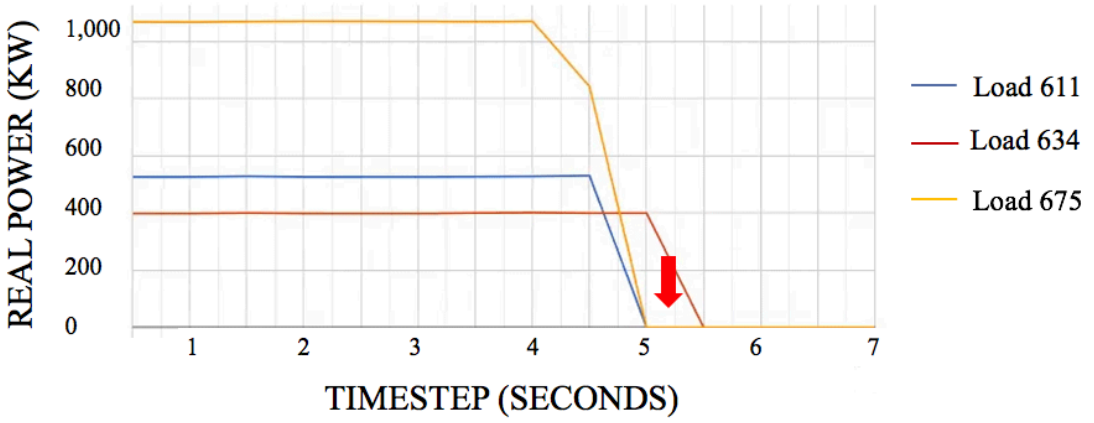

Figure 20 Cascading Service Outage Outcome. All power loads drop to zero.

The drops in Load 646 and 611 trigger a second order cascading failure, this time from the power network to the water network. It is assumed that Pumps 1 and 3 require power from the grid to operate. Therefore, when Loads 646 and 611 drop to zero, Pumps 1 and 3 fail from lack of power. Figure 21 shows a close up of the connections between the loads and the pumps.

Figure 21 Second Order Indirect Physical Failures. Pump 1 and pump 3 fail from loss of power at loads 646 and 611 respectively.

The second order cascading failure causes further service outage outcomes for the water network. The outages of Pumps 1 and 3 further decrease the pressures in the water network and EPANET calculates that the pressures at water junctions 16 and 17 drop below the reliability threshold of 40 psi. The pump failures also cause an escalating failure of junction 18 which drops even farther below the reliability threshold. Figure 22 shows a graph of the drop in pressure of junctions 16, 17, and 18.

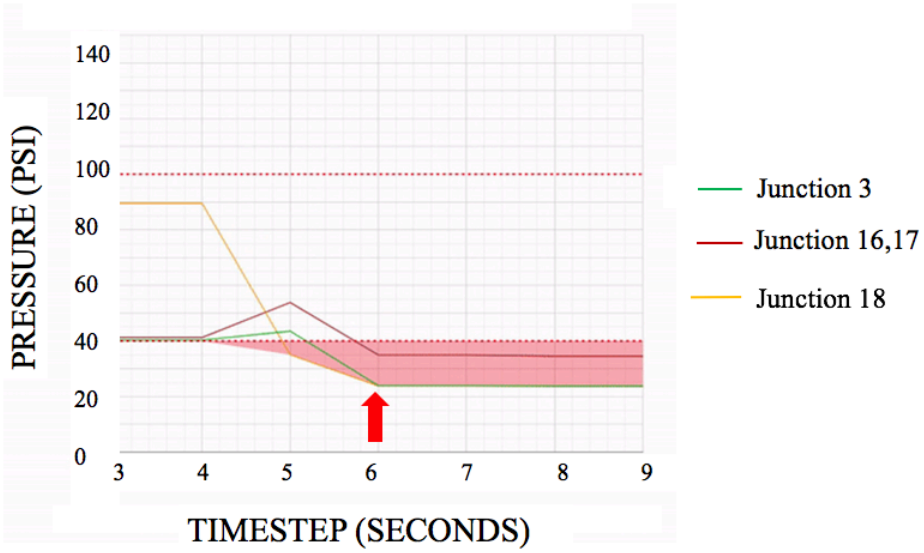

Figure 22 Cascading Service Outage Outcome. Water outages at junctions 16, 17, and 3 and escalating failure from interdependency causes an increased outage at Junction 18.

To evaluate the vulnerability interdependencies cause in terms of how many outages occur from the failure propagation, the number of outages that occurred in independent networks and the interdependent networks are compared. *Figure 8* shows a comparison of the failure events and outages that are anticipated. Without considering interdependencies in this scenario, water utilities would assume that only one water

demand node is vulnerable from a failure of Pump 2. From considering the cascading effects through the power system and back to the water system, they would know that three more demand nodes are vulnerable to failure and the node that initially failed, fails to an even larger degree due to the interdependencies. This translates to water outages of an additional 22% of demand nodes. Without exploring the interdependencies, all power outages are unanticipated (100% of all demand nodes). Figure 23 also shows the categories of failures based off Rinaldi et al 2001 and Markolf et al 2019 terminology.[92,212]

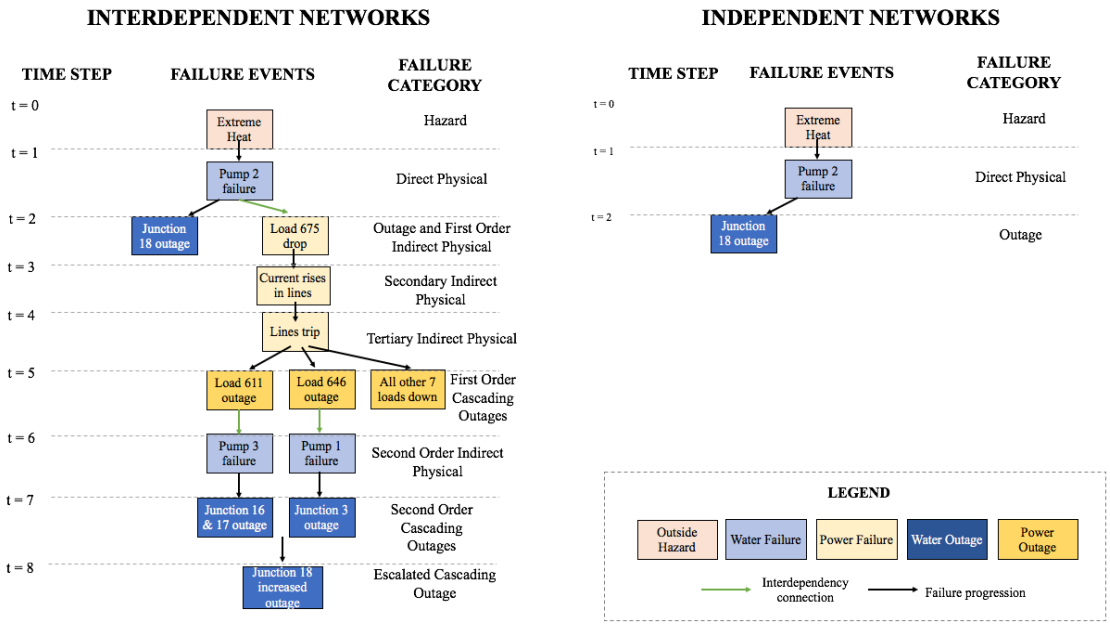

Figure 23 Comparison of Sequence of Events and Outages within Interdependent and Independent Networks

4.5 Potential of Coordinated Strategies Between Utilities

At each stage of propagation of failure, there are institutional strategies (including planning and operational) which could be implemented to either prevent hardware failure or prevent the cascade of failure. The RISE simulation of the single-hardware scenario

assumed no institutional actions were taken and therefore modeled a worst-case scenario cascade. Example actions which could prevent failures in the single-hardware scenario are listed below and categorized according to those which prevent hardware failure and which prevent cascades.

(1) Water utilities preventing hardware failure through either:
    a. Improved preventative maintenance (e.g. improved bearing lubrication and motor cooling[10])
    b. Rehabilitation (e.g. scheduled replacement of pumps[125])
    c. Robustness (e.g. improving pump insulation capacity[10])

(2) Water utilities preventing cascade of failure through either:
    a. Redundancy (e.g. water utilities installing redundant pumps[125])
    b. Operational response (e.g. increasing the levels of the water tanks to provide pressure[7]) Either handbook or EPANET manual.
    c. Repair response (e.g. repair Pump 2 in time to prevent load imbalance and junction outages[125])

(3) Power utilities preventing cascade of failure through:
    a. Operational response (e.g. using a congestion management procedure[213,214])

Figure 24 shows when in the progression of failure these institutional strategies could help prevent failure.

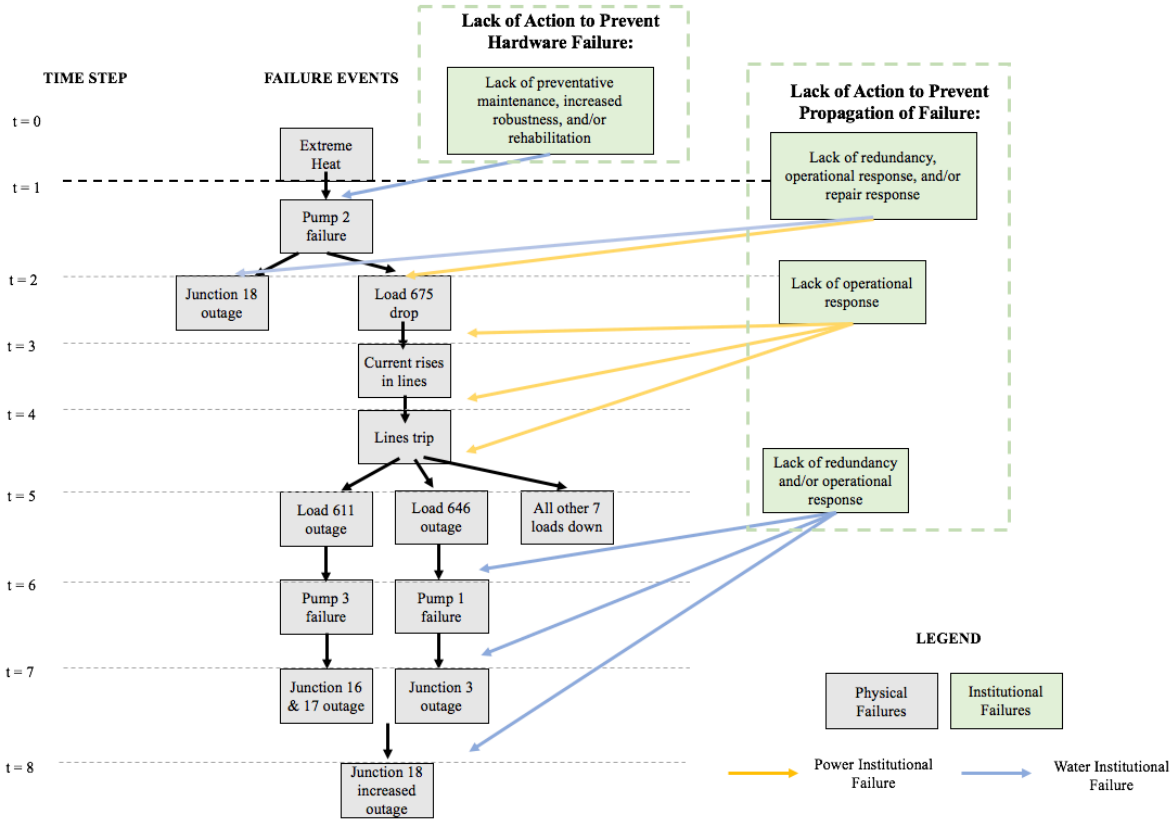

Figure 24 Institutional Failures Causing Physical Failures in Single-hardware Failure Scenario

We compare reductions of outages of each strategy to identify which have the most failure mitigation potential. The effect of the implementation of strategies estimated through the use of the fault progression generated by the single-hardware simulation in RISE. We assume that wherever a strategy would be implemented within the progression, it would prevent the next failure from happening and therefore all of the resulting cascades of that failure as well. We compare individual strategies independently, but in future studies multiple combined strategies could be considered. Figure 25 shows the percent of water, power, and total number of outages avoided under different institutional strategies as compared to the number of outages which occurred in the single-hardware scenario where no strategies were applied. The strategies which water utilities could use

to prevent cascades of failures were further separated into groups of strategies which produced the same outcomes (i.e. redundancy and operational response, and fast hardware repair). In contrast, power utilities only have one type of strategy that could prevent cascades, in this case -- operational response.

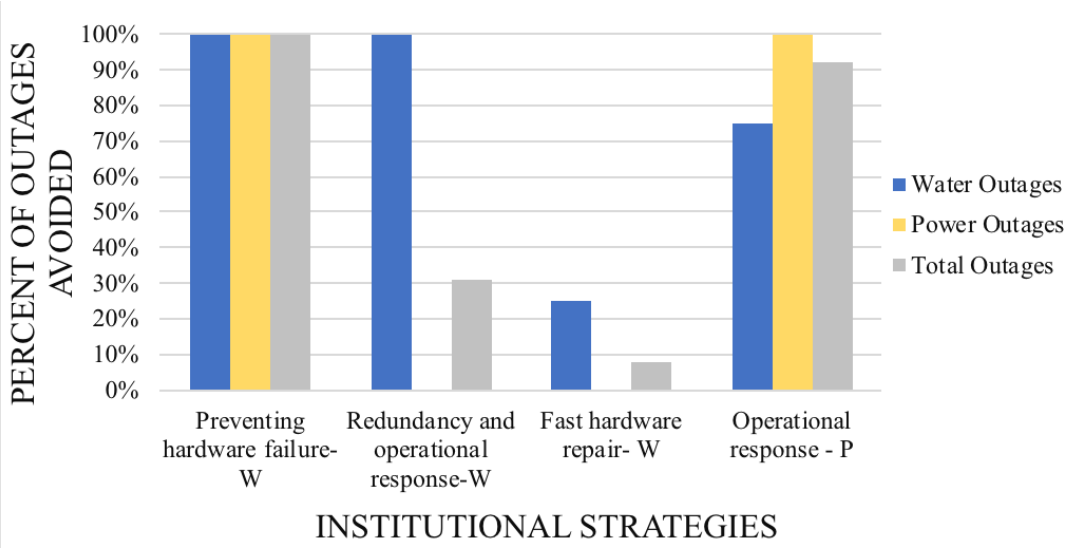

Figure 25 Percent of Outages Avoided from Institutional Strategies in Single-hardware Failure Scenario. (-W) signals that the strategy would be implemented by the water utility and (-P) signals that the strategy would be implemented by the power utility.

The outcomes of institutional strategies in this example coupled network show that when comparing institutional strategies, coordination between utilities has the potential to produce strategies that are most effective at reducing overall vulnerability from outages. The strategy which avoids the largest percentage of outages for both water and power utilities in this case study is preventing Pump 2 failure via preventative maintenance, rehabilitation, and/or robustness in the water system. This strategy was the only one to mitigate all power, water, and total outages. Power utility operational response would avoid the same amount of power outages, however, it is not as effective of a strategy for water utilities and the overall consumer base. Thus, when planning to prevent this pathway of failure propagation, if both power and water utilities channeled

resources toward preventing pump 2 hardware failure, this could be a more effective strategy than both utilities using resources on separate strategies for each system. When using this modeling framework to aid decision making, multiple initiating failure events should be explored to identify a variety of pathways of failure propagation and the different institutional strategies that best prevent outages from them.

It seems obvious that the prevention of the initiating failure would be the most effective strategy, but in a coupled network with different characteristics, other strategies maybe just as effective. The best strategy was a result of the characteristics of the pump that failed and its location within the coupled network. The size of the pump dictated the amount of power it demanded and therefore the amount of power load drop, and the water outages that occurred from the pump failure were an emergent outcome of the criticality of the pump within the network and the water flow calculations. If pump 2 did not have a load large enough to cause power imbalance, no cascades of failure would have happened. If pump 2 was in a less critical position in the network, Junction 18 may not have failed. If this was the case, the operational response from the power utilities would have the same percent of water outage reduction as preventing the hardware failure does.

4.6 Discussion and Future Research

This case study shows a framework for modeling how failures can propagate across infrastructure systems in real time, which improves the knowledge we have about how interdependencies can cause additional vulnerability for utilities. Instead of only considering the resource flows between networks or the number of connection points,

adding information about whether interdependencies cause failures given the resource flows within the network configurations, the operational settings of the components, and the operational management strategies, allows for anticipation of outages due to interdependencies. Anticipating outages from example propagations of failure in turn allows for the evaluation of outcomes from different institutional strategies both within and across systems. The result of the evaluation of strategies of this case study shows that there is potential for infrastructure systems managers to minimize impacts of interdependencies across systems by coordinating with other utilizes. We hope utilities use this finding as motivation to explore the possible benefits of coordinated strategies across utilities in their systems considering their specific network configurations and dependencies.

There are multiple avenues of future work that could enhance the modeling framework's capacity to aid decision making. We suggest exploring the impacts of simulating multiple networks, dependencies, and initial failures to gain general insights on how propagation of failures occur and how strategies reduce outages. We also suggest improving the characterization of institutional strategies, projecting impacts and benefits over longer periods of time, and modeling the response of coupled systems under future hazards. Institutional strategies could be better characterized in terms of types, levels, and cost. There are more types of planning and operational actions available to utilities besides preventative maintenance, corrective repair, and real time operational response. For example, utilities could redesign the structure of the networks or preventatively replace components. A model that includes all possible institutional actions would help utilities compare and prioritize actions for practical decision making. This would require

consulting utility managers to learn all of the actions available and developing ways to model those actions. Additionally, in reality, strategies provide levels of failure mitigation potential according to how many resources are invested in them. To model the avoided outages from different levels of strategies, aspects of the system should be dependent on quantities of strategies. For example, levels of preventative maintenance could be characterized by quantitative parameters in the probability distributions of hardware failure, and repair strategies could be characterized by the time it takes to repair like was done in the study about water distribution failure in Chapter 3 of this dissertation. Utilities could then also compare implementing levels of different strategies simultaneously, which more closely resembles reality than choosing only individual strategies to explore. Exploring levels of strategies according to the allocation of resources would shed light on the cost-effectiveness of strategies, which is a more realistic decision-making metric than failure mitigation effectiveness. Another improvement would be to simulate the cumulative impacts of strategies overtime. This would help explore whether choosing strategies for short term objectives provides a disadvantage for long-term goals. Additionally, if hardware failures were modeled probabilistically and their probability distributions were dependent on future hazards as well as institutional strategies, like was the case in the study about just water systems in Chapter 3, the future vulnerabilities from interdependencies and benefits from strategies could be assessed.

CHAPTER 5

SYNTHESIS

5.1 Summary

This dissertation advances the capability of water infrastructure utilities to anticipate and adapt to vulnerabilities in their systems from temperature increases and interdependencies with other infrastructure systems. Impact assessment models of increased heat and interdependencies were developed which incorporate probability, spatial, temporal, and operational information. Key findings from the work are that with increased heat the increased probability of water quality non-compliances is the greatest amongst a selection of water quality indicators and component failures (chapter 2), the anticipated increases in probability of hardware failures components is the greatest for iron pipes, then pumps, and then PVC pipes (chapter 3), the effects of temperature increase on hardware components and on service losses are non-linear due to spatial criticality of components (chapter 3), and vulnerabilities from interdependencies are dependent on spatial and operational complexity (chapter 4). Exploring different parameters of the models allowed for comparison of institutional strategies. Key findings are that either preventative maintenance or repair strategies can completely offset additional outages from increased temperatures (chapter 3), though improved repair times reduce overall duration of outages more than preventative maintenance (chapter 3), and that coordinated strategies across utilities could be effective for mitigating vulnerability (chapter 4).

A comparison of results across the two chapters which model the impacts of temperature increase (chapters 2 and 3), reveal different outcomes for component failures

and service losses, highlighting the importance of including spatial and temporal information in assessment models. The inputs of cumulative realistic temperature exposures in chapter 3 show different magnitudes and relative increases in failures across components than was estimated in chapter 2 using inputs of scenarios of average temperature exposures. The reason for the difference is that exposure-failure CDFs characterize probability of failure using the average of the entire range of daily temperatures over a year. The temperature-failure CDFs are averaged from only a range of summertime temperatures. The wider range of temperatures decreases the magnitude of increase in probabilities across all hardware components. Additionally, the relative sensitivities of components to temperature change became more apparent with the wider range of temperature inputs in chapter 3. The temperature-failure CDF curves developed in chapter 2 show that iron pipes have the greatest variance of curves for different temperatures, then pumps, then PVC pipes. This ended up characterizing the result given the full range of temperatures experienced in chapter 3. In chapter 2, under the limited range of temperatures the sensitivity of iron pipes to changes in temperature was not fully characterized. The ranking of the rest of the components in terms of their percent increase in failures remains the same as in chapter 2, however. Pumps have the second largest increase and then PVC pipes have the least increase. Additionally, the estimated increases in outages in chapter 3 is much fewer than those estimated in chapter 2 because chapter 2 assumes a direct relationship between component failures and service losses, but due to the various component criticalities, chapter 3 discovers that the relationship is non-direct.

5.2 Application

We suggest that water utilities incorporate the findings and insights from the dissertation into their decision-making processes when considering and preparing for impacts of additional heat and interdependencies. Anticipating the patterns of failure of their components and service losses can help generate effective institutional strategies regarding design of operations and hardware. Findings and recommendations from the dissertation should also be considered along with other challenges utilities anticipate facing to develop a comprehensive plan for the future. We also hope to broadly inspire utilities to start using impact assessment models to explore future changes within their systems.

The decision-making framework of water utilities may need to adapt to encourage anticipation and sensing of the increases in failures. The current budgeting structure has no formal process to incorporate future estimations of component reliability from either historical failure data or future climate models. According to the AWWA manual on utility management, budgets include the expenditures of the past year and the funds needed for new projects.[185] Because only the expenditures of the past year are considered, utilities are not encouraged to identify increases in failures that may be occurring over time and that may occur in the future. Therefore, adaptations typically are made when utilities recognize that an extreme event occurred during the year and decide to fund a new project to update the system for that extreme.[6] For stressors like heat which cause accumulated degradation overtime, and not dramatic events with many failures at once, utilities are less prepared to sense the threat and adapt. This necessary change to their decision making process could either come from within individual utilities or from a

regulatory body.[215] A program that could improve their ability to sense increased risk would be a conditions-based maintenance program, where utilities would monitor the temperature exposure to their hardware and water quality and plan maintenance based on the exposure values in addition to age.

In addition to operations, anticipation of risk to components could better inform design of hardware. More accurate estimates of probability of failure could improve the cost-benefit analyses of the sizing, number, and type of materials of components. Regarding sizing and numbers, smaller components (for example, pumps) running in parallel are less expensive than larger pumps, however having more pumps creates more chance for failure. Alternatively, larger pumps may give more chance of failure through their dependency with the power system (as demonstrated in the example in Chapter 4). The better understanding of risk of failures from heat and interdependencies can therefore help utilities determine the right balance of size and numbers of components. Additionally, better anticipation of risk could inform the cost benefit analysis of the use of more robust materials. For example, the knowledge of increases in risk of motor failure could justify the spending of funds to improve their insulation classes which would decrease the probability of failure.

Climate impacts to other infrastructure systems that depend upon network connections and operations of the flow of materials can also learn from this framework of modeling -- using specific mathematical formulations of degradation from the hazard, component operations, and the connections between components. We ultimately hope that using spatial and temporally explicit information becomes a more common practice

for anticipating and preparing for changing conditions which underlie successful provision of vital infrastructure services.

5.3 Future Work

There are many avenues for future work that would enhance the capacity of the models presented in this dissertation to facilitate decision making within water utilities. The characterization of institutional strategies could be improved in types, levels, and cost-effectiveness, and additional hazards and types of failures could be incorporated.

More types and levels of institutional strategies could be modeled to improve the ability for utilities to use the model to compare and prioritize strategies. There are more types of design, planning, and operational actions available to utilities besides preventative maintenance, corrective repair, and real time operational response. For example, utilities could redesign the structure of the networks, add redundancies, or preventatively replace components. A model that includes all possible institutional actions would help utilities compare and prioritize actions for practical decision making. This would require consulting utility managers to learn all of the actions available and developing ways to model those actions. Additionally, in reality, strategies provide levels of failure mitigation potential according to how many resources are invested in them. For example, corrective maintenance could be modeled at different levels according to different types of component replacement options. Water utilities have to manage the trade-offs between cost and reliability of new equipment when choosing replacement components. They have the option to buy full new equipment which provide low probabilities of failure or to buy inexpensive parts to replace only the damaged

components within the hardware which are associated with higher probabilities of failure.[216] For example, when motors and electronics overheat, either the burnt windings of the motor or the entire motor could to be replaced.[216] Including different options available to utilities for each of the strategies would expand the realistic decision-variables within the models.

The modeling efforts in this dissertation build towards the capability of utilities to do cost-benefit analyses of adaptation strategies to prioritize investments. Cost-effectiveness would be a better metric than outage reduction effectiveness for decision-making because it would help to compare outages on more realistic terms. For example, it is anticipated that though repair strategies are the most effective at reducing outages overall, a level of repair that costs the same amount as a level of preventative maintenance may not be more effective at reducing outages and therefore preventative maintenance would be a more attractive strategy. In order to allow for this comparison, costs of the strategies of repair and preventative maintenance and their ability to reduce outages at different levels of investment should be estimated. The social and economic costs of outages should also be estimated to fully characterize the cost of not preventing outages.

The cost of repair is dependent on the labor required to do the repair and the cost of replacement parts. There are at least three different types of labor forces that can be involved in the repair of failed components: (1) by operations staff during normal operating hours; (2) by operations staff during overtime hours; or (3) by outside contractors.[141,217] Throughout the year, water utilities may end up using a combination of these three approaches for repairs and replacements. When repairs or replacements are

done during normal hours, there is no extra cost to the utility in terms of man-hours. The overall cost of the labor time within a given time period could be estimated by multiplying the number of failures in a time period by the cost of the labor in that time period. The cost of the labor in the time period could be a weighted average of the different types of labor used by the utility with the weights being specific to each utility according to what percentage of the failures they use each type of labor. Furthermore, to estimate the cost of replacement of equipment after failure, the percentage of repairs where full replacements were used versus parts replacements should be considered. When estimating future costs, it would be a good idea to use a projection of the cost of labor and parts instead of the current costs.

Estimating the cost-effectiveness of different levels of preventative maintenance would require characterizing the non-direct relationship between investment levels and improvements to reliability. Investments into preventative maintenance improve reliability of components up to a point, but after all parts are functioning good-as-new, the phenomenon of diminishing marginal returns occurs where an additional unit of investment (e.g. installing a new part) generates much less improvement in reliability. The marginal return of the investment depends on the accuracy of reliability predictions. As utilities are better able to understand and predict the state of reliability of their components, they are better able to avoid wasteful investments and strategically invest in needy components. Therefore, as accuracy of prediction improves, there is more marginal return of investment. In order to calculate what the marginal return is for different levels of accuracy, a statistical regression could be generated using the following utility data for different components: their predictions of component failure times and the actual

component failure times -- the difference of which characterizes accuracy, and the amount invested in each component for preventative maintenance, along with the resulting reliability of the components.

The social and economic impacts resulting from the service outages should also be estimated and included in a future cost-benefit analysis. This would provide an understanding of the true costs of outages and could help utilities prioritize adaption strategies in different neighborhoods. There are different social and economic impacts in different neighborhoods of the distribution system based on the critical need of resources at those locations.[218] Therefore, weights could be assigned to each demand node in the network model and the outages which occur at the demand nodes could be weighted in order to calculate an overall impact. The component failures and institutional strategies that caused the most impact could be then prioritized for improvement.

In addition to realistically modeling strategies and their costs, there are additional elements that could be added to the models to improve their capacity to facilitate decision-making. Other climate and future hazards and components could be incorporated into the model in chapter 3. Temperature effects could be modeled in coincidence with other hazards which utilities are facing in semi-arid regions. One hazard that could be modeled simultaneously would be wildfires sparked from the increased temperature, which would decrease the quality of the incoming water into the water treatment plants. Additional dynamics could be added to the model in chapter 3 to incorporate the interactions between the difference hazards. For example, it could help answer the question: *what happens when there are water quality problems and increased hardware failure at the same time?* A survey of water utilities shows that "several

utilities have experienced dual extreme events with different outcomes – for example drought and flooding. These events can result in different impacts to assets and infrastructure and certainly make it more challenging for utilities to plan for the future".[6] Therefore, there is a need for exploration of the impacts of multiple hazards. Additionally, while water quality effects were modeled in chapter 2, they could also be incorporated into the network model in chapter 3 through the water quality modeling function of EPANET. This would allow for the estimation of the spatially-explicit impacts of water quality degradation. For example, it could help answer the question: *which demand nodes within the network are most susceptible to water quality issues from increasing temperatures*? It would also support the exploration of the interactions between water quality problems and hardware failures.

5.4 Adaptation Framework Landscape

This dissertation is part of a large and methodologically diverse effort to expand the decision-making metrics and frameworks which utilities use to adapt infrastructure to future conditions. ASCE states that "engineers should develop a new paradigm for engineering practice in a world in which climate is changing, but cannot be projected with a high degree of certainty".[2] This will require multiple different adaptation frameworks for different levels of uncertainty. "When it is not possible to fully define and estimate the risks and potential costs of a project and reduce the uncertainty in the timeframe in which action should be taken, engineers should use low-regret, adaptive strategies… to make the project more resilient to future climate and weather extremes. Engineers should seek alternatives that do well across a range of possible future

conditions".[2] The work of this dissertation modeling impacts therefore is an approach that is useful given the bounded uncertainty of climate models, but it is not sufficient for helping to prepare for future hazards that are not so well projected. Resilience and safe-to-fail are better overall decision-making frameworks to operate under for these conditions. However, the models presented in this dissertation can inform parts of these efforts.

Resilience frameworks focus on improving a utility's "ability to adapt to changing conditions and prepare for, withstand, and rapidly recover from disruption".[219] "This process can be modeled as a cycle encompassing at least four components that are often missing from the use phase of many engineering projects: (1) sensing, (2) anticipation, (3) adaptation, and (4) learning".[128] Modeling helps anticipate impacts in possible futures and preventatively adapt. Adaptation can also come from many different types of information, however.[128,220,221] "Adaptation can be either autonomous (e.g. reducing physical activity during a heatwave) or purposefully planned (e.g. adopting new building codes). Planned adaptation can be either reactive (i.e. after some impacts have been experienced) or proactive/ anticipatory (i.e. before major damage has occurred)".[222] Resilience can also mean adapting institutional and organizational structures when necessary to meet the entities truly important objectives.[189]

The safe-to-fail framework suggests that infrastructure managers should assume components will fail for some reason or another and that they should prioritize minimizing failure of delivery of critical services to society that can occur from those failures.[223] Therefore, estimating frequency of component failures is not a useful modeling exercise under this framework. The modeling of interdependencies, as was

done in chapter 4, could be useful, however. Since infrastructure systems are interdependent, there are all involved in providing the critical services. Therefore, utilities could use operational models of interdependency propagation to identify which pathways of vulnerability propagation between infrastructures threaten the provision of critical services and thus which pathways of failure they should minimize through institutional strategies.

REFERENCES

1. Allenby, B. & Chester, M. Infrastructure in the Anthropocene. 58–64 (2018).

2. Olsen, R. Adapting Infrastructure and Civil Engineering Practice to a Changing Climate. (American Society of Civil Engineers, 2015). doi:10.1061/9780784479193

3. Wayman, E. Chile's quake larger but less destructive than Haiti's. Earth (2010).

4. Jones, S. Why is Haiti vulnerable to natural hazards and disasters? The Guardian (2016).

5. Risk Analysis and Management for Critical Asset Protection (RAMCAP) Standard for Risk and Resilience Management of Water and Wastewater Systems. (2010).

6. Heyn, K. & Winsor, W. Climate Risks to Water Utility Built Assets and Infrastructure. in (2015).

7. Mays, L. W. Water Distribution System Handbook. (McGraw-Hill Professional Publishing, 2000).

8. Melillo, J. M., Richmond, T. (T. C. . & Gary W. Yohe, Eds., 2014. Climate Change Impacts in the United States Climate Change Impacts in the United States. (2014). doi:10.7930/j0z31WJ2

9. Clark, R. M., Li, Z. & Buchberger, S. G. Adapting water treatment design and operations to the impacts of global climate change. Front. Earth Sci. 5, 363–370 (2011).

10. Banerjee, A., Tiwari, A., Vico, J. & Wester, C. Motor protection principles. 2008 61st Annu. Conf. Prot. Relay Eng. 215–231 (2008). doi:10.1109/CPRE.2008.4515057

11. Cowern, E. The hot issue of motor temperature ratings. EC M Electr. Constr. Maint. 99, 104–106 (2000).

12. Csanyi, E. Heat as one of the most common cause of motor failure Service life. Electrical Engineering Portal 1–4 (2015).

13. Rockwell Automation. Basics for practical operation Motor Starting. 1, 46 (1998).

14. Kreeley, B. & Coulton, S. Increasing the Lifespan and Reliability of Electrical Components. 1–5 (2012).

15. Hoffman. Thermal Management: Heat Dissipation in Electrical Enclosures. (2017).

16. Whittle, A. & Stahmer, M. Temperature derating of PVC pipes for pressure applications. (2005).

17. Volk, C., Dundore, E., Schiermann, J. & Lechevallier, M. Practical evaluation of iron corrosion control in a drinking water distribution system. Water Res. 34, 1967–1974 (2000).

18. Toshiba. Application Guideline # 05 Temperature Rise – Insulation. 05, (2017).

19. Gauffre, P. Le et al. Impacts of climate change on maintenance activities: a case study on water pipe breaks. (2014).

20. Gilpin, R. R. The effects of dendritic ice formation in water pipes. Int. J. Heat Mass Transf. 20, 693–699 (1977).

21. Goulter, I. C. & Kazemi, A. Analysis of Water Distribution Pipe Failure Types in Winnipeg, Canada. J. Transp. Eng. 115, 95–111 (1989).

22. Kim, Y. H. Coagulants and Flocculants: Theory and Practice. (Tall Oaks Pub., 1995).

23. Hudak, P. F., Sadler, B. & Hunter, B. Analyzing underground water-pipe breaks in residual soils. (1998).

24. Azevedo de Almeida, B. & Mostafavi, A. Resilience of Infrastructure Systems to Sea-Level Rise in Coastal Areas: Impacts, Adaptation Measures, and Implementation Challenges. Sustainability 8, (2016).

25. Guhathakurta, S. & Gober, P. The Impact of the Phoenix Urban Heat Island on Residential Water Use. J. Am. Plan. Assoc. 73, 317–329 (2007).

26. USA Blue Book. USABlueBook Operator's Companion. (USABlueBook, 2013).

27. Smith, H. G., Sheridan, G. J., Lane, P. N. J., Nyman, P. & Haydon, S. Wildfire effects on water quality in forest catchments: A review with implications for water supply. J. Hydrol. 396, 170–192 (2011).

28. Semadeni-Davies, A., Hernebring, C., Svensson, G. & Gustafsson, L. G. The impacts of climate change and urbanisation on drainage in Helsingborg, Sweden: Combined sewer system. J. Hydrol. 350, 100–113 (2008).

29. Yordanova, L. Phoenix Historic September Monsoon Rainstorm Causes Unique Treatment Scenario at Tempe Water Treatment Plant. in 88th AZ Water Annual Conference (2015).

30. Barrett, B. CAP on Skunk Creek flooding. azcentral (2014).

31. ParkPioneer.net. Canal breaks near Bouse. ParkerPioneer.net (2012).

32. Hua, F., West, J. R., Barker, R. A. & Forster, C. F. Modelling of chlorine decay in municipal water supplies. Water Res. 33, 2735–2746 (1999).

33. Toroz, I. & Uyak, V. Seasonal variations of trihalomethanes (THMs) in water distribution networks of Istanbul City. 176, 127–141 (2005).

34. Graham, N. J. D., Collins, C. D., Nieuwenhuijsen, M. & Templeton, M. R. The Formation and Occurrence of Haloacetic Acids in Drinking Water. (2009).

35. Wadowsky, R. M., Wolford, R., McNamara, A. N. & Yee, R. B. Effect of Temperature Ph and Oxygen Level on the Multiplication of Naturally Occurring Legionella-Pneumophila in Potable Water. Appl. Environ. Microbiol. 49, 1197–1205 (1985).

36. Rogers, J., Dowsett, A. B., Dennis, P. J., Lee, J. V & Keevil ', A. C. W. Influence of Temperature and Plumbing Material Selection on Biofilm

Formation and Growth of Legionella pneumophila in a Model Potable Water System Containing Complex Microbial Flora. Appl. Environ. Microbiol. 60, 1585–1592 (1994).

37. Torvinen, E. et al. Mycobacteria in Water and Loose Deposits of Drinking Water Distribution Systems in Finland Mycobacteria in Water and Loose Deposits of Drinking Water Distribution Systems in Finland. 70, 1973–1981 (2004).

38. Archuleta, R., Mullens, P. & Primm, T. P. The relationship of temperature to desiccation and starvation tolerance of the Mycobacterium avium complex. Arch. Microbiol. 178, 311–314 (2002).

39. Pintar, K. D. M. & Slawson, R. M. Effect of temperature and disinfection strategies on ammonia-oxidizing bacteria in a bench-scale drinking water distribution system. Water Res. 37, 1805–1817 (2003).

40. Wild, H. E., Sawyer, C. N. & McMahon, T. C. Factors Affecting Nitrification Kinetics. Water Pollut. Control Fed. 43, 10 (1971).

41. Lipponen, M. T. T., Suutari, M. H. & Martikainen, P. J. Occurrence of nitrifying bacteria and nitrification in Finnish drinking water distribution systems. Water Res. 36, 4319–4329 (2002).

42. AWWA. Offfice of Ground Water and Drinking Water Distribution System Issue Paper: Nitrification. (2002).

43. One Hundred Fifteenth Congress of the United States of America. (2018).

44. Li, Z., Clark, R. M., Buchberger, S. G. & Yang, Y. J. Assessing the impact of climate change on drinking water treatment plant design and operation. World Environ. Water Resour. Congr. Am. Soc. Civ. Eng. 3, 52–60 (2008).

45. Friedl, F., Schrotter, S., Kogseder, B. & Fuch-Hanusch, D. Early Failure Detection Model for Water Mains due to Seasonal Climatic Impacts. in World Environmental and Water Resources Congress 1013–1023 (ASCE, 2012).

46. Bondank, E. N., Chester, M. V. & Ruddell, B. L. Water Distribution System Failure Risks with Increasing Temperatures. Environ. Sci. Technol. 52, 9605–9614 (2018).

47. Clark, S. S., Chester, M. V., Seager, T. P. & Eisenberg, D. A. The vulnerability of interdependent urban infrastructure systems to climate change: could Phoenix experience a Katrina of extreme heat? Sustain. Resilient Infrastruct. 4, 21–35 (2018).

48. Climate Resilience Evaluation and Awareness Tool Version 3.0 Methodology Guide.

49. Adaptation, C. C. AdaptWater TM online climate change analysis tool About Adaptation Good Practice.

50. Klise, K. A. et al. Water Network Tool for Resilience (WNTR) User Manual. (2017). doi:10.2172/1376816

51. Damelin, E., Shamir, U. & Arad, N. Engineering and economic evaluation of the reliability of water supply. Water Resour. Res. 8, (1972).

52. Cutter, S. L. et al. A place-based model for understanding community resilience to natural disasters. Glob. Environ. Chang. 18, 598–606 (2008).

53. Rowell, W. & Barnes, J. Obtaining the layout of water distribution systems. J. Hydraul. Div. 108, 137–148 (1982).

54. Tangena, B. H. & Koster, P. K. Reliability of drinking water supply systems. Water Supply 2 115–124 (1983).

55. Shamir, U. & Howard, C. Reliability and risk assessment for water supply systems. in Computer applications in water resources 1218–1228 (ASCE, 1985).

56. Tung, Y.-K. Evaluation of water distribution network reliability. in Hydraulics and hydrology in the small computer age (ASCE, 1985).

57. Hobbs, B. F. Reliability analysis of water system capacity. in Hydraulics and hydrology in the small computer age (ASCE, 1985).

58. Goulter, I. C. & Morgan, D. R. An integrated approach to the layout and design of water distribution networks. Civ. Eng. Syst. 2, 104–113 (1985).

59. Wagner, J. M., Shamir, U. & Marks, D. H. Reliability of water distribution systems. (1987).

60. Mays, L. W. & Cullinane, John, M. A Review and Evaluation of Reliability Concepts for Design of Water Distribution Systems. (1986).

61. Goulter, I. C. & Coals, A. V. Quantitative Approaches to Reliability Assessment in Pipe Networks. J. Transp. Eng. 112, 287–301 (1986).

62. Germanopoulos, G., Jowitt, P. W. & Lumbers, J. P. Assessing the Reliability of Supply and Level of Service for Water Distribution Systems. in Proceedings of the Institution of Civil Engineers 80.2 413–428 (1986).

63. Su, Y.-C., Mays, L. W., Duan, N. & Lansey, K. E. Reliability-based Optimization Model for Water Distribution Systems. J. Hydraul. Eng. 114, 1539–1556 (1987).

64. Bouchart, F. et al. in Reliability Analysis of Water Distribution Systems (1989).

65. Wagner, B. J. M., Shamir, U. & Marks, D. H. options proposed , a simulation of these options should be done to gain a better understanding of how the proposed alternative systems will be likely to behave under real-life conditions . This paper presents an event-oriented , discrete simulation progra. 114, 276–294 (1988).

66. Wagner, B. J. M., Shamir, U. & Marks, D. H. WATER DISTRIBUTION RELIABILITY: ANALYTIC METHODS. J. Water Resour. Plan. Manag. (1988). doi:10.1061/(ASCE)0733-9496(1988)114:3(276)

67. Hobbs, B. F. & Beim, G. K. Analytical simulation of water system capacity reliability: 1. Modified frequency-duration analysis. Water Resour. Res. (1988). doi:10.1029/WR024i009p01431

68. Cullinane, J. M., Lansey, K. E. & Basnet, C. Water distribution system design considering component failure during static conditions. in Unknown Host Publication Title (ASCE, 1989).

69. Bao, B. Y. & Mays, L. W. Model for Water Distribution System Reliability. 116, 1119–1137 (1990).

70. Duan, N., Mays, L. W. & Lansey, K. E. OPTIMAL RELIABILITY-BASED DESIGN OF PUMPING AND DISTRIBUTION SYSTEMS. J. Hydraul. Eng. (1990). doi:10.1061/(ASCE)0733-9429(1990)116:2(249)

71. Jacobs, P. & Goulter, I. Estimation of Maximum Cut-Set Size for Water Network Failure. J. Water Resour. Plann. Manag. 117, 588–605 (1991).

72. Cullinane, B. M. J., Lansey, K. E. & Mays, L. W. Optimization-availability-based design o f water-distribution networks. J. Hydraul. Eng. 118, 420–441 (1992).

73. Fujiwara, O. & Ganesharajah, T. Reliability assessment of water supply systems with storage and distribution networks. Water Resour. Res. 29, 2917–2924 (1993).

74. Gupta, R. & Bhave, P. R. Reliability Analysis of Water-Distribution Systems. J. Environ. Eng. 120, 447–461 (1994).

75. Xu, C. & Goulter, I. C. RELIABILITY-BASED OPTIMAL DESIGN OF WATER DISTRIBUTION NETWORKS. J. Water Resour. Plan. Manag. (1999). doi:10.1061/(ASCE)0733-9496(1999)125:6(352)

76. Tanyimboh, T. T., Burd, R., Burrows, R. & Tabest, M. Modelling and Reliability Analysis of Water Distribution of Water Distribution Systems. Water Sci. Technol. 39, 241–248 (1999).

77. Gargano, R. & Pianese, D. Reliability as Tool for Hydraulic Network Planning. J. Hydraul. Eng. 126, 354–364 (2000).

78. Bartos, M. D. & Chester, M. V. The Conservation Nexus: Valuing Interdependent Water and Energy Savings in Arizona. (2014).

79. Hwang, H. & Lansey, K. ARVIN : ARizona Value INtegrated Water , Energy , and Agriculture Planning Model ARVIN : ARizona Value INtegrated optimization model. (2015).

80. Berardy, A. & Chester, M. V. Climate Change Vulnerability in the Food, Energy, and Water Nexus: Concerns for Agricultural Production in Arizona and its Urban Export Supply. Environ. Res. Lett. (2017). doi:10.1042/BJ20101136>

81. Eisenman, D. P. et al. Health & Place Heat Death Associations with the built environment , social vulnerability and their interactions with rising temperature. Health Place 41, 89–99 (2016).

82. Basics for practical operation Motor Starting. 1, 46 (1998).

83. Hoffman's Industrial/Commercial Specifier's Guide: Technical Information. Hoffman (Hoffman, 2017).

84. Kreeley, B. & Coulton, S. Increasing the Lifespan and Reliability of Electrical Components. 1–5 (2012).

85. Climate Impacts Decision-Support Tool. USAID (2102).

86. Energy, E. & Division, T. E Rnest O Rlando L Awrence Estimating Risk To California Energy Infrastructure From Projected Climate Change. (2011).

87. Burillo, D., Chester, M. V., Ruddell, B. & Johnson, N. Electricity demand planning forecasts should consider climate non-stationarity to maintain reserve margins during heat waves. Appl. Energy (2017). doi:10.1016/j.apenergy.2017.08.141

88. Shahid, S. Vulnerability of the power sector of Bangladesh to climate change and extreme weather events. Reg. Environ. Chang. 12, 595–606 (2012).

89. Rasmussen, B., Morse, L., Perlman, D., Filosa, G. & Poe, C. A Framework for Considering Climate Change in Transportation and Land Use Scenario Planning Lessons Learned from an Interagency Pilot Project on Cape Cod. 298, (2012).

90. Integrating Climate Change into the Transportation Planning Process. (2008).

91. Can, W., Agencies, T., To, D. O., Resilience, B. & Responding, F. I. S. CHANGE CLIMATE RESILIENT Resources to Build Resilience. 1–3 (2012).

92. Rinaldi, S. M., Peerenboom, J. P. & Kelly, T. K. Identifying, understanding, and analyzing critical infrastructure interdependencies. IEEE Control Syst. Mag. 21, 11–25 (2001).

93. Pederson, P., Dudenhoeffer, D., Hartley, S. & Permann, M. Critical infrastructure interdependency modeling: a survey of US and international research. Idaho Natl. Lab. 1–20 (2006). doi:10.2172/911792

94. Lubega, W. N. & Farid, a M. A Reference System Architecture for the Energy–Water Nexus. Syst. Journal, IEEE PP, 1–11 (2014).

95. Wang, S., Hong, L. & Chen, X. Vulnerability analysis of interdependent infrastructure systems: A methodological framework. Phys. A Stat. Mech. its Appl. 391, 3323–3335 (2012).

96. Wang, S., Hong, L., Ouyang, M., Zhang, J. & Chen, X. Vulnerability analysis of interdependent infrastructure systems under edge attack strategies. Saf. Sci. 51, 328–337 (2013).

97. Johansson, J. & Hassel, H. An approach for modelling interdependent infrastructures in the context of vulnerability analysis. Reliab. Eng. Syst. Saf. 95, 1335–1344 (2010).

98. Carter, N. T. Energy-Water Nexus : The Energy Sector ' s Water Use. (2014).

99. Birol, F. et al. in World Energy Outlook 2012 1–33 (2012).

100. Haimes, Y. Y. & Jiang, P. Leontief - Based Model of Risk in Complex Interconnected Infrastructures. 7, 1–12 (2001).

101. Bagheri, E., Baghi, H. & Ghorbani, A. A. An Agent-based Service-Oriented Simulation Suite for Critical Infrastructure Behavior Analysis.

102. Barton, D. C., Edison, E. D., Schoenwald, D. A., Cox, R. G. & Rhonda, K. Simulating Economic Effects of Disruptions in the Telecommunications Infrastructure. (2004).

103. Panzieri, S., Setola, R. & Ulivi, G. AN APPROACH TO MODEL COMPLEX. (2003).

104. Veselka, T., Boyd, G., Conzelmann, G. & Koritarov, V. SIMULATING THE BEHAVIOR OF ELECTRICITY MARKETS WITH AN AGENT-BASED METHODOLOGY : THE ELECTRIC MARKET COMPLEX ADAPTIVE SYSTEMS (EMCAS) MODEL * Center for Energy , Environmental , and

Economic Systems Analysis Argonne National Laboratory Argonne , IL 6043. (2001).

105. Donzelli, P. Identifying and evaluating risks related to enterprise dependencies : a practical goal-driven risk analysis framework Roberto Setola *. 1120–1137 (2007).

106. Zhang, P., Peeta, S. & Friesz, T. Dynamic Game Theoretic Model of Multi-Layer. 147–178 (2005).

107. Eidson, E. D. & Ehlen, M. A. NISAC Agent-Based Laboratory for Economics (N-ABLE □): Overview of Agent and Simulation Architectures. (2005).

108. Barrett, C. L. et al. TRANSIMS : TRansportation ANalysis SIMulation System. (2003).

109. Pye, G. & Warren, M. Analysis and Modelling of Critical Infrastructure Systems.

110. Moini, N., Ph, D. & Asce, M. Modeling of Risks Threatening Critical Infrastructures : System Approach. 1–10 (2014). doi:10.1061/(ASCE)IS.1943-555X.0000263.

111. Rheinheimer, D. E., Ligare, S. T. & Viers, J. H. WATER AND ENERGY SECTOR VULNERABILITY TO CLIMATE WARMING IN THE SIERRA NEVADA : Simulating the Regulated Rivers of California ' s West Slope Sierra Nevada. (2012).

112. Rübbelke, D. & Vögele, S. Impacts of climate change on European critical infrastructures: The case of the power sector. Environ. Sci. Policy 14, 53–63 (2011).

113. Loggins, R. a & Wallace, W. a. Rapid Assessment of Hurricane Damage and Disruption to Interdependent Civil Infrastructures Systems. Accept. by J. Infrastruct. Syst. 21, 1–19 (2015).

114. Bella, J., Cascos, G., Ciaccia, J., Tripp, J. & Qussar, S. Emergency Backup Power Supply. 41–43 (2004).

115. Guinyard, T., Woo, O. & Arvin, C. Crews Investigating Newport Bech Water Main Break. NBC (2015).

116. Bartos, M. D. & Chester, M. V. The conservation nexus: Valuing interdependent water and energy savings in Arizona. Environ. Sci. Technol. 48, 2139–2149 (2014).

117. Gillette, J., Fisher, R., Peerenboom, J. & Whitfield, R. ANALYZING WATER / WASTEWATER INFRASTRUCTURE INTERDEPENDENCIES.

118. Lawrence, P. R. & Lorsch, J. W. Differentiation and Integration in Complex Organizations Linked references are available on JSTOR for this article : Differentiation and Integration in Complex Organizations. 12, 1–47 (1967).

119. Chester, M. V. & Allenby, B. Toward adaptive infrastructure: flexibility and agility in a non-stationarity age. Sustain. Resilient Infrastruct. (2018). doi:10.1080/23789689.2017.1416846

120. Sherehiy, B., Karwowski, W. & Layer, J. K. A review of enterprise agility: Concepts, frameworks, and attributes. Int. J. Ind. Ergon. doi:https://doi.org/10.1016/j.ergon.2007.01.007

121. Bureau of Reclamation. Downscaled CMIP3 an CMIP5 Climate and Hydrology Projections: Release of Downscaled CMIP5 Climate Projections, Comparison with preceding Information, and Summary of User Needs. Prepared by the U.S. Department of the Interior, Bureau of Reclamation, Technic. 47pp (2013).

122. Garfin, G. et al. in Climate Change Impacts in the United States: The Third National Climate Assessment 462–486 (U.S. Global Research Program, 462-486, 2014). doi:10.7930/J08G8HMN.On

123. U.S. Environmental Protection Agency. Reducing Urban Heat Islands: Compendium of Strategies - Urban Heat Island Basics. (2012).

124. Coughlin, K. & Goldman, C. Physical Impacts of Climate Change on the Western US Electricity System : A Scoping Study. (2008).

125. Reliability Analysis of Water Distribution Systems. (American Society of Civil Engineers, 1989).

126. Rubin, S. A call for reliability standards. J. / Am. Water Work. Assoc. 103, 22–24 (2011).

127. AWWA. Buried No Longer: Confronting America's water infrastructure challenge. Am. Water Work. Assoc. 37 (2011).

128. Park, J., Seager, T. P., Rao, P. S. C., Convertino, M. & Linkov, I. Integrating risk and resilience approaches to catastrophe management in engineering systems. Risk Anal. 33, 356–367 (2013).

129. Hu, Y., Wang, D., Cossitt, K. & Chowdhury, R. AC Pipe in North America : inventory , breakage , and working environments. J. Pipeline Syst. Eng. Pract. 1, 156–172 (2010).

130. Habibian, A. Effect of Temperature Changes on Water-Main Breaks. 120, 312–321 (1994).

131. Rajani, B., Zhan, C. & Kuraoka, S. Pipe-soil interaction analysis of jointed water mains. Can. Geotech. J. 33, 393–404 (1996).

132. Operator's Companion. (USA Blue Book, 2013).

133. Office of Ground Water and Drinking Water Distribution System Issue Paper: Nitrification. United States Environmental Protection Agency (2002).

134. Ralph, L., Heyn, K., Brooks, K. & Adams, A. AWWA Webinar Program: What You Need to Know About Climate Risks to Water Utility Infrastructure and Assets. (2016).

135. Chowdhury, S., Champagne, P. & McLellan, P. J. Models for predicting disinfection byproduct (DBP) formation in drinking waters: A chronological review. Sci. Total Environ. 407, 4189–4206 (2009).

136. Christensen, F. M., Andersen, O., Duijm, N. J. & Harremoës, P. Risk terminology - A platform for common understanding and better communication. J. Hazard. Mater. 103, 181–203 (2003).

137. Past Weather in Phoenix. timeanddate.com (2017). Available at: https://www.timeanddate.com/weather/usa/phoenix/historic. (Accessed: 1st January 2017)

138. Bureau, U. S. C. Population and Housing Unit Estimates. United States Census Bureau (2016).

139. US Climate Data. (2016). Available at: http://www.usclimatedata.com/climate/phoenix/arizona/united-states/usaz0166. (Accessed: 5th October 2016)

140. City of Phoenix. PHX Water Smart. (2016).

141. Operating and Capital Budget Plan: Fiscal Year 2015 - 2016. (2015).

142. Sakaue, K., Kamata, M., Iwamoto, S. & Nimiya, H. The Prediction Method of Water Temperature in Distribution Pipes. 1–15

143. Blokker, E. J. M. & Pieterse-Quirijns, E. J. Modeling temperature in the drinking water distribution system. J. Am. Water Work. Assoc. 105, E19–E28 (2013).

144. Randall-Smith, M. Guidance manual for the structural condition assessments of trunk mains. (WRC, 1992).

145. Palisade. @Risk. (2016).

146. Tobias, P. A. Applied Reliability. (CRC Press LLC, 1986).

147. Henley, E. J. & Kumamoto, H. Reliability Engineering and Risk Assessment. (Prentice-Hall, 1981).

148. United States Environmental Protection Agency. National Primary Drinking Water Regulations. Drink. Water Contam. 141–142 (2013). doi:EPA 816-F-09-004

149. USEPA. National Primary Drinking Water Regulations: Disinfectants and the disinfection byproducts. Public Law 351 (1998).

150. Association, F. R. W. Water Transmission and Distribution for Water Treatment Plant Operators. (2005).

151. Phoenix. 2013 Annual Water Quality Report. 1–8 (2013).

152. Adams, A. & Butterfield, J. 2014 Water Quality Report. (2014).

153. Dam, C. Water Quality Report. (2015).

154. Phoenix, C. of. 2012 Annual Water Quality Report. 1–8 (2009).

155. City of Phoenix. 2011 Annual Water Quality Report. 1–8 (2011).

156. 2016 Water Quality Report. (2016).

157. District, L. V. V. W. Operating and Capital Budget 2017. (2016).

158. Las Vegas, NV. Weather Underground

159. UN-WWAP. The United Nations World Water Development Report 2015: Water for a Sustainable World. (2015). doi:978-92-3-100071-3

160. E-c, N. Climate Change and Transportation. (2012).

161. Allen, M. et al. Managing the water distribution network with a Smart Water Grid. Smart Water 1, 4 (2016).

162. Milly, P. C. D. et al. Stationarity Is Dead: Whither Water Management? Science (80-.). 319, 573–574 (2008).

163. Bartos, M. D. & Chester, M. V. Impacts of climate change on electric power supply in the Western United States. Nat. Clim. Chang. 5, 748–752 (2015).

164. Melillo, J. M., Richmond, T. (T. C. . & Gary W. Yohe, Eds., 2014. Climate Change Impacts in the United States. (2014). doi:10.7930/j0z31WJ2

165. Application Guideline # 05 Temperature Rise – Insulation. 05, (2017).

166. Chinowsky, P. S., Strzepek, K., Larsen, P. & Opdahl, A. Adaptive Climate Response Cost Models for Infrastructure. J. Infrastruct. Syst. 16, 173–180 (2010).

167. Hughes, G., Chinowsky, P. & Strzepek, K. The costs of adaptation to climate change for water infrastructure in OECD countries. Util. Policy 18, 142–153 (2010).

168. Northwood, J. & Filion, Y. R. Impact of climate change on hydraulic performance in water distribution networks. Proc. 10th Annu. Water Distrib. Syst. Anal. Conf. WDSA 2008 163–172 (2009). doi:10.1061/41024(340)15

169. Wagner, B. J. M., Shamir, U. & Marks, D. H. Water Distribution Reliability: Analytical Methods. 114, 253–275 (1988).

170. Wagner, B. J. M., Shamir, U. & Marks, D. H. WATER DISTRIBUTION RELIABILITY: SIMULATION METHODS. 114, 276–294 (1988).

171. Fujiwara, O. & Ganesharajah, T. Reliability assessment of water supply systems with storage and distribution networks. Water Resour. Res. (1993). doi:10.1029/93WR00857

172. Duan, N., Mays, L. W. & Lansey, K. E. Optimal Reliability-Based Design of Pumping and Distribution Systems. 116, 249–268 (1990).

173. Kettler, A. & Goulter, I. Reliability consideration in the least cost design of looped water distribution networks. in Proceeding of 10th International Symposium on Urban Hydrology, Hydraulic and Sediment Control (1983).

174. Xu, C. & Goulter, I. Probabilistic Model for Water Distribution Reliability. J. Water Resour. Plan. Manag. 13, 5416–5421 (1998).

175. Climate Models. Climate.gov

176. City of Phoenix Water Services. (2018). Available at: https://www.phoenix.gov/waterservices/waterquality. (Accessed: 1st May 2018)

177. Water Distribution System Development Standards. (2009).

178. Sakarya, A. B. A. & Mays, L. W. Optimal Operation of Water Distribution Pumps Considering Water Quality. 126, 28–30 (2005).

179. Vasconcelos, J. J., Rossman, L. A., Grayman, W. M., Boulous, P. F. & Clark, R. M. Kinetics of chlorine decay. Am. Water Work. Assoc. 89, 54–65 (1997).

180. Rossman, L. A. EPANET Users Manual. (1994).

181. Goldman, F. E. & Mays, L. W. Water distribution system operation: Application of simulated annealing. Water Resouces Syst. Manag. Tools 5.1-5.18 (2005).

182. Rex, T. R. DEVELOPMENT OF METROPOLITAN PHOENIX : HISTORICAL , CURRENT AND FUTURE TRENDS August 2000 Prepared for the Morrison Institute for Public Policy School of Public Affairs College of Public Programs Arizona State University As part of the Brookings Growth Cas. 4011, (2000).

183. Cullinane, John, M. in Reliability Analysis of Water Distribution Systems (ed. Mays, L.) (American Society of Civil Engineers, 1989).

184. Farmer, L. The 7 Deadly Sins of Public Finance. Governing 5 (2014).

185. Water Utility Management: Manual of Water Supply Practices M5. (American Water Works Association, 2005).

186. Eisenberg, D. A. How to think about resilient infrastructure systems. (Arizona State University, 2018).

187. Hurd, T. et al. Networks: An Introduction. Phys. Rev. E (2010). doi:10.1093/acprof:oso/9780199206650.001.0001

188. Herrera, M., Abraham, E. & Stoianov, I. A Graph-Theoretic Framework for Assessing the Resilience of Sectorised Water Distribution Networks. Water Resour. Manag. 30, 1685–1699 (2016).

189. Woods, D. D. Four concepts for resilience and the implications for the future of resilience engineering. Reliab. Eng. Syst. Saf. 141, 5–9 (2015).

190. Leveson, N. A new accident model for engineering safer systems. 42, 237–270 (2004).

191. Derrible, S. Urban infrastructure is not a tree : Integrating and decentralizing urban infrastructure systems. (2017). doi:10.1177/0265813516647063

192. Leveson, N. G. System Safety Engineering : Back To The Future. (2002).

193. Reilly, A. C., Samuel, A., Guikema, S. D. & Reilly, A. C. Critical Infrastructure Interdependent Critical Infrastructure. (2015).

194. Complete, I. Emergency Backup Power Supply. (2004).

195. Liscouski, B. & Elliot, W. U.S.-Canada Power System Outage Task Force. System 40, 238 (2004).

196. Gilpin, K. N. Blackout Brings Water Shutdowns to Cleveland and Detroit. The New York Times (2003).

197. The Economic Impacts of the August 2003 Blackout. (2004).

198. Rinaldi, S. M., Peerenboom, J. P. & Kelly, T. K. Identifying, Understanding, and Analyzing Critical Infrastructure Interdependencies. IEEE Control Syst. Mag. (2001). doi:10.3406/sosan.1996.1375

199. What transients are and why you need protection Transient overvoltages. 44, (2012).

200. Lubega, W. N. & Farid, A. M. Quantitative engineering systems modeling and analysis of the energy–water nexus. Appl. Energy 135, 142–157 (2014).

201. Lall, U. & Mays, L. W. Model for planning water-energy systems. Water Resour. Res. 17, 853–865 (1981).

202. Pate, R., Hightower, M., Cameron, C. & Einfeld, W. OVERVIEW OF ENERGY-WATER INTERDEPENDENCIES AND THE EMERGING ENERGY DEMANDS ON WATER RESOURCES. (2007).

203. Brendan, B. AN OPERATIONAL MODEL OF INTERDEPENDENT WATER AND POWER DISTRIBUTION INFRASTRUCTURE SYSTEMS NAVAL POSTGRADUATE. (2018).

204. Data Sheets for IEEE 14 Bus System. Power Systems Test Case Archive (2003). Available at: http://labs.ece.uw.edu/pstca/pf14/pg_tca14bus.htm. (Accessed: 22nd April 2019)

205. Reliability Standards for the Bulk Electric Systems of North America. (2017).

206. Rossman, L. A. EPANET Manual. Soc. Stud. Sci. 38, 483–508 (2000).

207. Pinnacle West 2016 Annual Report. (2017).

208. U.S. Census Bureau QuickFacts. (2017). Available at: https://www.census.gov/quickfacts/fact/table/phoenixcityarizona/PST045218. (Accessed: 22nd April 2019)

209. Developer Handbook. (Western Municipal Water District, 2011).

210. Dugan, R. C. & Ballanti, A. OpenDSS Manual. Train. Mater. 1–184 (2016).

211. Hamel, D. et al. Resilient Infrastructure Simulation Environment (RISE). (2019).

212. Fraser, A., Chester, M. V., Hoehne, C., Markolf, S. A. & Underwood, B. S. Transportation resilience to climate change and extreme weather events – Beyond risk and robustness. Transp. Policy 74, 174–186 (2018).

213. Kirby, B. J. & Dyke, J. W. Van. Congestion Management Requirements. (2002).

214. Nerc. Technical Analysis of the August 14, 2003, Blackout: What Happened, Why, and What Did We Learn? 124 (2004).

215. Gim, C., Miller, C. A. & Hirt, P. W. The resilience work of institutions. Environ. Sci. Policy 97, 36–43 (2019).

216. Penrose, H. W. Electric motors: Repair or replace? Plant Services (2011).

217. City of Phoenix. The Phoenix Detail Budget 2015-16. (2015).

218. Bojórquez-tapia, L. A. et al. Spatially-explicit simulation of two-way coupling of complex socio- environmental systems : Socio-hydrological risk and decision making in Mexico City. 1, 1–15

219. DHS Risk Lexicon. (2010).

220. Ahern, J. From fail-safe to safe-to-fail: Sustainability and resilience in the new urban world. Landsc. Urban Plan. 100, 341–343 (2011).

221. Linkov, I. et al. Changing the resilience paradigm. Nat. Clim. Chang. 4, 407–409 (2014).

222. Füssel, H. M. Adaptation planning for climate change: Concepts, assessment approaches, and key lessons. Sustain. Sci. 2, 265–275 (2007).

223. Kim, Y. et al. Fail-Safe and Safe-to-Fail Adaptation: Decision-making for Urban Flooding under Climate Change. Clim. Change In Press, (2017).

224. Gifford, M. Personal Communication. (2016).

225. City of Phoenix. 2011 Water Resource Plan City of Phoenix. 85 (2011).

226. Arizona Safe Drinking Water Information System 3.0 (AZSDWIS). Available at: http://azsdwis.azdeq.gov/DWW_EXT/. (Accessed: 12th January 2016)

227. Nevada, S. of. Nevada Drinking Water Information System (NDWIS). (2014). Available at: http://ndep.nv.gov/bsdw/ndwis.htm. (Accessed: 12th January 2016)

228. AMERICAN Products Lay the Foundation for Major Water Improvements in South Dakota. (2017).

229. WEB Water Treatment Plant - 'Heart' of the WEB Water System. (2014). Available at: http://www.webwater.org/web-water-treatment-plant-heart-of-the-web-water-system/.

230. Folkman, S. Water Main Break Rates In the USA and Canada. 1–26 (2012).

231. Spellman, F. & Drinan, J. Piping and Valves. (CRC Press LLC, 2001).

232. Brown, P. Personal Communication. (2015).

233. Special Thickness Classes. American Cast Iron Pipe Company (2016). Available at: http://www.american-usa.com/products/ductile-iron-pipe-and-fittings/unrestrained-joint-pipe/fastite-joint-pipe/special-thickness-classes. (Accessed: 3rd October 2016)

234. Medinger, C. Helping motors keep their cool. Reliable Plant

235. Association, A. W. W. Effects of Water Age on Distribution System Water Quality. United States Environ. Prot. Agency (2002).

236. Monteiro, L., Viegas, R. M. C., Covas, D. I. C. & Menaia, J. Modelling chlorine residual decay as influenced by temperature. Water Environ. J. 29, 331–337 (2015).

237. Zerbe, J. & Siepak, J. Drinking water quality standards and methods of its enforcement in Poland. Przegl. Lek. 58 Suppl 7, 5–9 (2001).

238. Wagenet, L., Heidekamp, A. & Lemley, A. Water Treatment: Notes. Water Treatment (2005). doi:10.5772/2883

239. Bromide in Drinking-Water. World Heal. Organ. (2009). doi:05.03.2015

240. Chawla, R., Varma, M., Balram, A., Murali, M. & Natarajan, P. Trihalomethane Removal and Formation Mechanism in Water. (1983).

241. CL17 Free Chlorine Analyzer. Hach (2017). Available at: https://www.hach.com/cl17-free-chlorine-analyzer/product?id=7640295880.

242. AW400 Residual chlorine monitor. (2016).

243. Reliability Basics: How Good Is Your Assumed Distribution's Fit? Reliability HotWire (2007). Available at: http://www.weibull.com/hotwire/issue71/relbasics71.htm. (Accessed: 14th April 2018)

244. D'Agostino & Stephens. Goodness-Of-Fit Techniques. (Marcel Dekker, Inc., 1986).

245. NIST/SEMATECH e-Handbook of Statistical Methods. U.S. Department of Commerce (2012). Available at: https://www.itl.nist.gov/div898/handbook/eda/section3/eda35e.htm.

APPENDIX A

SUPPLEMENTARY INFORMATION FOR CHAPTER 2

A.1 Overall methodology process flow

The sequential steps of the risk projection and suggestion of prioritization of operational strategies is shown in Figure 26.

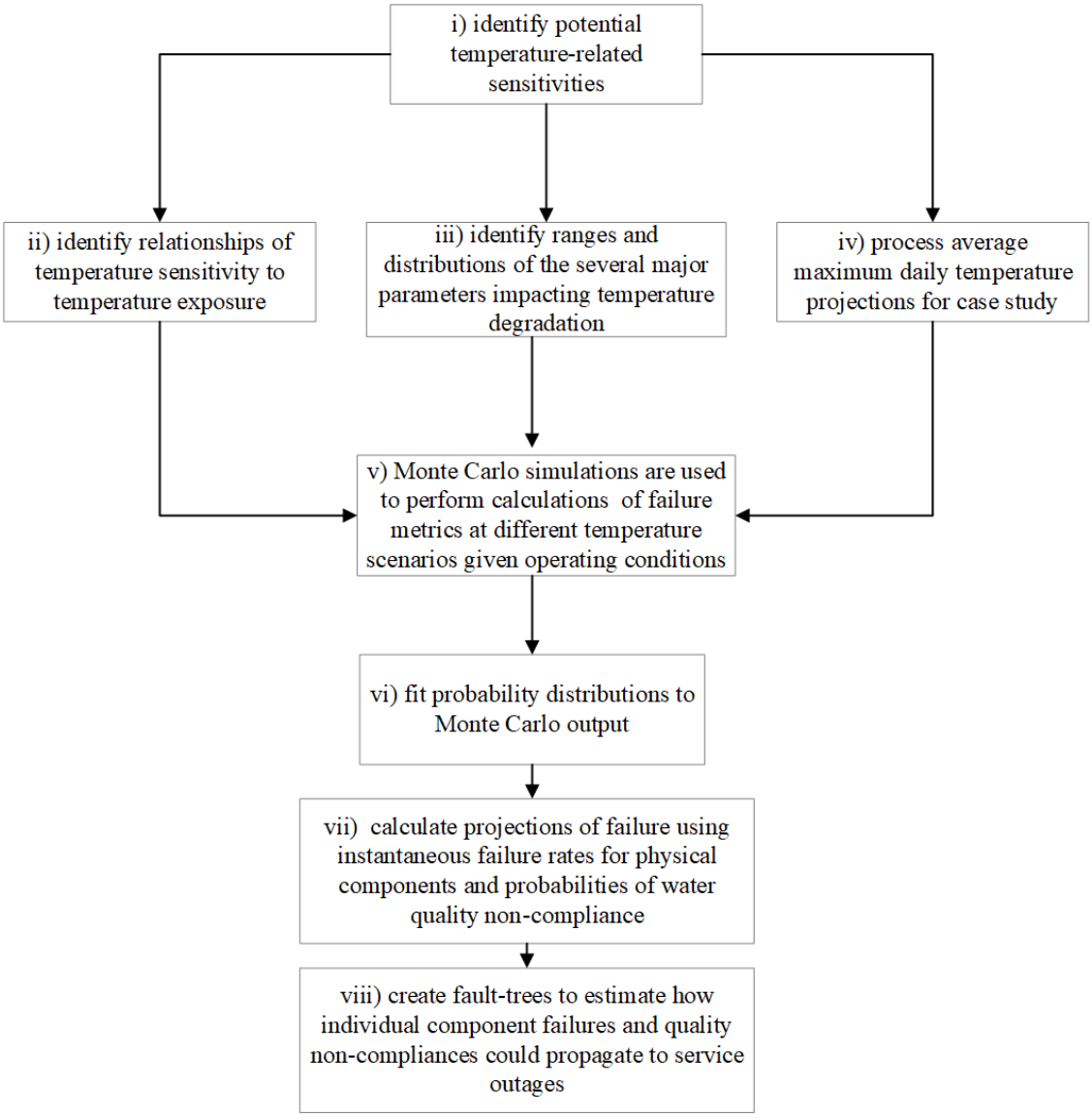

Figure 26 Methodology Process Flow

A.2 Identifying Temperature-Related Sensitivity and Exposure

A literature review was conducted to identify which infrastructure components within water treatment and distribution systems are sensitive to temperatures. These components, including their mechanisms of temperature-sensitivity, are shown in Table 2.

Table 2 Temperature Sensitive Components Identified through Literature Review

Infrastructure Component	Temperature-Sensitivity	Type of Temperature Stress over summertime period	Source(s)
Motor	Overheating	Ambient temperature surrounding motor	[10–12,82]
Electronics	Overheating	Ambient temperature surrounding electrical cabinet	[83,84]
Plastic pipe	Degradation	Water temperature	[16]
Metal pipe	Corrosion	Water temperature	[17]
Pipe	Fracture from soil expansion	Soil temperature	[129]
Water quality	Chlorine residual decay	Water temperature	[32]
Water quality	Total trihalomethane (TTHM) growth	Water temperature	[33]

Water quality	Trihaloactic acid (THAA) growth	Water temperature	[34]
Water quality	*Legionella* growth	Water temperature	[35,36]
Water quality	*Mycobacterium avium* complex (MAC) growth	Water temperature	[37,38]
Water quality	Nitrification increase	Water temperature	[39–41,133]
Water demand	Increase	Ambient air temperature	[25]
Operators	Heat fatigue	Ambient air temperature	[132]

The degradation rate of the motors and electronics is theoretically related to the cumulative difference between the operating temperature (ambient temperature plus temperature from dissipated heat) and the design temperature during the summer. The studies of other environmental and public health hazards have found that the impact of a hazard depends on "the concentration, amount or intensity of a particular agent that reaches a target system in terms of its duration, frequency, and intensity".[136] It is therefore assumed that physical components experiencing degradation would have varying levels of degradation for different durations of exposure along with magnitudes of temperature exposure. A proposed equation for the rate of component degradation of motors and electronics over a time for period as a function of exposure temperature, has been formulated as shown in Equations 3 – 5.

$$r_d = \int_{t_1}^{t_2} \alpha \cdot \max\left(0, T(t)\right)^{\beta} dt \quad (3)$$

$$T(t) = T_O(t) - T_d \quad (4)$$

$$T_O(t) = T_a(t) + T_h(t) \quad (5)$$

r_d is rate of degradation [lifespan/^{o}C], T is the ambient of temperature of exposure [^{o}C], α and β are the linear and exponential parameters of degradation, T_O is the operating temperature of the component [^{o}C], T_d is the designed maximum allowable temperature of a component [^{o}C], T_a is the ambient temperature [^{o}C], and T_h is the change in temperature surrounding the component as a result of the heat dissipation from friction of operation [^{o}C]. The temperature from dissipated heat, Th, is modeled as an average range, and the ambient temperature is assumed to be $T_{a,max}$, the 3-month average of maximum daily ambient temperatures. T_h is 105- 115 ^{o}C for motors and 5.5-55.5 ^{o}C for electronics as described in SI Table S6. T_o and consequentially are r_d averages as well. The modifications to the degradation rate made for the purposes of modeling are shown in Equations 6 - 8. The bounds of integration are defined as the summertime period, t_1 = June 1st and t_2 = August 31st.

$$\overline{r_d} = \alpha \cdot \max\left(0, \overline{T}\right)^{\beta} \quad (6)$$

$$\overline{T} = \overline{T_O} - T_d \quad (7)$$

$$\overline{T_O} = \overline{T_{a,max}} + \overline{T_h} \quad (8)$$

Similarly, little is known about how long it takes for chemical reactions to change given a change in water temperature.

A.3 Urban Water System Case Study

The potable water distribution and treatment systems within the overall water system were chosen for the analysis as highlighted in Figure 27. The temperature projections for Phoenix, Arizona and Las Vegas, Nevada from global climate models are shown in Figure 28.

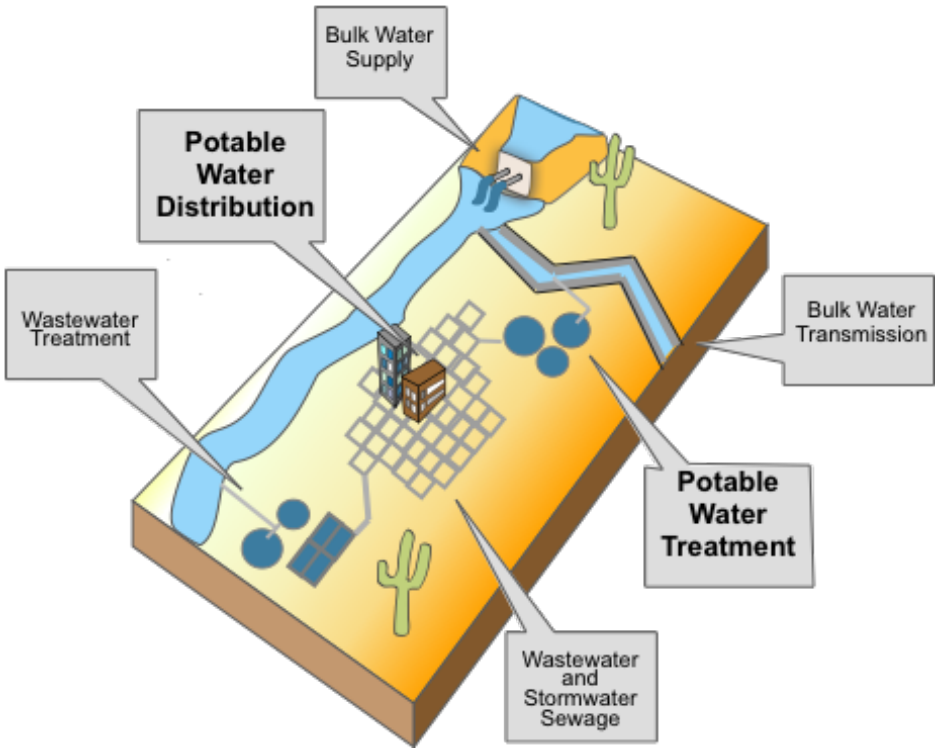

Figure 27 Urban Water Infrastructure Systems. The potable water treatment and distribution infrastructure systems (bolded text) are analyzed because the failure of components could most logically be linked to the failure of municipal residents not receiving sufficient amounts and quality of water.

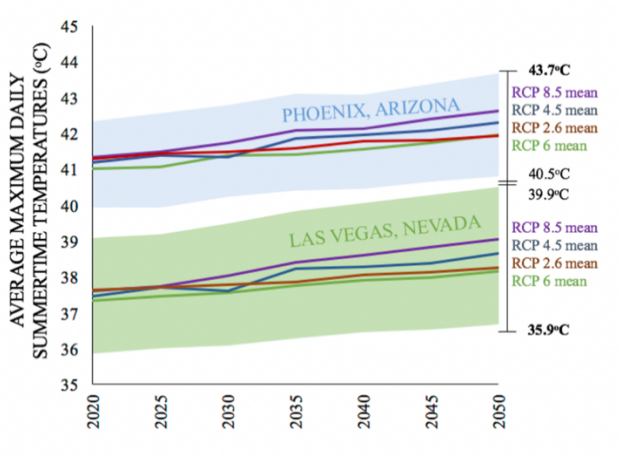

Figure 28 Average of Maximum Daily Summer Air Temperature (3x3) Projections from Global Climate Models for Phoenix, Arizona and Las Vegas, Nevada. Air temperatures in Phoenix and Las Vegas are projected to significantly increase by 2050 in all RCP scenarios.

A potable water treatment and distribution system with representative Phoenix and Las Vegas characteristics was selected for the analysis. Characteristics of the Phoenix and Las Vegas are shown in Table 3.

Table 3 Potable Water Treatment and Distribution System Characteristic Comparison in Phoenix, Arizona and Las Vegas, Nevada.

Characteristic	City of Phoenix, Arizona	Las Vegas Water District, Nevada	Source
Projected temperature range from 2020 - 2050	39.9 – 43.7°C	35.9 – 40.5°C	[121]

Projected temperature increase from 2020 - 2050	0.4 – 1.7°C	0.6 – 2.0°C	[121]
Treatment Capacity (MGD)	700 MGD	900 MGD	[155,157]
Number of pumping stations in distribution system	110	100	[140,224]
Miles of pipe in whole system	7,000	7,000	[140,224]
Number of WTPs	6	2	[157,225]
Number of Quality Sampling Stations	70	No record	[226,227]

In many ways, the Phoenix and Las Vegas water infrastructure are similar, thus a water system with combined characteristics between the two places was modeled. The number of components in the combined system is shown in Table 4. The redundancies of components modeled are shown in Table 5. The number of opportunities for water outages are shown in Table 6, and the modeled operating characteristics are shown in Table 7. Inputs into the model listed in Tables S3-S6 represent scenarios. Some of the scenarios are representative of Phoenix/Las Vegas specifically, some are generic to all modern water infrastructure systems, and some are reasonable scenarios based on engineering judgement as guided by textbooks and interviews with utility engineers. The scenario type was chosen based on the amount of data available. All scenarios were specific to Phoenix and Las Vegas where possible.

Table 4 Case Study Water System Components

Modeled Component	Phoenix and Las Vegas – type system	Type of Scenario	Explanation of Scenario
Total number of pumping stations in overall water system	100	specific	Data from Las Vegas and Phoenix city documents and conversations with engineers. 140,224

Number of WTPs	4	specific	Data found from Las Vegas and Phoenix city documents.[157,225]
Number of pumping stations in each WTP	2	reasonable	The situation for pumping units is applied to pumping stations. [183]
Number of pumping units per pumping station	2 (1 standby)	reasonable	This is stated as a minimal case for most water systems. This series system behavior allows for propagation of failure rates. [183]
Number of motors per pumping unit	1	reasonable	Motor is referred to singularly as housed in a pump casing.[12]
Number of electronic controls per pumping unit	1	reasonable	Controls are needed to operate each motor. [183]
Treatment Capacity (MGD)	800	realistic	Average value between Las Vegas and Phoenix. [140,224]
Miles of pipe in WDS	7,000	reasonable	Data from Las Vegas and Phoenix city documents and engineers. [140,224]
Miles of pipe in WTP	540	reasonable	A pipe manufacturer's website disclosed how many miles of pipe were used in an expansion of a water treatment plant for a certain number of counties.[228] The

			counties per MGD fraction for that water utility[229] was used to translate the mileage to a Las Vegas and Phoenix type system.
Percentage PVC pipes in WDS	30%	realistic	This is the average percentage reported for AZ, NM, TX, OK, AR, & LA.[230]
Percentage cast iron pipe in WDS	20%	realistic	This is the average percentage reported for AZ, NM, TX, OK, AR, & LA.[230]
Percentage PVC pipes in WTP	0%	reasonable	"PVC is only used for low pressure applications and transportation of coarse solids" in WTPs.[231]
Percentage cast iron pipe in WTP	100%	reasonable	"Metal is one of the principle materials" used for piping in WTPs. [231]
Sampling Stations	70	specific	Data found from City of Phoenix non-compliance reporting website. [226]

Redundancies prevent component failures from cascading to system failures [125]. Table 5 shows the number of redundancies of various processes within the system that are available when other components fail. The number of components and amounts of backup resources in Table 5 are inputs to estimating systemic failures. These values are scenarios either pulled from examples from an engineering text, or are from discussions with water treatment and distribution engineers.

Table 5 Redundancy Scenarios

Characteristic	Number for modeled scenario	Type of Scenario	Explanation of Scenario
Number of pumping units needed to be in operation for pumping station to deliver water	2	reasonable	This is stated as the typical case for most water systems. [183]
Number of WTPs that can supply a pressure zone	2	reasonable	City of Tempe engineer told authors a story of how a lightning storm caused the two WTPs in the city to fail which caused a pressure decrease in a pressure zone. [232]

Number of WTPs needed to be operational for all water to be delivered	2	reasonable	City of Tempe engineer told authors a story of how a lightning storm caused the two WTPs in the city to fail which caused a pressure decrease in a pressure zone. When only one WTP was down, the pressure was adequate. [232]
Amount of emergency storage of treated water at WTP	Insufficient Amount	reasonable	Depending on the outage time of components, the backup storage water could eventually become insufficient. [194]

Table 6 shows the annual systemic failure opportunities by process. These are the count of possible events where if components failed, they would cause some level of outage in a water distribution pressure zone (PZ). The values are estimated from the number of components in the system in Table 4. All scenarios are "reasonable" because predicting whether or not a pressure zone is more accurately dependent upon relational spatial and temporal information about components and demands.[125]

Table 6 Number of Modeled Opportunities for Systemic Failures.

Type of Systemic Failure	Phoenix and Las Vegas – type system value	Type of Scenario	Explanation of Scenarios
Pressure zone (PZ) from pumping station (PS) outage in WDS	82	reasonable	same as pumping stations
Pressure zone from PS outage in WTP	6	reasonable	same as number of WTPs
Pressure Zone from any PS outage	88	reasonable	PZ from PS outage in WDS + PZ from PS

			outage in WTP
Pressure zone from WTP pipe break	540	reasonable	miles of pipe in WTP that are cast iron or PVC
Pressure zone from WDS pipe break	3,500	reasonable	miles of pipe that are cast iron or PVC
Pressure zone failure opportunities from any pipe break	4,040	reasonable	Miles of pipe in WDS and WTP that are cast iron or PVC
Pressure zone outage from chlorine residual decay below threshold	70	reasonable	Number of sampling stations
Pressure zone outage from TTHM above threshold	70	reasonable	Number of sampling stations
Pressure zone outage from water quality non-compliance	70	reasonable	Number of sampling stations

Operating characteristics are shown in Table 7. The values were possible ranges or means found from literature. The ranges of operating characteristics are used as parameters in the failure metric equations used to create probability distributions that characterize physical component failure or water quality non-compliance.

Table 7 Modeled Operating Characteristics

Operating Characteristic	Distribution Parameters	Assumed Distribution type	Type of Scenario	Explanation of Scenario
Water temp. regression coefficient	range: 0.52 – 0.89	Uniform	generic	From empirical data from 9 Japanese WTPs.[142]
Water temp. regression constant (°C water/ °C air)	mean: 3.8113, std. dev.: 1.890	Normal	generic	From empirical data from 9 Japanese WTPs.[142]
Age of PVC pipes (yr)	min: 20, max: 80	Points	generic	From US and Canadian empirical data.[230]
Age of Iron pipes (yr)	min: 30, max: 70	Normal	generic	From US and Canadian empirical data.[230]
Pipe diameter (in)	range: 12-24	Uniform	generic	Range reported in text book.[7]

Pipe thickness (mm)	min: mean: 9.4615, std. dev.: 1.5875, max: mean: 12.6365, std. dev.: 1.5875	Lognormal	generic	Range from a pipe manufacturer.[233]
Insulation Class of Motors	F	Point	specific	Class of insulation used in hot climates[234]
Maximum rated motor temperature (ºC)	155	Point	specific	Maximum rated temperature for class F insulation [11]
Temperature rise of motor (dependent upon use) (ºC)	range: 105-115	Uniform	specific	Possible temperature rise range for class F insulation[11]
Age of Motor (years)	min: 5 max: 10	Points	reasonable	Low and high points equidistant from MTTF

Temperature rise in electronic cabinets (°C)	range: 5.5-55.5	Uniform	generic	Range reported for unfinished aluminum and stainless steel, and painted metallic and non-metallic enclosures with an 2-16 W/ft^2 input power[83]
Electronic Cabinet % temperature reduction from shielding	range: 25% - 46%	Uniform	reasonable	This is the range reported, assuming there is some amount of shielding[83]
Electronic cabinet % temperature reduction from circulating fans	10%	Point	reasonable	Assumption that even in worst case conditions, there is still a circulating fan. [83]
Electronic cabinet % temperature reduction from air	50% - 100%	Uniform	reasonable	Reasonable considering it is reported that AC can reduce temperature by up to 30°C[83]

conditioning (AC)				
Age of electronic component (years)	min: 7 max: 12	Points	reasonable	Low and high points equidistant from MTTF
Water age (h)	range: 32-72	Uniform	generic	Range found in EPA report.[235]
Specific UV absorbance (SUVA) (l/mg*m)	range: 1.04-1.21	Uniform	generic	Empirical range from journal article.[236]
TOC (mg/L)	range: 1.3 - 5.6	Uniform	generic	Range from white paper on water quality.[237]
pH	range: 6.5-8.5	Uniform	specific	Reported range from city water quality reports[152]
Initial chlorine concentration (mg/L)	range: 0.4-3	Uniform	generic	Reported range from white paper on water treatment.[238]
Bromide concentration (mg/L)	range: 0-0.5	Uniform	generic	Reported range from EPA report.[239]

$MTTF_{T1}$ of Pipes (yr)	scale (characteristic life): 47, shape: 2	Weibull	reasonable	The mean of 47 is reported. The shape parameter is chosen to be greater than one. [125,230]
$MTTF_{T1}$ of Motor (yr)	scale (characteristic life): 7.5, shape: 2	Weibull	reasonable	The mean of 7.5 is reported. The shape parameter is chosen to be greater than one. [125]
$MTTF_{T1}$ of Electronics (yr)	scale (characteristic life): 9.5, shape: 2	Weibull	reasonable	The mean of 9.5 is reported. The shape parameter is chosen to be greater than one. [125]

A.4 Modeling increases in component and water quality failure

A.4.1 Failure Metric Calculation

The equations used for each component are described in the following subsections.

A.4.1.1 Motor Degradation

An increase in ambient temperature poses a threat of overheating to the operation of motors and electronics that are vital to the operation of the pumping units. Motors can overheat from the combined dissipated heat from motor windings and the ambient

temperature surrounding the motor, causing destruction of the insulation which can lead to burnt stator windings [10–12,82]. For every 10°C increase in the operating temperature over the capacity of the insulation, the lifespan decreases by one-half [10–12,82]. The lifespan from this relationship was assumed to be the ETTF. All equations used for calculating motor ETTF are shown in Equations 9 - 11.

$$r_d = 0.5 \tag{9}$$

$$r_d = lifespan\ degradation\ rate\ per\ 10℃\ above\ insulation\ capacity$$
$$Lifespans = ETTF = lifespan\ or\ mean\text{-}time\text{-}to\text{-}failure\ of\ component$$

To calculate new ETTFs with temperature change, the following exponential decay model was created from the degradation rate information.

$$ETTF_{T2} = MTTF_{T1} * (1 - r_d)^{T/10} \tag{10}$$

Where

$$T = \left[\overline{T_{a,max}} + \overline{T_h}\right] - T_d \tag{11}$$
$$T_d = 155°C$$
$$MTTF_{T1} = the\ ETTF\ at\ an\ original\ temperature$$
$$ETTF_{T2} = the\ ETTF\ at\ a\ new\ temperature$$
$$T = temperature\ rise\ in\ the\ motor\ above\ the\ insulation\ capacity\ [℃]$$

T_h
$= temperature\ rise\ of\ motor\ due\ to\ dissapated\ heat\ from\ operation\ of\ windings\ [℃]$

$T_{a,max} = temperature\ rise\ of\ motor\ due\ to\ ambient\ temperature, scenarios\ [℃]$

$T_d = \max allowable\ operating\ temperature\ based\ on\ \ class\ F\ insulation\ capacity\ [°C]$

A.4.1.2 Electronic ETTF Degradation

Similar to motors, the electronic controls that are used for pump operation are typically stored in electrical cabinets, and for every 10°C rise in enclosure temperature above 40°C, the lifespan of the electronics decreases by one-half [83,84]. The enclosure temperature is the combination of dissipated heat from the electric load inside the enclosure and the outside ambient temperature minus the temperature reduction from cooling devices. The equation used for calculating the electronic's ETTF are shown in Equation 12.

$$T = \left[\overline{T_{a,max}} + R\overline{T_h}\right] - T_d \qquad (12)$$

$$T_d = 40°C$$

$T_h = temperature\ rise\ inside\ enclosure\ due\ to\ dissapated\ heat\ from\ electric\ load$ [℃]

$T_{a,max} = temperature\ rise\ inside\ enclosure\ due\ to\ ambient\ temperature$[℃]

$T = temperature\ rise\ in\ the\ enclosure\ above\ the\ allowable\ threshold$ [℃]

$R = Percent\ temperature\ reduction\ from\ shielding, circulating\ fans, and\ AC$ [%]

A.4.1.3 PVC Pipe ETTF Degradation

With high water temperatures, thermoplastic pipes can experience overbearing pressures, and PVC experiences the greatest degradation of all types of thermoplastic pipes [16]. The derating of the pipe is linear with increasing water temperatures. The Rate of Lifespan degradation for every 1° C above insulation exceedance threshold is shown in Table 8. [16] The Plastics Industry Pipes Association of Australia Limited states that linear interpolation can be used to estimate derating factors in between the temperatures listed. Thus, a linear regression is applied to the data points to estimate derating for the different temperature scenarios.

Table 8 PVC Pressure Derating Factors [16]

Temperature (ºC)	Pressure Derating Factor
20	1
30	0.87
40	0.7
50	0.58

The linear equation for derating factor obtained from these data is:

$$D = -0.0123T_w + 1.293 \quad (13)$$

$D = pressure\ derating\ factor$

$T_w = water\ temperature\ (°C)$

We assume that pressure degradation is not corrected in operations so that it directly correlates with lifespan degradation:

$$r_d = D \quad (14)$$

$r_d = lifespan\ degradation\ rate\ per\ °C\ increase$

ETTF decay model:

$$ETTF_{T2} = ETTF_{T1} * r_d \quad (15)$$

$$ETTF_{T2} = ETTF_{T1} * (-0.0123T_w + 1.293) \quad (16)$$

A.4.1.4 Iron Pipe ETTF Corrosion

For iron pipes, the temperature-related mechanism of failure is internal corrosion[17]. The relationship between corrosion rate and temperature has been reported in the literature for only the cast iron type of pipe. Temperature may have a similar effect on the corrosion rate of ductile iron and steel pipes though no relationship was found in literature. Corrosion rates for cast iron pipes are reported to be empirically different for water treatment plants (WTPs) and the water distribution system (WDS) (Equations 17 & 18). External and internal pit corrosion are relative to the original pipe thickness and were calculated from empirical corrosion rates where external pit depth was assumed to be one-half of the internal pit depth[17]. Corrosion rates and pipe age were used to calculate pit depth. The average age of pipes in the Southwest US is about 50 years[230].The pit depth was then used to calculate the remaining life of the pipe according to Randall-Smith et al.[144] Then the ETTF was assumed to be the current age of the pipe plus its remaining life as shown in the Equations 19-25.

External and internal pit corrosion were relative to the original pipe thickness and were calculated with empirical corrosion rates [17].

For iron pipes in a water distribution system:

$$r_c = 0.0272 * T_w + 0.0915 \quad (17)$$

For iron pipes in a water treatment plant:

$$r_c = 0.0774 * T_w - 0.1073 \quad (18)$$

Corrosion rates and pipe age were used to calculate the internal pit depth:

$$P_i = r_c * t \quad (19)$$

It was assumed that the external pit depth, P_e, would be half of the internal pit depth due to lack of information.

$$P_e = 0.5P_i \tag{20}$$

$$P_e = 0.5t(0.0774 * T_w - 0.1073) \tag{21}$$

The pit depth is the depth of the hole that appears in the pipe from the corrosion. The size of the hole determines how much life is left in the pipe [144].

$$\rho = \left(\frac{t}{P_e + P_i}\delta\right) - t \tag{22}$$

$$\rho = remaining\ life\ [years]$$
$$t = age\ of\ water\ main\ [years]$$
$$\delta = thickness\ of\ original\ pipe\ wall\ [in.]$$
$$P_i = internal\ pit\ depth\ [in.]$$
$$P_e = external\ pit\ depth\ [in.]$$

Remaining life (in time) equation including values of external and internal pit corrosion was translated into mean time to failure calculation using the assumption that ETTF equaled the sum of current age of the pipe and the remaining life of the pipe.

$$ETTF = t + \rho \tag{23}$$

$$ETTF = \frac{t}{P_e + P_i}\delta \tag{24}$$

$$ETTF = \frac{t}{0.5t(0.0774 * T_w - 0.1073) + P_i}\delta \tag{25}$$

A.4.1.5 TTHM Formation

Water quality is also affected by an increase in water temperature. The water temperature change increases the rates of production of cancerous chemical compounds. Total Trihalomethanes (TTHMs) are disinfection byproducts formed from organic reactions with chlorine and can cause cancer in consumers.[240] Temperature is one of the factors influencing TTHM formation because temperature increases the reaction rates between the organics and disinfectants (Equation 26).[33] Equation 26 was generated from empirical data from within the water distribution system of Istanbul City, Turkey which is supplied by surface water and goes through the following treatment steps: "aeration, prechlorination, coagulation, flocculation-sedimentation, filtration, and postchlorination." The parameters of the THM formation distribution were used to calculate the cumulative probability that a concentration from the distribution would be above the EPA regulated threshold of 80 µg/L for THMs.[148]

$$TTHM = 11.967 * (TOC)^{0.398} * {T_w}^{0.158} * Cl_2^{0.702} \quad (26)$$

$$TOC = Total\ organic\ carbon\ \left[\frac{mg}{L}\right]$$

$$Cl_2 = Chlorine\ dosage\ \left[\frac{mg}{L}\right]$$

$$T_w = Water\ temperature\ [°C]$$

A.4.1.6 THAA Formation

Total Haloacetic Acids (THAAs) are another temperature-sensitive disinfection byproduct and carcinogen. The concentration of THAAs is dependent upon the

concentration of TTHMs and temperature where temperature was represented by the seasonality factor (Equation 27).[34] Equation 27 was generated from an empirical study of three drinking water systems in the United Kingdom which represent a range of source water conditions – "upland surface water, a lowland surface water, and groundwater" with standard treatment mechanisms: aeration, filtration, coagulation, sedimentation, and chlorination.

$$THAA = 0.99\,(TTHM)^{0.64} * (Cl)^{0.15} * (SUVA)^{0.09} * (Br^{-} + 0.005)^{-0.12} * (ResT + 5)^{0.07} * (Season) \quad (27)$$

THAA = Total haloacetic acid [μ g/l]

TTHM = Total trihalomethanes [μ g/l]

Cl = Total chlorine [mg/l]

SUVA = Specific UV absorbance [l/mg.m]

Br = Bromide [mg/l]

ResT = Water age (residence time) [h]

Season = Season, expressed numerically as: 1 for spring, 1.46 for summer, 1.31 for autumn, 1.01 for winter

A.4.1.7 Chlorine residual concentration

Another type of quality concern is that of chlorine residual decay as water travels to the consumer. "The residual disinfectant concentration in the distribution system, measured as total chlorine, combined chlorine, or chlorine dioxide, as specified in § 141.74 (a)(2) and (b)(6), cannot be undetectable in more than 5 percent of the samples each month, for

any two consecutive months that the system serves water to the public".[149] An average detectable limit found from reviewing details of monitoring equipment is 0.0175 mg/L.[241,242]

The decay constant's relationship with temperature was taken from the empirical study of two water distribution systems in Birmingham, Alabama, by Hua et al. [32] (Equation 28). Water quality non-compliance counts are for individual sampling stations. This study shows the counts of non-compliant stations. This could lead to an increased likelihood in 2 months being non-compliant in a row.

$$k_b = \frac{0.0050e^{0.0841T_w}}{C_o} \tag{28}$$

$$k_b = chlorine\ decay\ constant$$

$$T_w = water\ temperature\ [°C]$$

$$C_0 = initial\ chlorine\ concentration\ [\frac{mg}{L}]$$

The concentration of remaining chlorine residual was calculated using Equation 29 & 30.[32]

$$C = C_o e^{-k_b t} \tag{29}$$

$$C = C_o e^{-\frac{0.0050e^{0.0841T_w}}{C_o}t} \tag{30}$$

$$C = final\ chlorine\ concentration\ [\frac{mg}{L}]$$

$$t = age\ of\ water\ [hr]$$

A.4.2 Probability Distribution Creation Method

The outputs were used to characterize the distributions by performing 5,000 iterations of Monte Carlo simulations on the degradation equations and sampling from the lower and upper halves of the ranges of operational characteristics, representing best case (lowest consequential probability of failure) and worst case (highest consequential probability of failure) of normal operating conditions (Table 9 & 10 respectively). Palisade© @Risk software was used to fit the output data from the simulations into probability distributions using the Anderson Darling (AD) Statistics, probability plots, visualization and judgement about the process underlying the data.[145] Figures 29-45 show fit comparisons for all components and water quality aspects under worst-case operating conditions and 40ºC temperature scenario (although any other scenario would show similar results for all components and aspects of water quality except for chlorine residual—for which we show both scenarios). Figures show possible fits listed in order of AD Statistics and probability plots with fits listed in order of AIC rankings. For physical components, the Weibull distribution was chosen because it is typically used to characterize the general forms of degradation components experience with age, and it also had reasonable fits in terms of AD statistic and linear probability plots as shown in figures 29-36.[146,243] Parameters of the distributions and AD Statistics for one Monte Carlo simulation are shown in Table 9 and 10 (values vary slightly for every run of the simulation--due to

random nature of sampling in Monte Carlo). Generally, the better the distribution fits the data, the smaller the AD Statistic is. Table S10 shows the critical AD Statistics from the theoretical Weibull distribution for comparison with the AD statistics for the components fitted with Weibull to help evaluate the reasonableness of fit.[244] When the AD Statistic from the fit is less than the critical statistic, the null hypothesis that the data fit a Weibull distribution is not rejected.[245] Motors and PVC pipes were the only components that had outputs that were statistically equal to the Weibull to the 10% significance level. The physical components with non-statistical Weibull fits have other poor fits shown on the figures as a point of comparison with Weibull. The output distributions for chlorine residual concentration were fitted as exponential distributions based on best fit and the need to be consistent across operating scenarios as shown in Figures 37-41. The exponential distribution was visually the best fit for the output for the worst-case operating conditions scenario, though the AD statistics suggested the gamma distribution was the better fit. Additionally, though the type of distribution of inputs were constant, the output of chlorine residual was so sensitive to the different ranges of inputs for different operating scenarios that it changed the output shape of the output. The worst-case scenario could only fit an exponential whereas the best-case scenario looked much more of a bell shape characteristic of a normal or Weibull distribution. Exponential fits were used for both scenarios, however, so that the difference in probability of failure between scenarios would not be characterized by the difference in fitted distributions but rather only the increase in temperature. The exponential distribution was the only distribution that was in common between scenarios, so it was the one that was used. The

fits for DBP production were selected based on best fit as shown in figures 42-45. The best statistical fits for both TTHM and THAA was the Gamma distribution.

Table 9 Output Distribution Parameters and Anderson-Darling Statistic of Failure Metrics from Monte Carlo Simulation for Low Failure Probability (Best-case Operational Characteristics).

Component/ Chemical	Distribution Type	Distribution Parameter Type	Ambient Temperature Scenario (°C)								
			36	**37**	**38**	**39**	**40**	**41**	**42**	**43**	**44**
Motors	Weibull	scale	18.9	17.4	16.1	14.9	13.7	12.7	11.7	10.8	10.0
		shape	1.9	1.9	1.9	1.9	1.9	1.9	1.9	1.9	1.9
		AD statistic	0.84								
Electronics	Weibull	scale	22.3	20.9	19.3	18.1	16.9	15.8	14.7	13.8	12.8
		shape	1.7	1.7	1.7	1.7	1.7	1.7	1.7	1.7	1.7
		AD statistic	8.50								
PVC pipe	Weibull	scale	45.8	45.5	45.1	44.8	44.4	44.1	43.7	43.3	43.0
		shape	2.0	2.0	2.0	2.0	2.0	2.0	2.0	2.0	2.0
		AD statistic	0.07								
Iron Pipe in WDS	Weibull	scale	447	438	429	420	412	405	397	389	383
		shape	6.4	6.4	6.4	6.5	6.5	6.4	6.5	6.7	6.5
		AD statistic	--								
Iron Pipe in WTP	Weibull	scale	190	185	180	177	173	169	165	162	158
		shape	5.9	5.9	5.9	6.0	5.9	5.9	5.9	6.0	6.1
		AD statistic	60.35								
Chlorine Residual	Exponential	failure rate	1.69	1.64	1.59	1.53	1.48	1.43	1.37	1.32	1.26

		AD statistic	920.53								
THM production	Gamma	scale	4.1	4.1	4.1	4.2	4.2	4.1	4.2	4.3	4.2
		shape	7.7	7.6	7.7	7.7	7.7	7.8	7.6	7.6	7.7
		AD statistic	39.76								
THAA production	Gamma	scale	13.8	13.8	13.8	13.8	14.1	13.8	14.0	13.7	14.0
		shape	1.7	1.7	1.7	1.7	1.7	1.7	1.7	1.7	1.7
		AD statistic	9.34								

Table 10 Output Distribution Parameters and Anderson-Darling Statistic of Failure Metrics from Monte Carlo Simulation for High Failure Probability (Worst-case Operational Characteristics)

Component/ Chemical	Distribution Type	Distribution Parameter Type	Ambient Temperature Scenario (°C)								
			36	**37**	**38**	**39**	**40**	**41**	**42**	**43**	**44**
Motors	Weibull	scale	12.7	11.7	10.7	10.0	9.2	8.5	7.9	7.3	6.8
		shape	1.9	1.9	1.9	1.9	1.9	1.9	1.9	1.9	1.9
		AD statistic	0.45								
Electronics	Weibull	scale	13.5	12.6	11.8	11.0	10.2	9.5	8.9	8.3	7.7
		shape	1.8	1.8	1.8	1.8	1.8	1.8	1.8	1.8	1.8
		AD statistic	4.15								
PVC pipe	Weibull	scale	42	41.5	41.0	40.6	40.1	40.0	39.2	38.7	38.3
		shape	2.0	2.0	2.0	2.0	2.0	2.0	2.0	2.0	2.0
		AD statistic	0.08								
Iron Pipe in WDS	Weibull	scale	275	269	263	257	252	247	242	237	233
		shape	5.4	5.4	5.5	5.5	5.4	5.4	5.5	5.5	5.5
		AD statistic	2.29								
Iron Pipe in WTP	Weibull	scale	112	109	107	104	102	99	97	95	93
		shape	5.2	5.4	5.3	5.3	5.3	5.4	5.4	5.3	5.4
		AD statistic	65.0								
	Exponential	failure rate	0.077	0.067	0.057	0.047	0.039	0.033	0.022	0.018	0.014

Chlorine Residual		AD statistic	3180								
TTHM production	Gamma	scale	1.5	1.5	1.5	1.5	1.5	1.6	1.6	1.6	1.6
		shape	53.6	54.5	53.9	54.0	54.4	54.5	53.9	53.2	54.3
		AD statistic	19.1								
THAA production	Gamma	scale	0.4	0.4	0.4	0.4	0.4	0.4	0.4	0.4	0.4
		shape	113	112	111	113	114	111	112	113	113
		AD statistic	10.1								

Table 11 Critical AD Statistics of Theoretical Weibull Distribution for Different Significance Levels, α. [244]

α	0.1	0.05	0.025	0.01
AD critical statistic	0.637	0.757	0.877	1.038

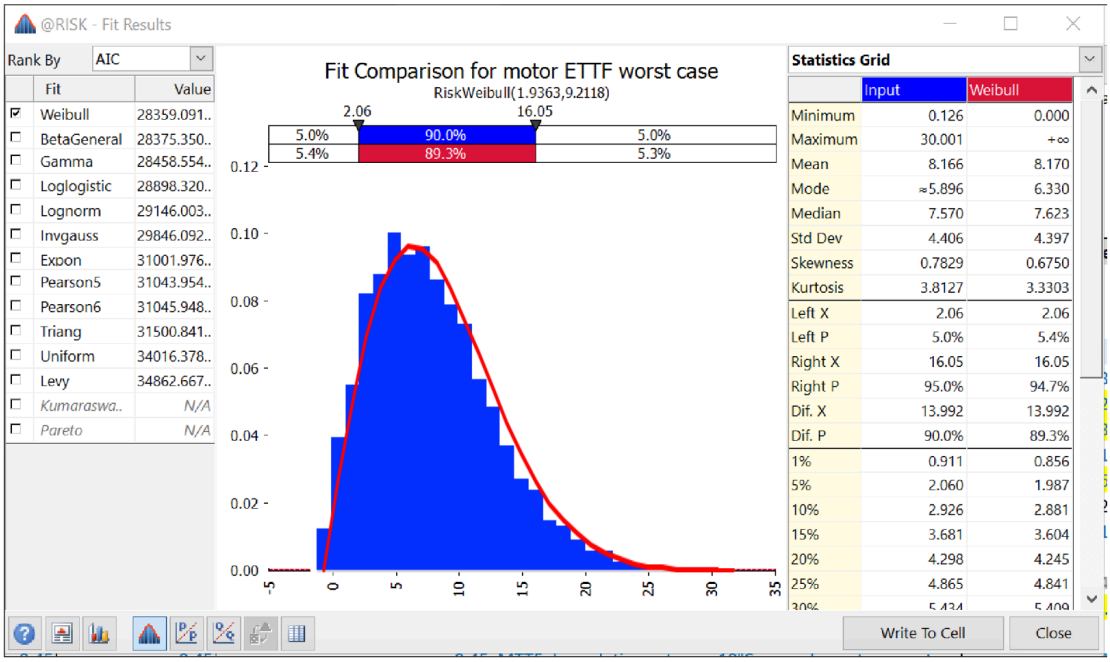

Figure 29 Fit Comparison for Motors

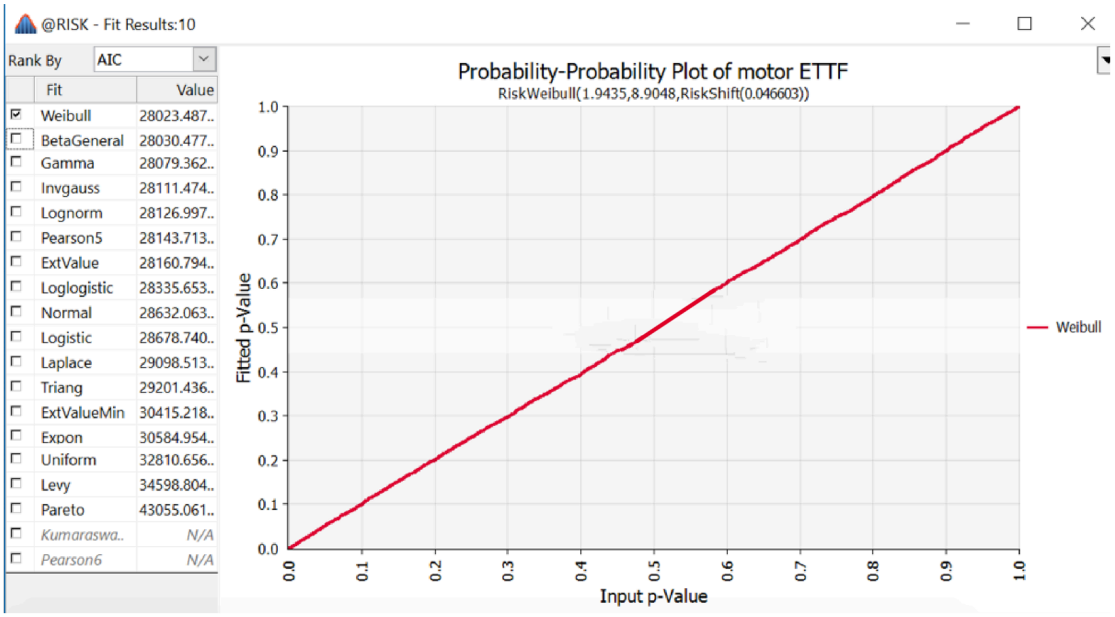

Figure 30 Probability Plot for Motors

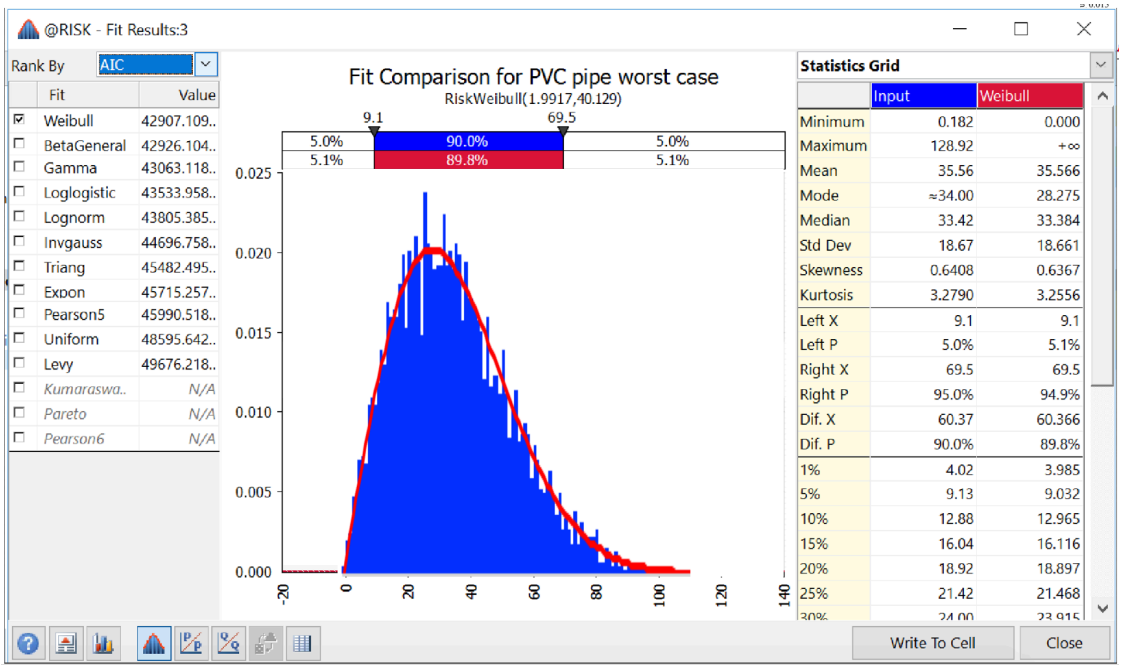

Figure 31 Fit Comparison for PVC Pipes

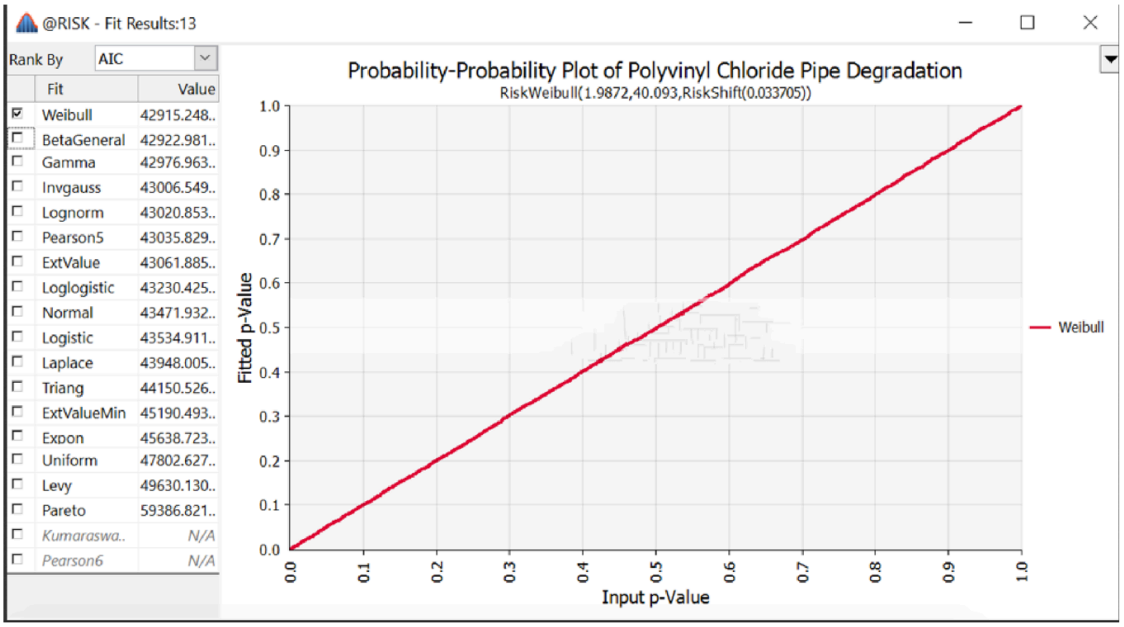

Figure 32 Probability Plot for PVC Pipes

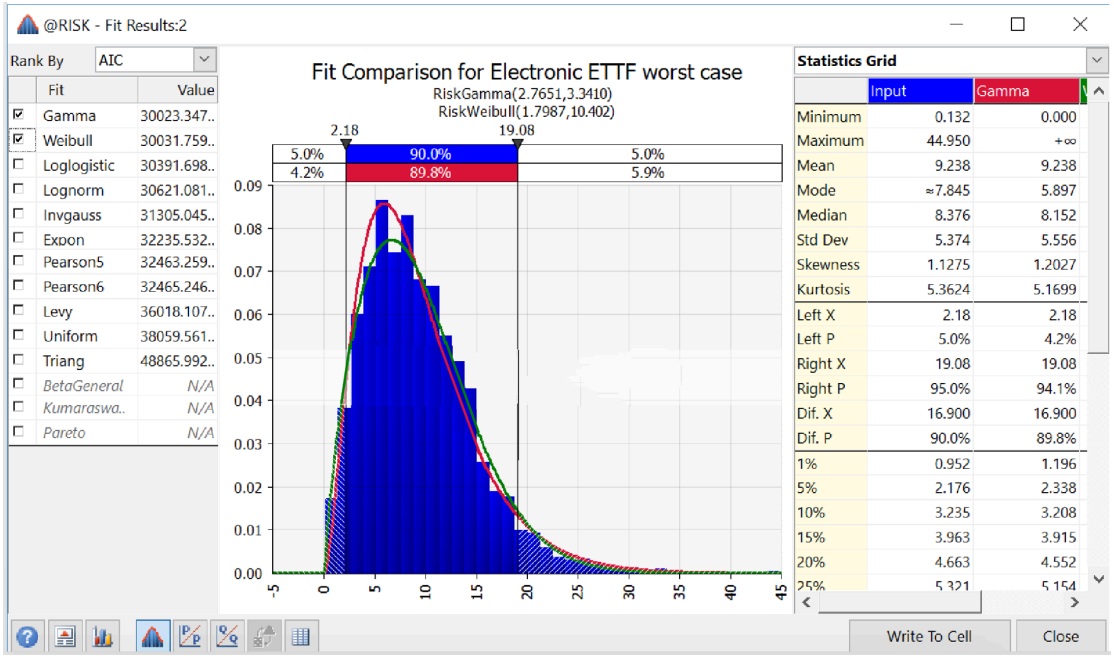

Figure 33 Fit Comparison for Electronics

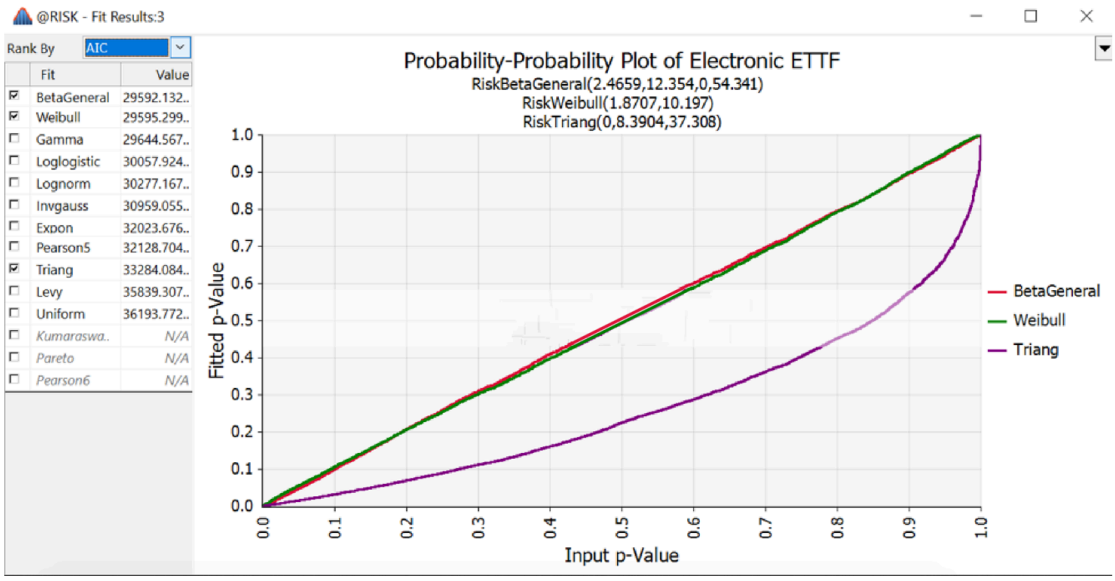

Figure 34 Probability Plot for Electronics. The probability plot of the Triangular fit is plotted to show an example of a non-linear and therefore poor fit.

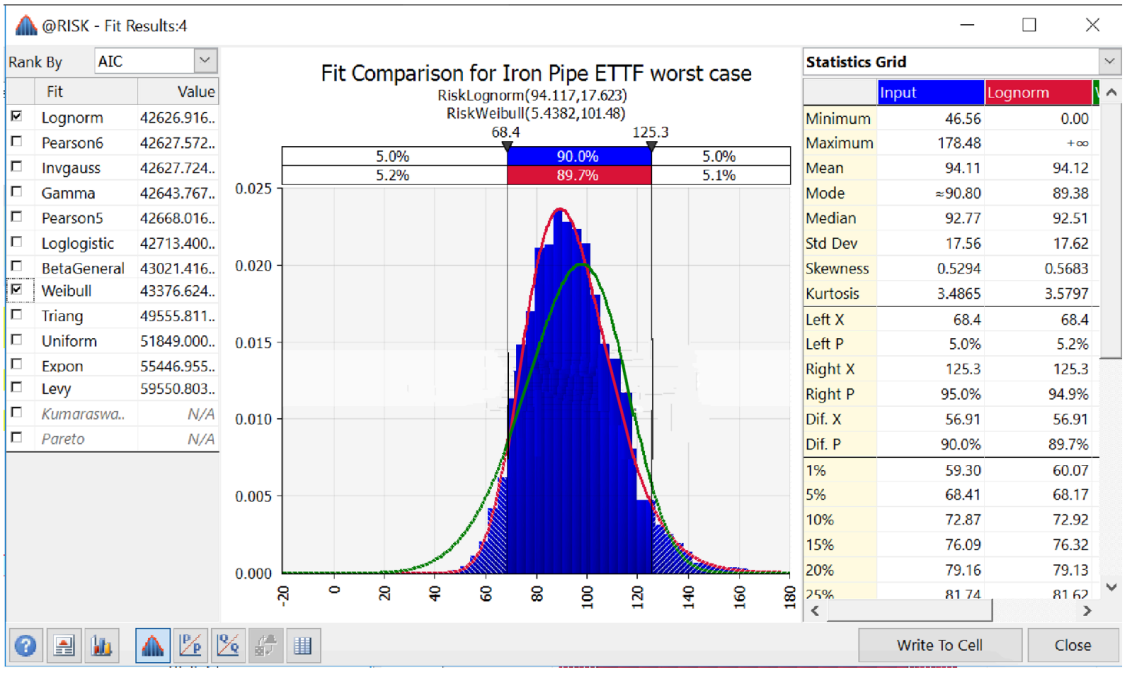

Figure 35 Fit Comparison for Iron Pipes

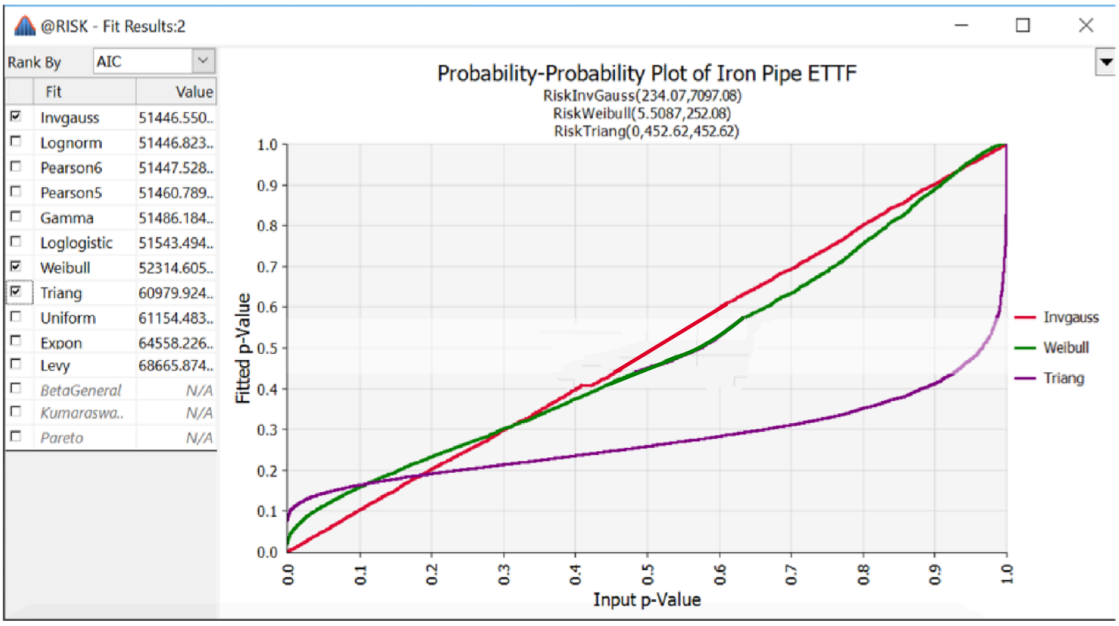

Figure 36 Probability Plot for Iron Pipes. The probability plot of the Triangular fit is plotted to show an example of a non-linear and therefore poor fit.

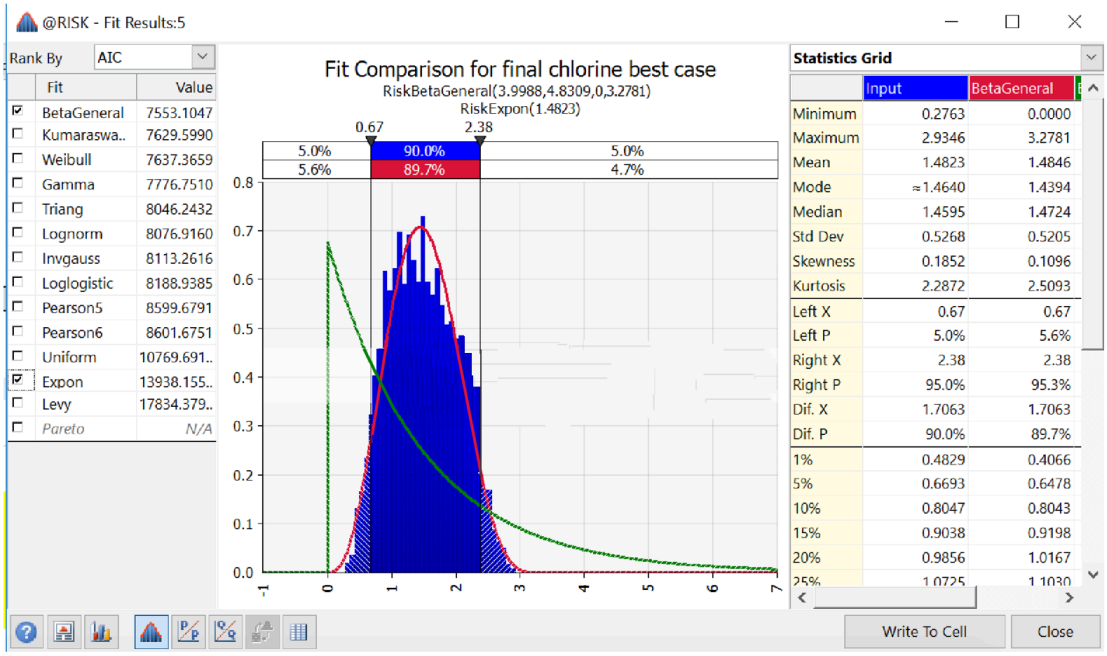

Figure 37 Fit Comparison for Chlorine Residual Under Best-Case Operating Conditions

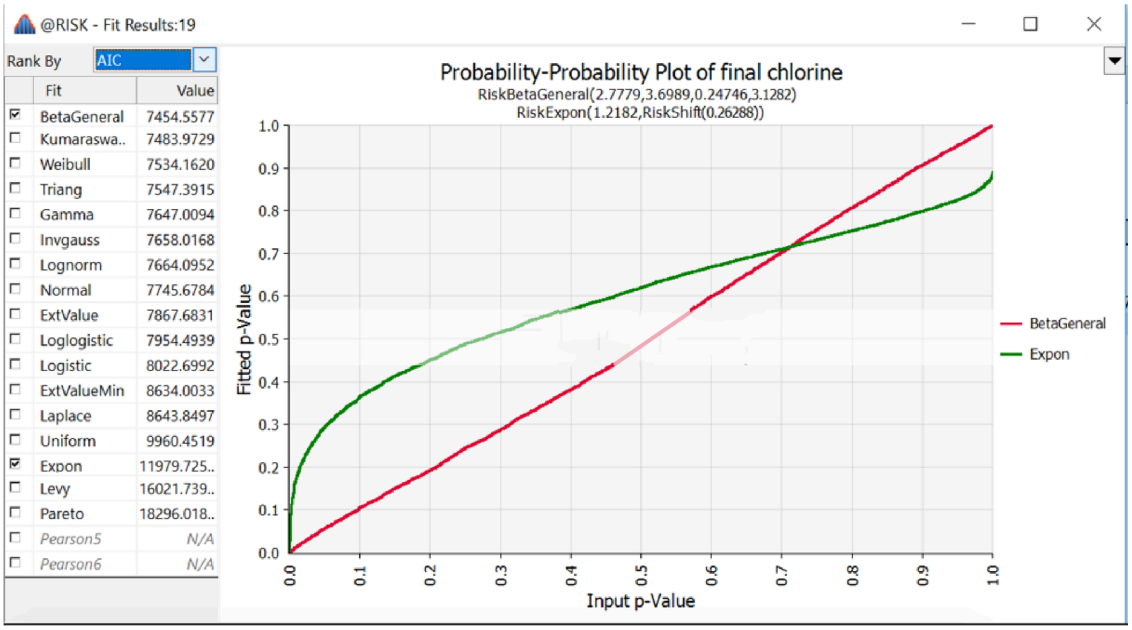

Figure 38 Probability Plot for Chlorine Residual Under Best-Case Operating Conditions

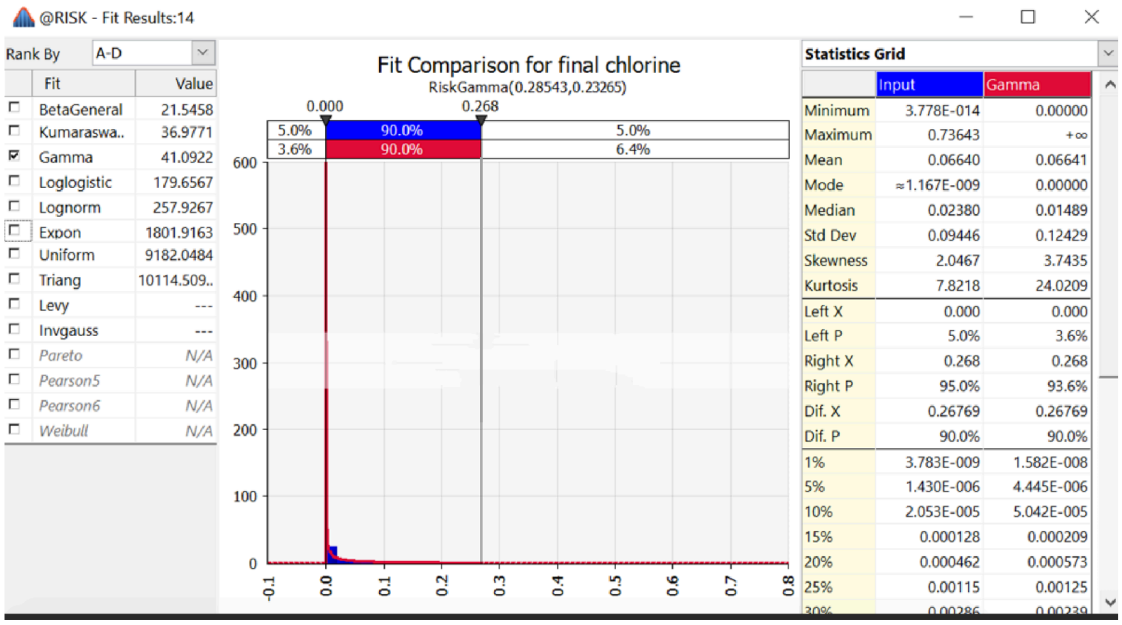

Figure 39 Fit Comparison for Chlorine Residual Under Worst-Case Operating Conditions—Gamma

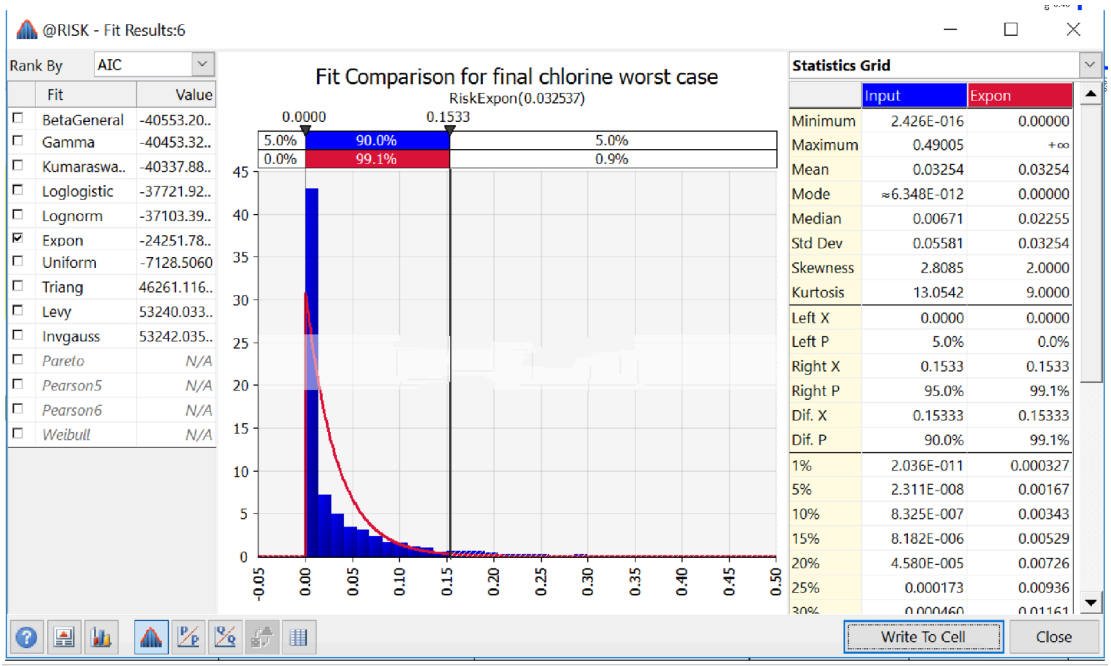

Figure 40 Fit Comparison for Chlorine Residual Under Worst-Case Operating Conditions -- Exponential

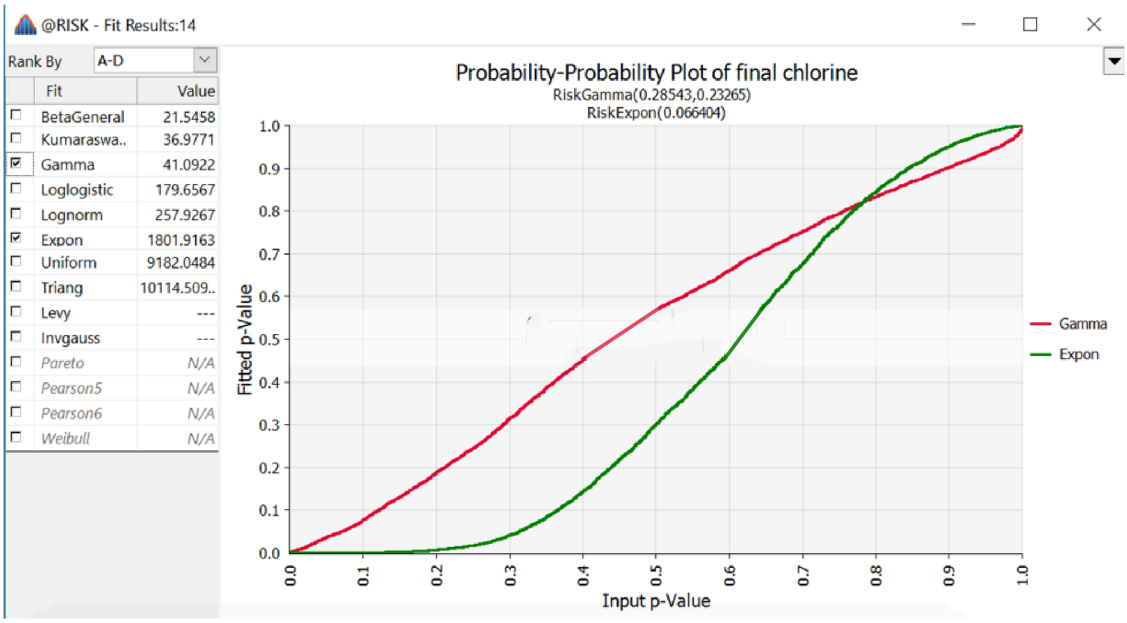

Figure 41 Probability Plot for Chlorine Residual Under Worst-Case Operating Conditions

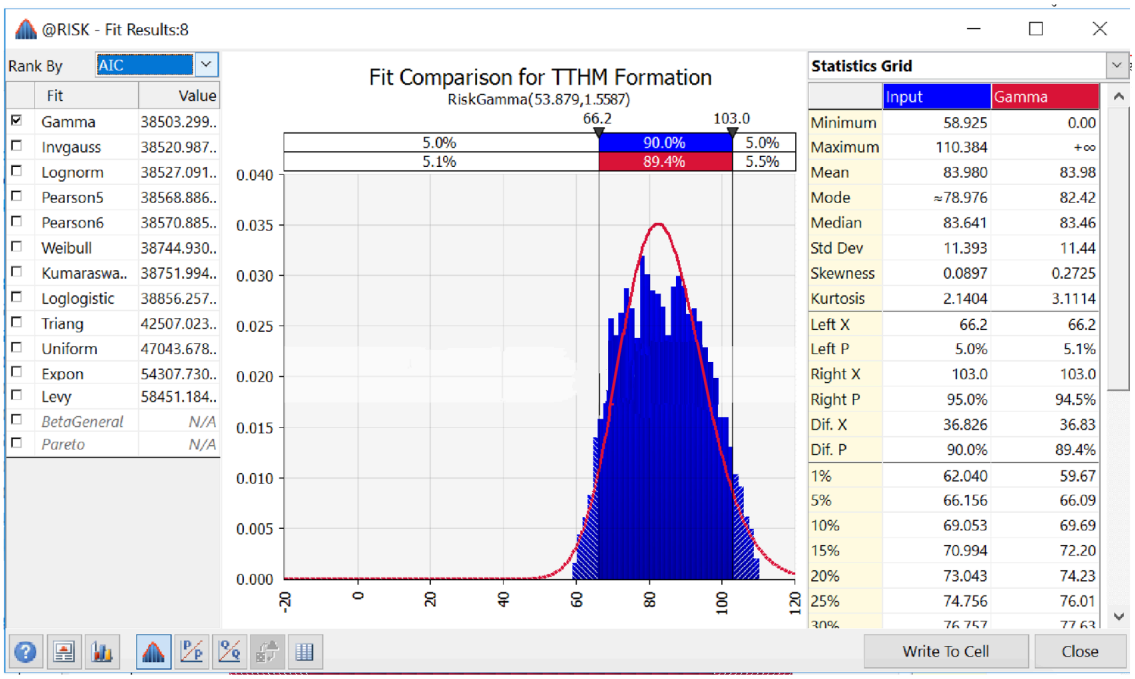

Figure 42 Fit Comparison for THM Production

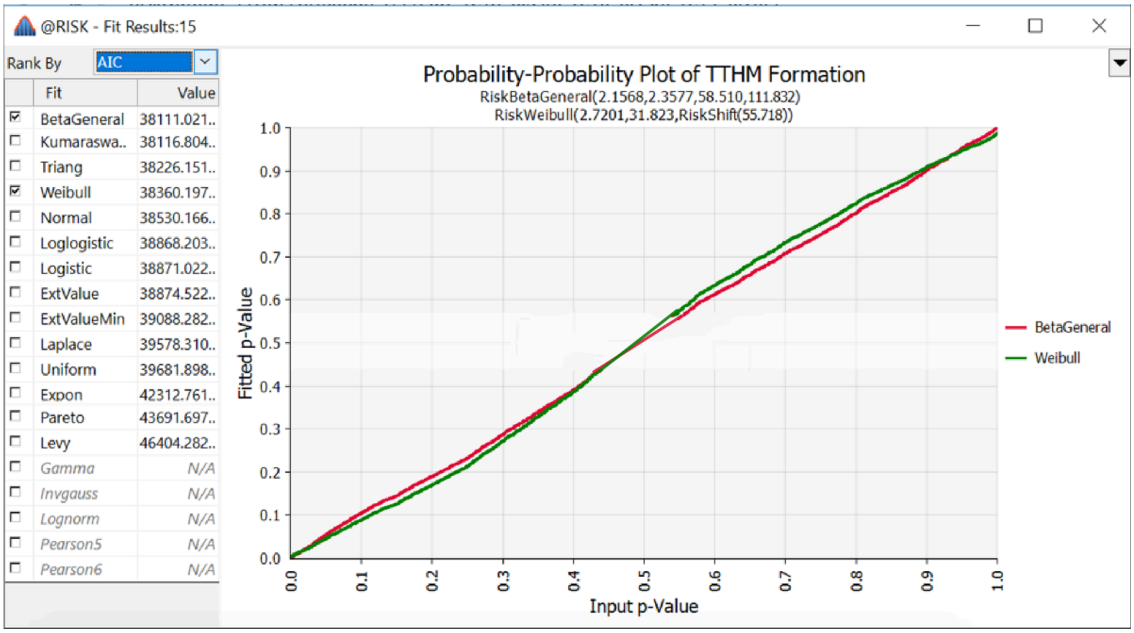

Figure 43 Probability Plot for TTHM Production

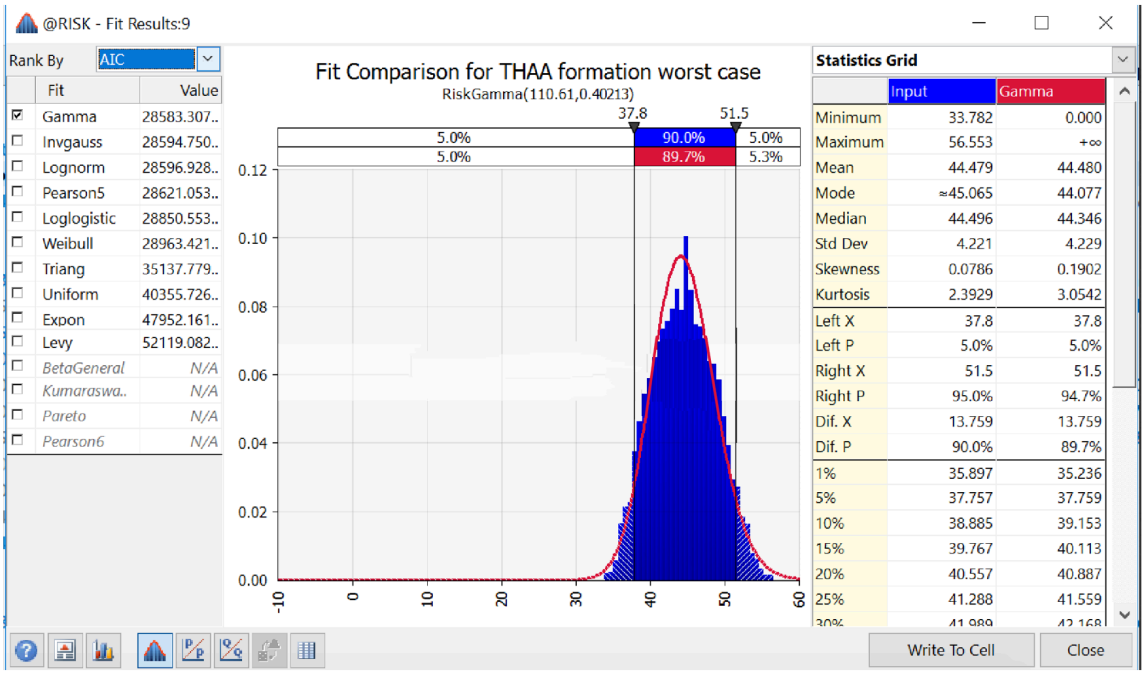

Figure 44 Fit Comparison for THAA Production

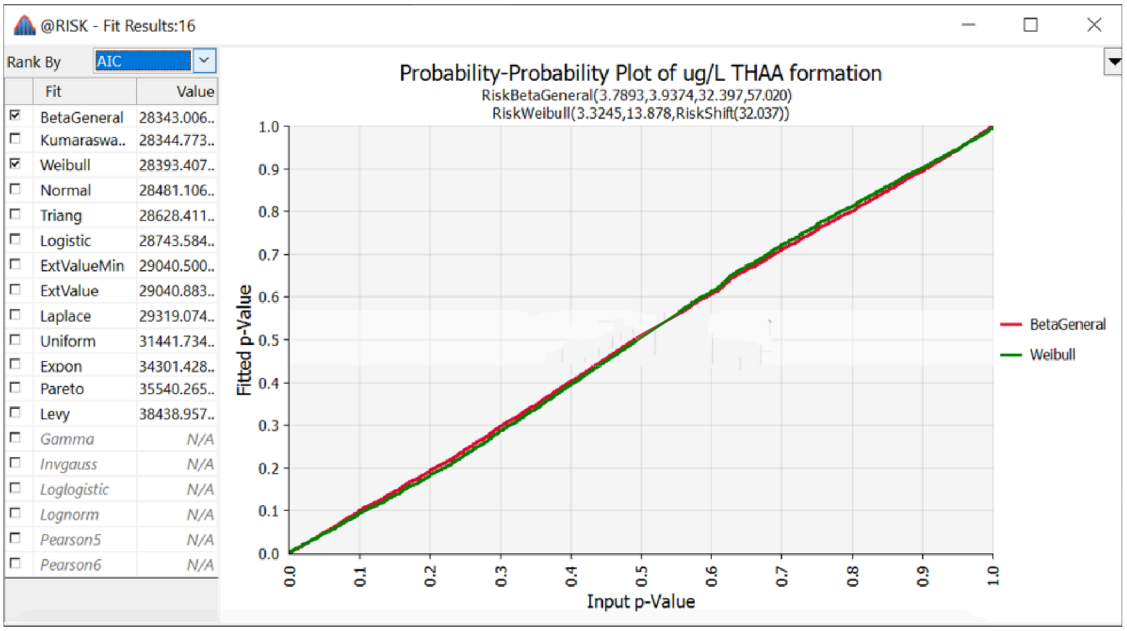

Figure 45 Probability Plot for THAA Production

A.4.3 Projection of Failure Calculation Method

A.4.3.1 Physical Component Failure: Failure Rate Method

The failure distributions were integrated to attain rate of failure. The component failure rates are calculated using the failure rate method, which is the rate of instantaneous failure immediately after its current age, given that the component has survived to its current age [146,147] as shown in equations 31 - 33. This method was used to calculate failure rates of motors, electronics, and pipes.

$$\lim_{\Delta t \to 0} \Pr\left(T < t + \Delta t \middle| T > t\right)/\Delta t = \frac{lim_{\Delta t \to 0}[F(t + \Delta t) - F(t)]/\Delta t}{1 - F(t)} \tag{31}$$

$$h(t) = \frac{f(t)}{R(t)} \tag{32}$$

$$For\ Weibull: h(t) = \frac{\alpha}{\beta}\left(\frac{t}{\beta}\right)^{\alpha-1} \tag{33}$$

where *h(t)* is the instantaneous failure rate, *t* is the current age of the component, Δt is an incremental time period, *f(t)* is the probability of failure of a component within the time period, and R(t) is the reliability or chance of component survival up until its current age, α is the shape parameter of the Weibull distribution, and β is the scale parameter of the Weibull distribution.

A.4.3.2 Probability of Water Quality Non-Compliance Method

Parameters of probability distribution functions from output Monte Carlo simulation were used in Excel to calculate failure as either exceeding the EPA maximum threshold regulation or being below an EPA minimum threshold regulation. The TTHM formation distribution were used to calculate the cumulative probability that a concentration from the distribution would be above the EPA regulated threshold of 80 µg/L for TTHMs.[148] Therefore, P(x> 80 µg/L) was calculated. The EPA regulation for THAAs is 60 µg/L[148] so the probability that P(x> 60 µg/L) was calculated. The chlorine residual distributions were used to calculate the probability that a concentration from a sampling station would be undetectable according to the EPA regulation. [149] Therefore, the P(x<0.0175 mg/L) was calculated based on the average detectable limit of monitoring equipment. [241,242]

The cumulative distribution functions of the Weibull distribution used to calculate probabilities are shown in Equation 34.

$$P(x) = \begin{cases} 1 - e^{-\lambda x^{\alpha}}, & if\ P(x < X) \\ e^{-\lambda x^{\alpha}}, & if\ P(x > X) \end{cases} \quad (34)$$

A.5 Modeling Failure Cascades to Service Outages: System Failure Laws

To model component failures leading to systemic failures stochastically, “AND” and “OR” logic gates were used to denote the parallel and series behavior within the system,

based on standard reliability engineering methods.[147] The laws of probability translate this logic into quantitative probabilities.

As shown in equation 35, a system failure rate "can be calculated by summing up the failure rates of all individual components" assuming a series behavior of the system[146]. This equation was used to calculate pumping unit, pumping station, water outage from pumping station outage in WDS, water outage from pumping station outage in WTP, overall water outage from pumping station, water outage from iron pipe break in WTP, water outage from iron pipe break in WDS, water outage from PVC pipe break in WTP, water outage from PVC pipe break in WDS, and overall water outage from pipe break.

$$h_s(t) = \sum_{i=1}^{n} h_i\,(t) \tag{35}$$

The probability that A and B occur simultaneously (corresponding to AND gates or joint probabilities) is shown in Equation 36.[147] This equation was used to estimate the probability of simultaneous types of water outages.

$$P(A \cap B) = P(A)P(B) \tag{36}$$

The probability of either A or B occurring (corresponding to OR gates and the union of probabilities) is shown in Equation 37.[147] This equation was used to estimate the probability of water quality non-compliance from either TTHM production or chlorine residual decay.

$$P(A \cup B) = P(A) + P(B) - P(A \cap B) \tag{37}$$

A.6 Projected Increases in Service Outages: Failure Percent Increases

Table ***12*** shows the resulting increase in failure rates in the period of 2020-2050 for all components and outage events in Phoenix, Las Vegas, and the case study system.

Table 12 Failure Percent Increases

Component/ Event	Phoenix-Las Vegas Average over Maximum Temperature Ranges					
	Mean Percent Increase	Mean Std. Deviation	Greatest Difference in Expected Failures Between Best and Worst Operating Conditions	Greatest Difference in Failure Rate	Percent Increase Under Good Operations	Percent Increase Under Bad Operations
Motors	92%	9%	2	1%	102%	83%
Electronics	76%	4%	2	1%	71%	80%
Pumping Units	72%	12%	5	2%	62%	82%
Pumping Stations	76%	15%	3	3%	62%	91%
PVC pipe	10%	0.2%	0	0.0%	10%	10%

Iron pipe WDS	52%	12%	0	0.0%	40%	65%
Iron pipe WTP	76%	8%	0	0.0%	68%	83%
TTHM Production	17%	10%	45	64.3%	27%	7%
Chlorine decay at station	53%	36%	41	59%	17%	90%
Water Outage from Pipe Break	10%	3%	22	1%	7%	13%
Water Outage from Pump Station Outage	76%	15%	14	15%	62%	91%
Water Quality Non-Compliance	17%	0.40%	55	79%	17%	17%
Any Pumping Station Outage -	25%	2%	89	2%	25%	25%

Water Main Break - Water Quality Non-Compliance						
Simultaneous Pumping Station Outage - Water Main Break - Water Quality Non-Compliance	105%	5%	6	0%	103%	107%
Simultaneous Pumping Station Outage - Water Main Break	95%	21%	6	0%	74%	116%
Simultaneous Pumping Station	106%	17%	32	20%	89%	123%

Outage - Water Quality Non-Compliance						
Simultaneous Water Main Break - Water Quality Non-Compliance	29%	3%	23	1%	26%	32%

A.7 Model Uncertainty

An exploration of the model's sensitivity to the important model assumptions (that were not characterized as parameters with ranges and probability distributions) is described in this section. If the information for soil and pipe parameters were made available to model the water temperature inside underground pipes, the modeled water temperature might decrease,[142,143] causing fewer failures in pipes and water quality. If the relationship between degradation of motors and electronics per duration of temperature exposure were made available, the current degradation modeled might slightly over-predict the degradation rate from not considering variations in daily and seasonal temperature. When the degradation rate is decreased in the model by 10%, the motor and

electronic probabilities of failure have a percent decrease of 0-22%, where the highest percent change is associated with the failure rates at the lowest temperatures under the worst- case operating conditions, and there is 0% change for all temperatures in the best-case operating conditions. When the rate of degradation of motors decreases by 10%, the probability of motor failure has a percent decrease of 0-13%. When the rate of degradation of electronics decreases by 10%, the probability of electronic failure has a percent decrease of 0-22%. Additionally, hind-casted probabilities of motor failure are validated by historical failure rates, so current results are reasonable. If component redundancy data and spatial and temporal information about the WDS network were to be made available for specific utilities, a better estimate of probability of systemic failure could be made. Assuming that there is a 50% chance (instead of 100% chance) of an inadequate amount of water storage decreases the likelihood of outage from pipe break by 50% and an outage from pumping station failure by 50%. If quantitative relationships to describe the effect of water hammer from one component failure causing another became available, the frequency of component systemic failure might increase. Lastly, it is hard to know what the resulting risk will be when normal structural and operational characteristics change overtime from urban expansion, transformative designs, etc.

APPENDIX B

SUPPLIMENTARY INFORMATION FOR CHAPTER 3

B.1 Introduction

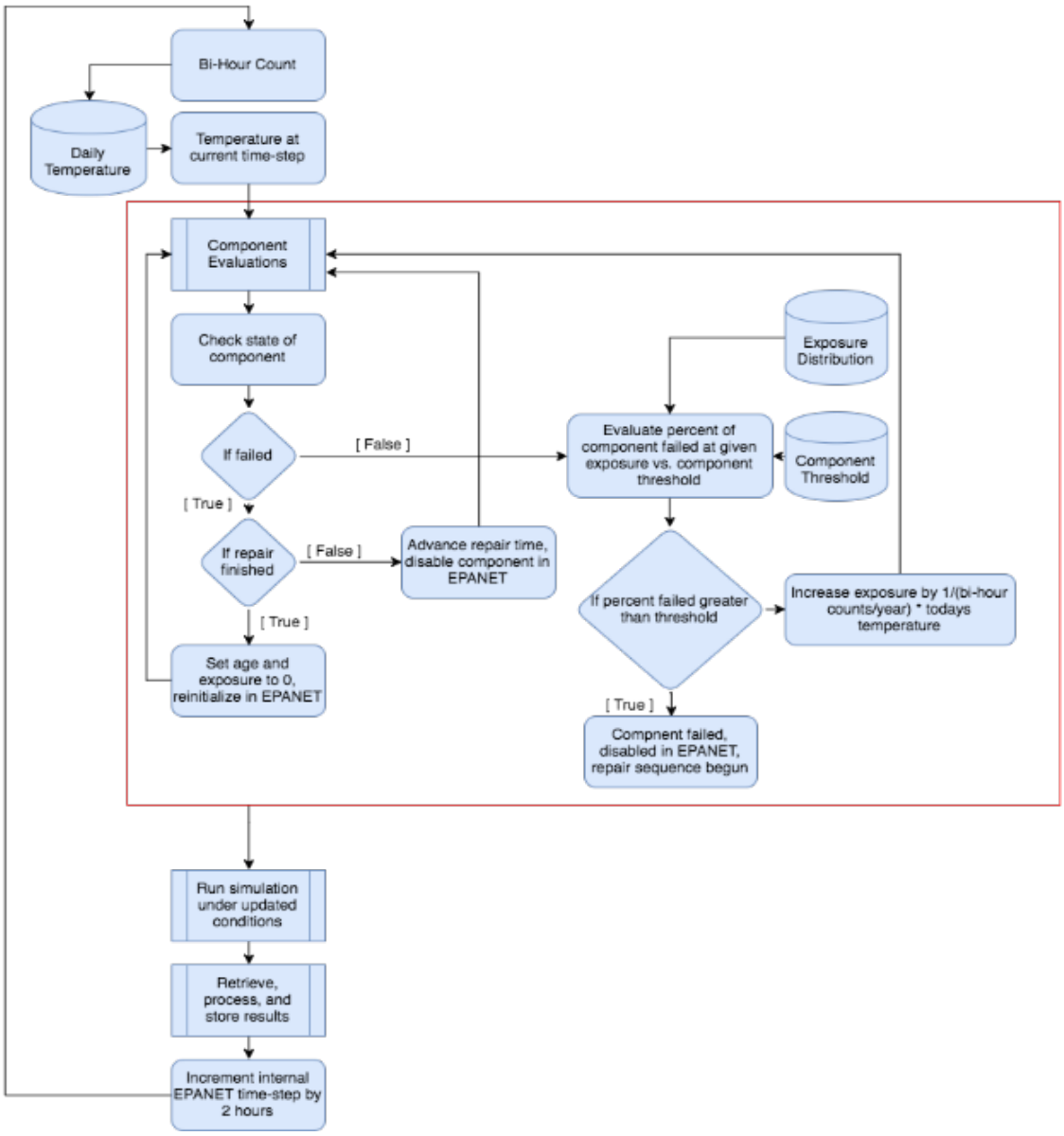

Figure 46 Perses Modeling Overview

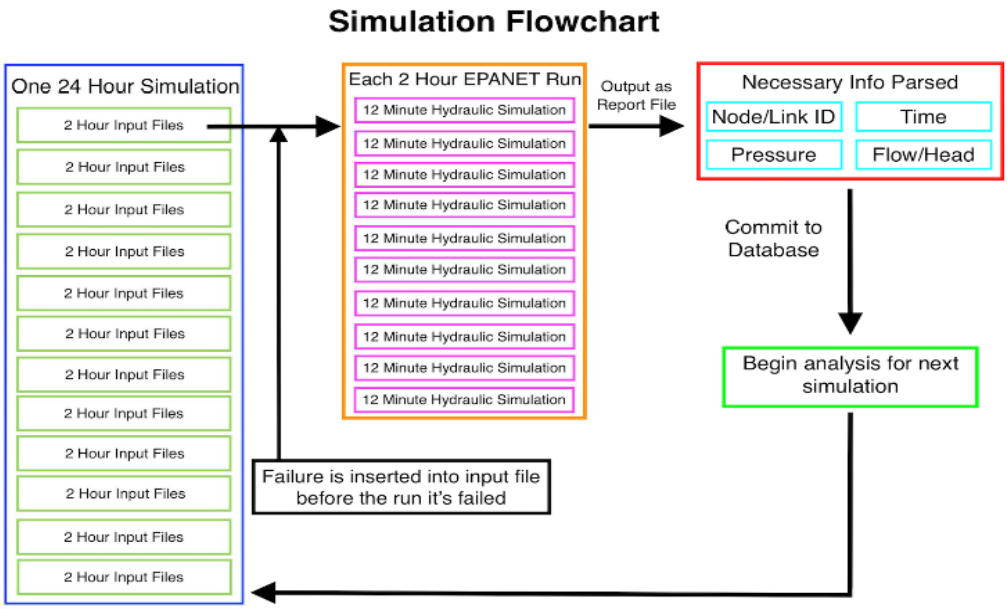

Figure 47 Simulation Overview

B.2 Methodology

B.2.1 Modeling Component Probability of Failure

The method used to estimate the mean time to failure of various components in this system is based off of fixed Weibull curves generated from the model given by [Emily's Paper]. Programmatically this is done by accessing the temperature at surface max at the given day from the previously loaded list of temperatures. Once the temperature at a certain time step is estimated the corresponding Weibull curve is retrieved from the list of Weibull curves previously loaded in. On these curves we match the age of the component in years to the age in years on the x-axis, and due to these being cumulative failure Weibull curves, are able to estimate a likelihood of failure at this time step with accuracy.

B.2.2 Modeling Component States

Since we estimate the mean time to failure for each component before we estimate the failure state, we are able to as accurately as possible determine each components failure state at each discrete time step, with some level of "random-ness" factored in. The estimation of failure is done by comparing the percent of components that we have estimated to be failed under the given conditions versus a random value from a uniform distribution ranging from 0 to 1. If the value for the percent of components failing is greater than the value obtained from the normal distribution, the given component is disabled, and the necessary changes made to the model.

Component repair is handled in a similar fashion as component failure. Once failed, the component will be assigned a standard duration for that failure, which models the time to repair the outage in the real world. One important aspect to note is that when the components return to the functioning state they do so at 100% capacity, meaning that there is no period in which they function at a fraction of their total capacity.

B.3 Case Study

B.3.1 North Marin Input File

[TITLE]
North Marin Water District Zone I

[JUNCTIONS]

;ID	Elev	Demand	Pattern	
10	147	0.00		;
15	32	620.00	3	;
20	129	0.00		;

35 12.5 1856 4 ;
40 131.9 0 ;
50 116.5 0 ;
60 0 0 ;
61 0 0 ;
101 42 189.95 1 ;
103 43 133.2 1 ;
105 28.5 135.37 1 ;
107 22 54.64 1 ;
109 20.3 231.4 1 ;
111 10 141.94 1 ;
113 2 20.01 1 ;
115 14 52.1 1 ;
117 13.6 117.71 1 ;
119 2 176.13 1 ;
120 0 0 ;
121 -2 41.63 1 ;
123 11 1859 2 ;
125 11 45.6 1 ;
127 56 17.66 1 ;
129 51 0 ;
131 6 42.75 1 ;
139 31 5.89 1 ;
141 4 9.85 1 ;
143 -4.5 6.2 1 ;
145 1 27.63 1 ;
147 18.5 8.55 1 ;
149 16 27.07 1 ;
151 33.5 144.48 1 ;
153 66.2 44.17 1 ;
157 13.1 51.79 1 ;

159 6 41.32 1 ;
161 4 15.8 1 ;
163 5 9.42 1 ;
164 5 0 ;
166 -2 2.6 1 ;
167 -5 14.56 1 ;
169 -5 0 ;
171 -4 39.34 1 ;
173 -4 0 ;
177 8 58.17 1 ;
179 8 0 ;
181 8 0 ;
183 11 0 ;
184 16 0 ;
185 16 25.65 1 ;
187 12.5 0 ;
189 4 107.92 1 ;
191 25 81.9 1 ;
193 18 71.31 1 ;
195 15.5 0 ;
197 23 17.04 1 ;
199 -2 119.32 1 ;
201 0.1 44.61 1 ;
203 2 4643 5 ;
204 21 0 ;
205 21 65.36 1 ;
206 1 0 ;
207 9 69.39 1 ;
208 16 0 ;
209 -2 0.87 1 ;
211 7 8.67 1 ;

213 7 13.94 1 ;
215 7 92.19 1 ;
217 6 24.22 1 ;
219 4 4.32 1 ;
225 8 22.8 1 ;
229 10.5 64.18 1 ;
231 5 16.48 1 ;
237 14 15.61 1 ;
239 13 44.61 1 ;
241 13 0 ;
243 14 4.34 1 ;
247 18 70.38 1 ;
249 18 0 ;
251 30 24.16 1 ;
253 36 54.52 1 ;
255 27 40.39 1 ;
257 17 0 ;
259 25 0 ;
261 0 0 ;
263 0 0 ;
265 0 0 ;
267 21 0 ;
269 0 0 ;
271 6 0 ;
273 8 0 ;
275 10 0 ;

[RESERVOIRS]
;ID Head Pattern
4 220.0 ;

```
5                 167.0                 ;

[TANKS]
;ID             Elevation       InitLevel       MinLevel        MaxLevel        Diameter
        MinVol          VolCurve
1                       131.9                   13.1                    0.1
        32.1            85                      0.1                             ;
2                       116.5           23.5            6.5             40.3            50
        0.1                             ;
3               129.0                   29.0                    4.0
        35.5                    164             0.1                             ;

[PIPES]
;ID             Node1           Node2           Length          Diameter        Roughness
        MinorLoss       Status
20              3               20              99
        24              199             0               Open    ;
40              1               40              99
        24              199             0               Open    ;
50              2               50                      99
        24              199                     0               Open    ;
60              4               60                      1231
        24              140             0               Open    ;
101             10              101                     14200
        18              110             0               Open    ;
103             101             103             1350                            16
        130             0               Open    ;
105             101             105                     2540
        12              130             0               Open    ;
107             105             107             1470                            12
        130             0               Open    ;
```

109 103 109 3940
16 130 0 Open ;
111 109 111 2000 12
130 0 Open ;
112 115 111 1160 12
130 0 Open ;
113 111 113 1680
12 130 0 Open ;
114 115 113 2000
8 130 0 Open ;
115 107 115 1950 8
130 0 Open ;
116 113 193 1660 12
130 0 Open ;
117 263 105 2725 12
130 0 Open ;
119 115 117 2180 12
130 0 Open ;
120 119 120 730
12 130 0 Open ;
121 120 117 1870 12
130 0 Open ;
122 121 120 2050
8 130 0 Open ;
123 121 119 2000 30
141 0 Open ;
125 123 121 1500 30
141 0 Open ;
129 121 125 930
24 130 0 Open ;

131 125 127 3240 24
130 0 Open ;
133 20 127 785
20 130 0 Open ;
135 127 129 900
24 130 0 Open ;
137 129 131 6480 16
130 0 Open ;
145 129 139 2750 8
130 0 Open ;
147 139 141 2050 8
130 0 Open ;
149 143 141 1400
8 130 0 Open ;
151 15 143 1650
8 130 0 Open ;
153 145 141 3510 12
130 0 Open ;
155 147 145 2200 12
130 0 Open ;
159 147 149 880
12 130 0 Open ;
161 149 151 1020 8
130 0 Open ;
163 151 153 1170 12
130 0 Open ;
169 125 153 4560
8 130 0 Open ;
171 119 151 3460 12
130 0 Open ;

173 119 157 2080
30 141 0 Open ;
175 157 159 2910
30 141 0 Open ;
177 159 161 2000
30 141 0 Open ;
179 161 163 430
30 141 0 Open ;
180 163 164 150
14 130 0 Open ;
181 164 166 490
14 130 0 Open ;
183 265 169 590
30 141 0 Open ;
185 167 169 60
8 130 0 Open ;
186 187 204 99.9
8 130 0 Open ;
187 169 171 1270
30 141 0 Open ;
189 171 173 50
30 141 0 Open ;
191 271 171 760
24 130 0 Open ;
193 35 181 30
24 130 0 Open ;
195 181 177 30
12 130 0 Open ;
197 177 179 30
12 130 0 Open ;

199 179 183 210
12 130 0 Open ;
201 40 179 1190
12 130 0 Open ;
202 185 184 99.9 8
130 0 Open ;
203 183 185 510
8 130 0 Open ;
204 184 205 4530
12 130 0 Open ;
205 204 185 1325
12 130 0 Open ;
207 189 183 1350 12
130 0 Open ;
209 189 187 500
8 130 0 Open ;
211 169 269 646
12 130 0 Open ;
213 191 187 2560 12
130 0 Open ;
215 267 189 1230
12 130 0 Open ;
217 191 193 520
12 130 0 Open ;
219 193 195 360
12 130 0 Open ;
221 161 195 2300
8 130 0 Open ;
223 197 191 1150
12 130 0 Open ;

225 111 197 2790 12
130 0 Open ;
229 173 199 4000 24
141 0 Open ;
231 199 201 630
24 141 0 Open ;
233 201 203 120 24
130 0 Open ;
235 199 273 725
12 130 0 Open ;
237 205 207 1200
12 130 0 Open ;
238 207 206 450
12 130 0 Open ;
239 275 207 1430 12
130 0 Open ;
240 206 208 510
12 130 0 Open ;
241 208 209 885
12 130 0 Open ;
243 209 211 1210
16 130 0 Open ;
245 211 213 990
16 130 0 Open ;
247 213 215 4285
16 130 0 Open ;
249 215 217 1660
16 130 0 Open ;
251 217 219 2050 14
130 0 Open ;

257 217 225 1560
12 130 0 Open ;
261 213 229 2200
8 130 0 Open ;
263 229 231 1960
12 130 0 Open ;
269 211 237 2080
12 130 0 Open ;
271 237 229 790
8 130 0 Open ;
273 237 239 510
12 130 0 Open ;
275 239 241 35
12 130 0 Open ;
277 241 243 2200
12 130 0 Open ;
281 241 247 445
12 130 0 Open ;
283 239 249 430
12 130 0 Open ;
285 247 249 10
12 130 0 Open ;
287 247 255 1390
10 130 0 Open ;
289 50 255 925
10 130 0 Open ;
291 255 253 1100
10 130 0 Open ;
293 255 251 1100
8 130 0 Open ;

295 249 251 1450
12 130 0 Open ;
297 120 257 645
8 130 0 Open ;
299 257 259 350
8 130 0 Open ;
301 259 263 1400
8 130 0 Open ;
303 257 261 1400 8
130 0 Open ;
305 117 261 645
12 130 0 Open ;
307 261 263 350
12 130 0 Open ;
309 265 267 1580 8
130 0 Open ;
311 193 267 1170
12 130 0 Open ;
313 269 189 646
12 130 0 Open ;
315 181 271 260
24 130 0 Open ;
317 273 275 2230
8 130 0 Open ;
319 273 205 645
12 130 0 Open ;
321 163 265 1200
30 141 0 Open ;
323 201 275 300
12 130 0 Open ;

```
325             269             271             1290
        8       130     0       Open    ;
329     61      123             45500
        30      140     0       Open    ;



[PUMPS]
;ID             Node1           Node2           Parameters
 10             5               10              HEAD 10
        SPEED 1 ;
 335            60              61              HEAD 335
        SPEED 1 ;


[VALVES]
;ID             Node1           Node2           Diameter        Type    Setting
        MinorLoss

[TAGS]

[DEMANDS]
;Junction       Demand          Pattern         Category

[STATUS]
;ID             Status/Setting
 10             Closed
 335            Closed

[PATTERNS]
;ID             Multipliers
```

;

1	1.34	1.94	1.46	1.44	0.76	0.92	0.85	1.07	0.96	
1	1.10	1.08	1.19	1.16	1.08	0.96	0.83	0.79	0.74	
1	0.64	0.64	0.85	0.96	1.24	1.67				
2	0		0		0		0		0	0.656
	0		0		0					
2	1.0037	0.988	0.978	0.978	0.98	0.980	0.977	0.981	0.976	
2	0.986	0.984	0.984	0.975	0.989	1.00				
3	1		1		1		1		1	0.580
	0.580	0		0						
3	0		0		0.580	0.580	0.580	0.580	0.580	0
	0									
3	0		0		0		0		0.580	0.580
4	0.882	0.919	0.926	0.926	0.964	0.980	0.957	0.992	0.977	
4	0.983	1.00	0.970	0.980	0.934	0.896	0.872	0.869	0.872	
4	0.870	0.887	0.876	0.876	0.900	0.898				
5	0.956	0.975	0.971	0.986	0.975	0.986	0.984	0.993	1.00	
5	1.00	0.989	0.993	0.975	0.973	0.958	0.956	0.958	0.960	
5	0.956	0.951	0.940	0.947	0.962	0.964				

[CURVES]

;ID	X-Value	Y-Value
;PUMP: PUMP:		
10	0	104
10	3000	92

10	6000	63

;PUMP: PUMP:

335	0	200
335	8000	138
335	14000	86

[CONTROLS]

pump 10 open at time 0

pump 335 open at time 0

pump 10 open at time 1

pump 335 open at time 1

pump 10 open at time 2

pump 335 open at time 2

pump 10 open at time 3

pump 335 open at time 3

pump 10 open at time 4

pump 335 open at time 4

pump 10 open at time 5

pump 335 open at time 5

pump 10 open at time 6

pump 335 open at time 6

pump 10 open at time 7

pump 335 open at time 7

pump 10 open at time 8

pump 335 open at time 8

pump 10 open at time 9

pump 335 open at time 9

pump 10 open at time 10

pump 335 open at time 10

pump 10 open at time 11

pump 335 open at time 11
pump 10 open at time 12
pump 335 open at time 12
pump 10 open at time 13
pump 335 open at time 13
pump 10 open at time 14
pump 335 open at time 14
pump 10 open at time 15
pump 335 open at time 15
pump 10 open at time 16
pump 335 open at time 16
pump 10 open at time 17
pump 335 open at time 17
pump 10 open at time 18
pump 335 open at time 18
pump 10 open at time 19
pump 335 open at time 19
pump 10 open at time 20
pump 335 open at time 20
pump 10 open at time 21
pump 335 open at time 21
pump 10 open at time 22
pump 335 open at time 22
pump 10 open at time 23
pump 335 open at time 23
pump 10 open at time 24
pump 335 open at time 24
pump 10 open at time 25
pump 335 open at time 25
pump 10 open at time 26
pump 335 open at time 26

pump 10 open at time 27
pump 335 open at time 27
pump 10 open at time 28
pump 335 open at time 28
pump 10 open at time 29
pump 335 open at time 29
pump 10 open at time 30
pump 335 open at time 30
pump 10 open at time 31
pump 335 open at time 31
pump 10 open at time 32
pump 335 open at time 32
pump 10 open at time 33
pump 335 open at time 33
pump 10 open at time 34
pump 335 open at time 34
pump 10 open at time 35
pump 335 open at time 35
pump 10 open at time 36
pump 335 open at time 36
pump 10 open at time 37
pump 335 open at time 37
pump 10 open at time 38
pump 335 open at time 38
pump 10 open at time 39
pump 335 open at time 39
pump 10 open at time 40
pump 335 open at time 40
pump 10 open at time 41
pump 335 open at time 41
pump 10 open at time 42

pump 335 open at time 42
pump 10 open at time 43
pump 335 open at time 43
pump 10 open at time 44
pump 335 open at time 44
pump 10 open at time 45
pump 335 open at time 45
pump 10 open at time 46
pump 335 open at time 46
pump 10 open at time 47
pump 335 open at time 47
pump 10 open at time 48
pump 335 open at time 48
;link 335 OPEN IF Node 1 BELOW 17.1
;Link 335 CLOSED IF Node 1 ABOVE 19.1
;Link 10 CLOSED IF Node 1 BELOW 17.1
;Link 10 OPEN IF Node 1 ABOVE 19.1
[RULES]
RULE 1
IF TANK 1 LEVEL ABOVE 19.1
THEN PUMP 335 STATUS IS CLOSED
AND LINK 10 STATUS IS OPEN

RULE 2
IF TANK 1 LEVEL BELOW 17.1
THEN PUMP 335 STATUS IS OPEN
AND LINK 10 STATUS IS CLOSED

[ENERGY]
Global Efficiency 75
Global Price 0

```
 Demand Charge       0

[EMITTERS]
;Junction       Coefficient

[QUALITY]
;Node           InitQual

[SOURCES]
;Node           Type            Quality         Pattern

[REACTIONS]
;Type           Pipe/Tank       Coefficient


[REACTIONS]
 Order Bulk              1
 Order Tank              1
 Order Wall              1
 Global Bulk             0
 Global Wall             0
 Limiting Potential      0
 Roughness Correlation   0

[MIXING]
;Tank           Model

[TIMES]
 Duration                48
 Hydraulic Timestep      1:00
 Quality Timestep        0:06
```

Pattern Timestep	1:00
Pattern Start	0:00
Report Timestep	1:00
Report Start	0:00
Start ClockTime	12 am
Statistic	None

[REPORT]

Status	No
Summary	No
Page	0

[OPTIONS]

Units	GPM
Headloss	H-W
Specific Gravity	0.998
Viscosity	1

[COORDINATES]

;Node X-Coord Y-Coord

10 9.00 27.85

15 38.68 23.76

20 29.44 26.91

35 25.46 10.52

40 27.02 9.81

50 33.01 3.01

60 23.90 29.94

61 23.71 29.03

101 13.81 22.94

103 12.96 21.31

105 16.97 21.28
107 18.45 20.46
109 17.64 18.92
111 20.21 17.53
113 22.04 16.61
115 20.98 19.18
117 21.69 21.28
119 23.70 22.76
120 22.08 23.10
121 23.54 25.50
123 23.37 27.31
125 24.59 25.64
127 29.29 26.40
129 30.32 26.39
131 37.89 29.55
139 33.28 24.54
141 35.68 23.08
143 37.47 21.97
145 33.02 19.29
147 30.24 20.38
149 29.62 20.74
151 28.29 21.39
153 28.13 22.63
157 24.85 20.16
159 23.12 17.50
161 25.10 15.28
163 25.39 14.98
164 25.98 15.14
166 26.48 15.13
167 25.88 12.98
169 25.68 12.74

171 26.65 11.80
173 26.87 11.59
179 25.71 10.40
181 25.72 10.74
183 25.45 10.18
184 25.15 9.52
185 25.01 9.67
187 23.64 11.04
189 24.15 11.37
191 22.10 14.07
193 22.88 14.35
195 23.18 14.72
197 20.97 15.18
199 29.42 8.44
201 30.89 8.57
203 31.14 8.89
204 23.80 10.90
205 29.20 6.46
206 31.66 6.64
207 31.00 6.61
208 32.54 6.81
209 33.76 6.59
211 34.20 5.54
213 35.26 6.16
215 39.95 8.73
217 42.11 8.67
219 44.86 9.32
225 43.53 7.38
229 36.16 3.49
231 38.38 2.54
237 35.37 3.08

239 35.76 2.31
241 35.87 2.11
243 37.04 .00
247 35.02 2.05
249 35.02 1.81
251 34.15 1.10
253 32.17 1.88
255 33.51 2.45
257 21.17 23.32
259 20.80 23.40
261 20.79 21.45
263 20.32 21.57
265 25.39 13.60
267 23.38 12.95
269 25.03 12.14
271 25.97 11.00
273 29.16 7.38
275 31.07 8.29
4 24.15 31.06
5 8.00 27.53
1 27.46 9.84
2 32.99 3.45
3 29.41 27.27

[VERTICES]
;Link X-Coord Y-Coord

[LABELS]
;X-Coord Y-Coord Label & Anchor Node

[END]

B. 4 Results

B.4.1 Long-term Increase in Failures in Large-Scale System

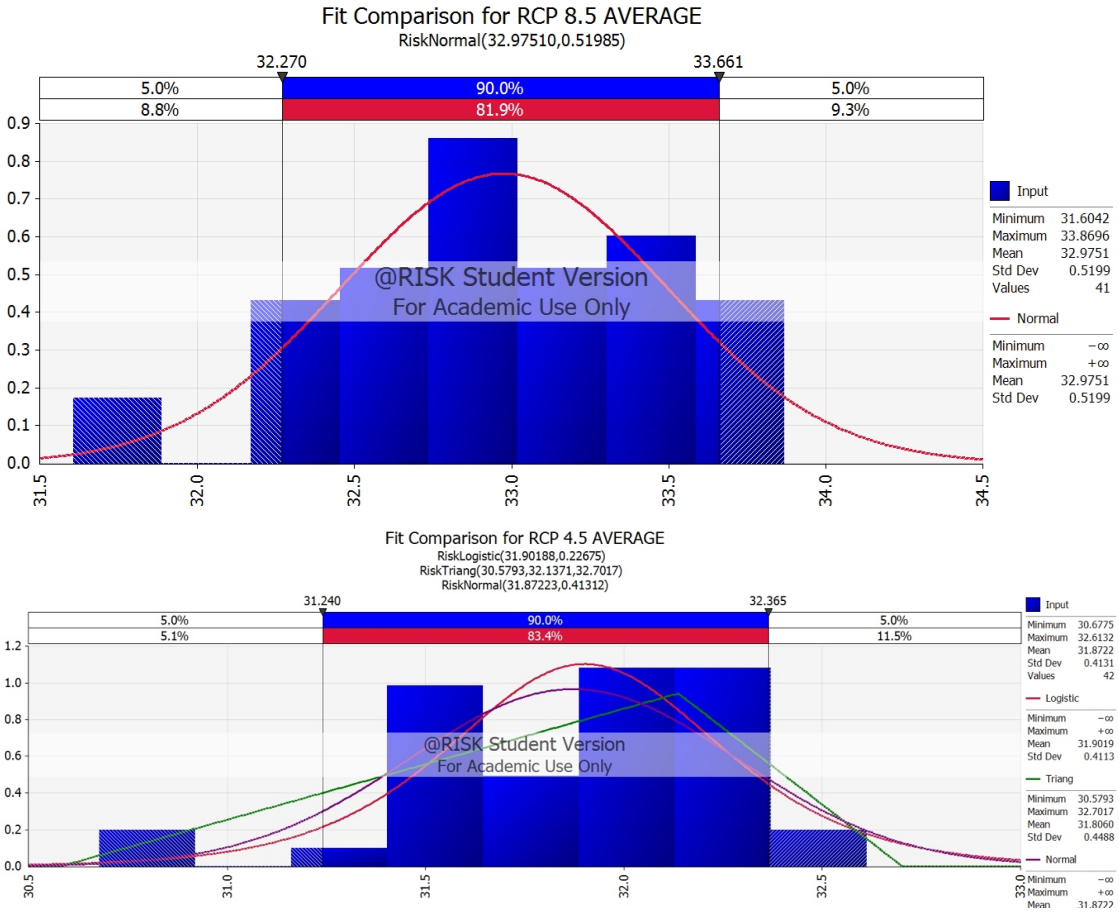

Figure 48 Projection Probability Distribution Functions

APPENDIX C

CO-AUTHOR PERMISSION FOR PUBLISHED MATERIAL

Chapter 2 was published in *Environmental Science & Technology* and appears as published with the exception of text and figure formatting. The citation for the article is: Bondank, E. N., Chester, M. V., & Ruddell, B. L. (2018). Water Distribution System Failure Risks with Increasing Temperatures. *Environmental science & technology*, *52*(17), 9605-9614. All co-authors have granted permission for use the material in this dissertation.